CHAPTER 1

Excretion of cytokinins into the cultivation medium by suspension-cultured tobacco cells

Jan Petrášek, Alena Březinová, Josef Holík, Eva Zažímalová

Plant Cell Reports 21, 97-104, 2002

This chapter describes how plant cells of the cytokinin-autonomous tobacco cell line VBI-0, when cultivated in medium without addition of cytokinins, can keep balanced levels of physiologically active cytokinins by means of their secretion into the cultivation medium.

My contribution to this article was in the preparation and cultivation of plant material, determination of all growth characteristics, development of suitable large-scale cultivation method, adaptation of method for extraction of cytokinins from cultivation medium, processing and interpretation of all measured data and the editing of the manuscript text.

Alena Březinová and Josef Holík were involved in cytokinin determination by radioimmunoassay (RIA), and Eva Zažímalová in writing and editing of the manuscript (corresponding author). HPLC separation of cytokinins was done by Josef Eder and Petre Dobrev.

This research was supported by grants to Eva Zažímalová from the Grant Agency of the Academy of Sciences of the Czech Republic, project no. A6038706, and by the Ministry of Education, Youth and Sports, project no. OK 379/1999.

Plant Cell Rep (2002) 21:97–104
DOI 10.1007/s00299-001-0433-9

PHYSIOLOGY AND BIOCHEMISTRY

J. Petrášek · A. Březinová · J. Holík · E. Zažimalová

Excretion of cytokinins into the cultivation medium by suspension-cultured tobacco cells

Received: 1 June 2001 / Revised: 4 December 2001 / Accepted: 6 December 2001 / Published online: 28 May 2002

Abstract The dynamics of individual cytokinins were determined in both the cells and the cultivation medium during the subculture interval of cell suspension cultures of *Nicotiana tabacum* L., line VBI-0. The amounts of cytokinins detected in the cultivation medium were less than 1 pmol ml^{-1} of suspension. In the late stationary phase, the levels of isopentenyladenosine, as well as that of dihydrozeatin and its riboside, increased significantly. However, when expressed per cell number, the levels of zeatin- and isopentenyladenine-type cytokinins in both the cells and medium were at a maximum at the beginning of the subculture interval and then gradually decreased. Cytokinins were excreted from the cells during the whole subcultivation period, and their concentrations in the cultivation medium were found to be approximately in proportion to their momentary levels inside the cells. The excretion might thus represent one of the mechanisms controlling endogenous cytokinin concentrations.

Keywords Cytokinins · Plant cell cultures · Growth cycle · *Nicotiana tabacum* L.

Abbreviations *Ade*: Adenine · *Ado*: Adenosine · *BA*: N^6-Benzyladenine · *BAP*: N^6-Benzyladenosine · *2,4-D*: 2,4-Dichlorophenoxyacetic acid · *DHZ*: Dihydrozeatin · *DHZR*: Dihydrozeatin riboside · *iP*: N^6-(Δ^2-Isopentenyl)adenine · *iPR*: N^6-(Δ^2-Isopentenyl)adenosine · *NAA*: α-Naphthaleneacetic acid · *RIA*: Radioimmunoassay · *RP-HPLC*: Reverse phase high-performance (pressure) liquid chromatography · *SBI*: Subculture interval · *Z*: *trans*-Zeatin · *ZR*: *trans*-Zeatin riboside

Communicated by G. Hahne

J. Petrášek · A. Březinová · J. Holík · E. Zažimalová (✉)
Institute of Experimental Botany,
The Academy of Sciences of the Czech Republic,
Rozvojová 135, 16502 Prague 6-Lysolaje, Czech Republic
e-mail: eva.zazim@ueb.cas.cz
Tel.: +420-2-20390429, Fax: +420-2-20390474

Introduction

Cytokinins and auxins are the main phytohormones controlling the growth and development of in vitro cultured plant cells (Skoog and Armstrong 1970; Meins 1989; Kamínek 1992). At the level of the isolated plant cell (grown in cell suspension culture) one can distinguish two main processes apparently controlled by a co-operation between cytokinins and auxins – cell division and cell elongation. The free auxin:cytokinin ratio represents a significant signal for the onset and maintenance of cell division (John et al. 1993; recently summarised in Pasternak et al. 2000) as well as for the establishment of cell phenotype (Stickens et al. 1996). This ability of the auxin:cytokinin ratio to control key events in plant morphogenesis was first recognised by Skoog and Miller (1957), who altered the regulation of organogenesis in vitro by manipulating the cytokinin and auxin content in defined culture media. Recent investigations also support the inter-relationships between auxin and cytokinin levels and morphogenic responses of various plants and plant cells (e.g. Li et al. 1995; Centeno et al. 1996; Leyser et al. 1996). Most of the physiological responses induced by the exogenous application of cytokinins have also been observed in transgenic plant cells expressing various specific genes, the products of which are involved in cytokinin biosynthesis (Akiyoshi et al. 1983; Klee and Romano 1994). The endogenous cytokinin level was significantly increased in these transgenic plants, resulting in typical physiological effects such as the inhibition of root growth, formation of a shooty phenotype and delay of leaf senescence (Van Loven et al. 1993; Hewelt et al. 1994). However, the transformation of tobacco cells by an *Agrobacterium tumefaciens* strain lacking the *tmr* cytokinin biosynthesis locus resulted in the production of unorganised tumours growing in a cytokinin-independent manner similar to the growth of transformants bearing the original *tmr* locus (Black et al. 1994).

There is no doubt that in plant cells the internal level of cytokinins (as well as that of other phytohormones) is

precisely regulated, and there are several reports describing this phenomenon (e.g. Akiyoshi et al. 1983; Hansen et al. 1987; Vaňková et al. 1992; Fosket 1993; Zhang et al. 1995; Zažimalová et al. 1996, 1999; Redig et al. 1996; summarised in Kamínek et al. 1997). Reports on cytokinin regulation of plant cell development have mostly focused on the effects of exogenous application and the regulation of endogenous levels of individual cytokinin derivatives. The excretion of cytokinins from cells into the cultivation medium has largely been ignored, and only a few reports are available on this topic. These include limited information on cytokinin production and excretion by bacteria and fungi (Barea et al. 1976; Gogala 1991; Strzelczyk et al. 1994) and one report (Vaňková et al. 1987) describing the production and excretion of zeatin derivatives (Z and ZR) by immobilised tobacco cells. The excretion of cytokinins into the medium by those cytokinin-autonomous cells was much higher than that by cytokinin-dependent cells. The same column flow-through arrangement with immobilised tobacco cells was used also for studies on the production and excretion of isoprenoid cytokinins following the application of auxin (NAA; Vaňková et al. 1992).

In a previous investigation (Zažimalová et al. 1996), we studied the dynamics of individual endogenous cytokinins during the growth cycle (subculture interval) of the auxin-dependent and cytokinin-independent cell suspension culture of *Nicotiana tabacum* L. (strain VBI-0). In cells grown at an optimum auxin concentration, the transient maxima of iP and iPR (and also to a lesser extent those of Z and ZR) correlated with the onset of cell division during the exponential growth phase. A partial lack of auxin in the cultivation medium induced an accumulation of endogenous cytokinins, predominantly in the form of physiologically very active free bases, a finding which might reflect a mechanism "compensating" for the lack of one hormone by the increased accumulation of another one.

In this report, the same auxin-dependent and cytokinin-autonomous tobacco cell strain, VBI-0, was used to detect and to quantify the excretion of various cytokinins from the cells to the cultivation medium. The data have been related to the individual phases of the growth cycle of suspension-cultured VBI-0 cells and to internal cytokinin levels in the cells.

Materials and methods

Plant material

Tobacco cell strain VBI-0, derived from the stem pith of *Nicotiana tabacum* L. cv. Virginia Bright Italia (Opatrný and Opatrná 1976), was used as a model experimental material. Batch cell cultures were grown in suspension in standard liquid Heller medium (Heller 1953), supplemented with the auxins NAA and 2,4-D (5×10^{-6} *M* each) and subcultured routinely at 2-week intervals. Two-week-old cell suspension was used for the inoculation. The initial cell density was 7.3×10^4 cells ml^{-1}. For the extraction and determination of cytokinins in the cultivation medium, 'large-scale' cultivation was carried out in 2-l Erlenmeyer flasks, each containing 800 ml of cell suspension, in darkness at 25°C on an orbital shaker (INR-200; Sanyo-Gallenkamp, UK) at 120 rpm.

Determination of cell number and cell viability

The cells were counted using a Fuchs-Rosenthal haemocytometer, and cell density was expressed as the number of cells per milliliter of cell suspension. Viability of the cells in suspension was estimated by the trypan blue dye exclusion test (Phillips 1973) using 0.4% trypan blue solution (Sigma, St. Louis, Mo.). For the whole SBI, cell viability did not decrease below 80% of the total cell number (data not shown).

Extraction of cytokinins from the cultivation medium

The cultivation medium was collected in 50-ml aliquots during the SBI under large-scale cultivation conditions, and the cells were removed by careful filtration through filter paper under reduced pressure. Three separate samples of medium were analysed in parallel. Cell cakes were discarded. The filtrate was subjected to the extraction procedure described in Zažimalová et al. (1996) adapted for the extraction of cytokinins from the cultivation medium (Fig. 1). The individual cytokinin derivatives (iP, iPR, Z, ZR, DHZ and DHZR) were then separated by RP-HPLC using the protocol modified by Březinová et al. (1992). A Separon SGX RPS 7-µm column (250×4.6 mm; Tessek, Prague, Czech Republic) was used, and cytokinins were eluted with a linear methanol gradient (24–73%, v/v) in 10^{-2} *M* citrate-acetate buffer at pH 6.3. Under these conditions, cytokinins were distributed into five fractions: fraction 1 contained ZR; fraction 2, Z+DHZR; fraction 3, DHZ; fraction 4, iPR; fraction 5, iP. The two cytokinins included in fraction 2 were separated in a second run on a LiChrospher 100 RP-18 5-µm column (250×4 mm, Merck) and eluted with a linear gradient of methanol:acetonitrile (1:1, v:v) in 40 m*M* triethylammonium acetate buffer (10–42%), pH 3.9 (Vaňková et al. 1998). The individual cytokinins were then quantified by RIA. Recovery rates were estimated using [^{3}H]-labelled standards (Z, ZR, iP, iPR, DHZ, DHZR; approx. 2×10^4 dpm per cytokinin per sample). The specific radioactivity of iPR was 1.3 TBq $mmol^{-1}$; the specific radioactivity of all other cytokinins used was 1.1 TBq $mmol^{-1}$. All these preparations were synthesised by Dr. Jan Hanuš (Radioisotope Laboratory, Institute of Experimental Botany, Prague, Czech Republic).

Parallel extraction and purification of cytokinins from the cells and the cultivation medium

The VBI-0 cells were grown under standard cultivation conditions (250-ml Erlenmeyer flasks containing 40 ml of cell suspension at an initial cell density 4.3×10^4 cells ml^{-1}). At intervals during a subculture period, cells (approx. 1 g fresh mass) were harvested by gentle filtration (see above); at the same time aliquots of the cultivation medium (35–50 ml) were collected. Sampling was carried out on days 2, 8, 16 and 23 – i.e. at the lag phase, exponential, late exponential/early stationary and late stationary growth phases, respectively. The cells were homogenised using a pestle and mortar in liquid nitrogen, and the cytokinins were then extracted as described by Zažimalová et al. (1996). The extraction and purification of cytokinins from the cultivation medium were performed as described above.

Determination of individual cytokinins by RIA

The protocol of Weiler (1984), as modified by Březinová et al. (1992), was followed. For the quantification of individual cytokinins, polyclonal rabbit antibodies (their characteristics are given in the Table 1) and [^{3}H]-labelled cytokinins (iPR and ZR, see above) were used. Each RIA determination was carried out a minimum of three times.

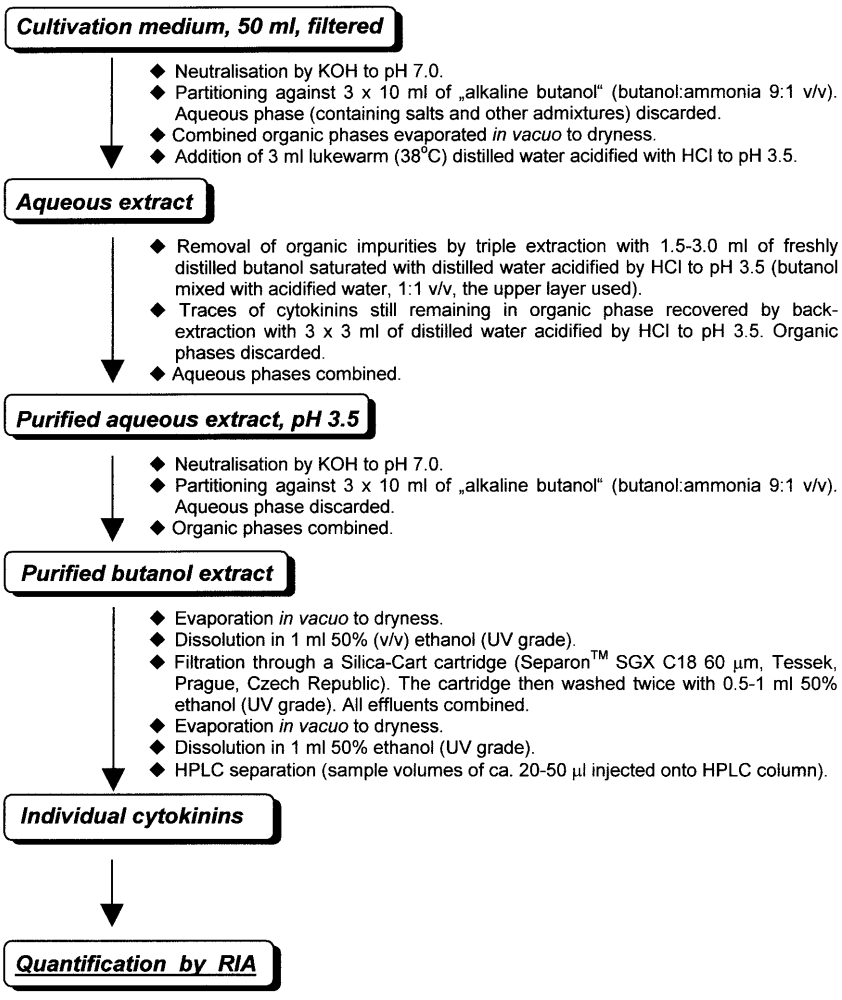

Fig. 1 Protocol for the extraction and purification of cytokinins from the cultivation medium

Table 1 Characteristics of the antibodies used for cytokinin determination and quantification

Antibody against	Cross-reactivity against other cytokinins		Cross-reactivity against Ade and Ado	Titre
iPR	iP	100%	<1%	1:2,000
	Z	0.1%		
	ZR	0.2%		
	DHZ	<0.1%		
	BA	0.1%		
	BAP	0.1%		
	Kinetin	0.2%		
	Other cytokinins	<0.2%		
ZR	Z	98%	<2%	1:1,000
	DHZ	88%		
	DHZR	40.4%		
	iP	0.2%		
	iPR	0.9%		
	Other cytokinins	<2%		

Results and discussion

The tobacco cell strain VBI-0 possesses some specific properties advantageous for both cytological and biochemical studies, including a specific filamentous phenotype and time-separated processes of cell division and cell elongation (Fig. 2). It is relatively well characterised from both a cytological (Opatrný and Opatrná 1976; Petrášek et al. 1998) and a biochemical (Cvikrová et al. 1988; Zažimalová et al. 1995, 1996) point of view. The strain is highly friable, and the number of cells per unit of volume (e.g. 1 ml) and/or fresh mass (e.g. 1 g) can be determined easily. Therefore, analytical data can be expressed on either a fresh mass or cell number basis. Consequently, the biochemical characteristics obtained may ultimately provide more complex information about the relationships

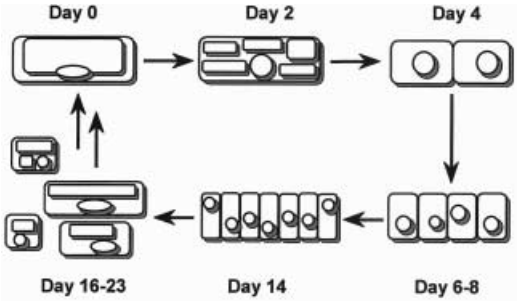

Fig. 2 Timing of events during large-scale subcultivation of the VBI-0 cell strain in liquid medium. The inoculum consisted of individual highly vacuolated cells which after a 2-day lag phase gradually produced cell filaments (within exponential growth phase, approx. day 4–14). The disintegration of cell chains and the subsequent elongation of each individual cell occurred consecutively from day 14

between cell development and metabolic activities. In order to determine the cytokinins in the cultivation medium, we used large-scale cultivation (in one 2-l Erlenmeyer flask) to provide a sufficient amount of experimental material for the analyses. The results presented here were obtained from one particular subculture, thereby allowing us to follow and compare the dynamics of individual cytokinin levels more precisely. Whole large-scale subcultivation was repeated twice, with analogous results.

The cytokinins were extracted from the cultivation medium during various phases of the SBIs using classical partitioning methods based on the different solubilities of the various forms of cytokinin molecules in either water or organic solvents depending on pH. The recovery rates for individual cytokinins varied from approximately 70% to 85%, with coefficients of variation between 6.0% and 9.5% (n=3). Since RIA was used for the final cytokinin determination, the radiolabelled standards were added in concurrent samples to prevent 'overload' by the radioactivity of samples where 'native' cytokinins from the medium were to be determined. This extraction procedure has been used for the extraction of cytokinins from various tissues and – as determined using various internal standards (see above, and [^{3}H]-*m*-hydroxybenzyladenosine) – gives reproducible recoveries of approximately 85% (Auer et al. 1999).

During the SBIs, the pH value in the cultivation medium underwent slight changes: From a starting value of pH 5.8, there was an increase to pH 6.6 on day 11, followed by a decrease to 5.9 on day 23 (data not shown). Since the pH value of the medium was adjusted to 7.0 at the beginning of the extraction procedure (see Fig. 1), the changes in pH of the cultivation medium during SBI could not influence the partitioning itself and, consequently, the comparability of final results.

The first sample (day 0) was taken 30 min following the inoculation of the cells into fresh medium and thus represented the fast response of the cell culture upon transfer into the fresh medium rather than the properties of the inoculum itself. Therefore, the cytokinin contents at day 0 did not correspond to those at day 14, despite

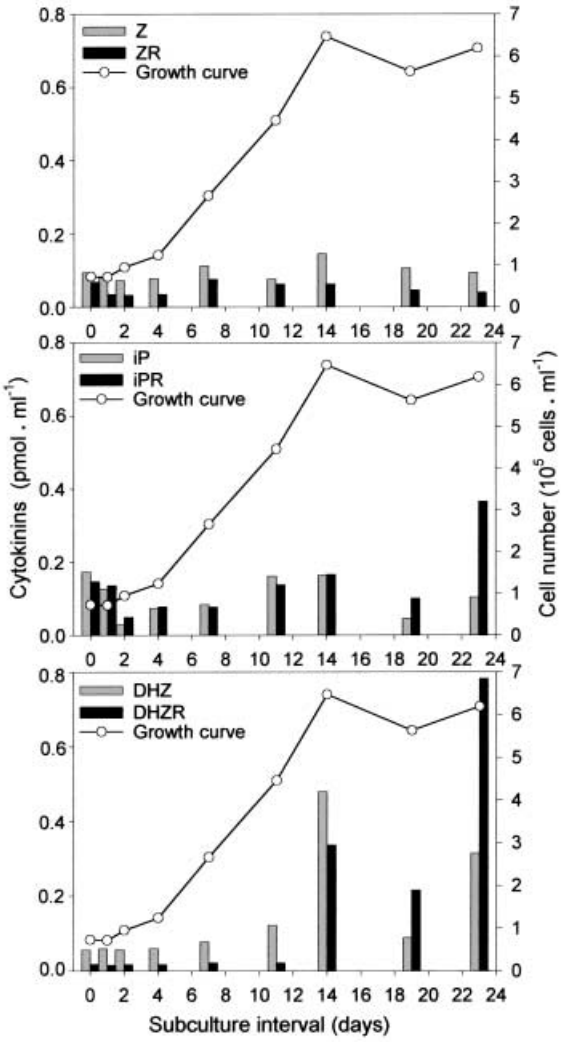

Fig. 3 Dynamics of individual cytokinin levels in the cultivation medium during the SBI of the VBI-0 tobacco cell strain grown in suspension culture, as expressed per milliliter of cultivation medium. The zeatin-type cytokinins (*Z* zeatin, *ZR* its riboside) are depicted in the *upper panel*, the isopentenyladenine-type cytokinins (*iP* N^6-(Δ^2-isopentenyl)adenine, *iPR* its riboside) in the *middle panel* and dihydrozeatin-type cytokinins (*DHZ* dihydrozeatin, *DHZR* its riboside) in the *lower panel*. The line shows the growth curve of the large-scale subculture used as the representative experiment. Standard deviations of cytokinin determinations were less than 3% of the means (n=3)

the fact that 14-day-old cells were used for inoculation (cf. Materials and methods).

As the VBI-0 cell strain is cytokinin-autonomous, no cytokinins were added into the cultivation medium. Therefore, the cells themselves must have produced all the cytokinins detected.

Generally, the amounts of all cytokinins tested were very low, from hundredths of picomoles to nearly 1 pmol per millilitre of cultivation medium (Fig. 3). Levels of Z and ZR (Fig. 3, upper panel) varied around 0.1 pmol, with the amount of riboside decreasing from approximately 80% of the free base at the beginning of SBI to approximately 40% at the end. During the whole SBI, there were

no significant changes in the levels of zeatin-type cytokinins expressed per milliliter of cultivation medium, and their concentrations were near the detection limits.

The amounts of iP and iPR were approximately twofold greater than those of Z and ZR in the lag phase and only slightly higher than those in the exponential growth phase (Fig. 3, middle panel). In contrast, towards the end of SBI in the late stationary phase, the concentration of iPR increased significantly. In the case of iP-type cytokinins, a different ratio between free base and riboside was also observed: in the lag and exponential growth phases, the amounts of both were more or less the same; however, in the late stationary phase, there was a threefold increase in iPR compared with iP.

The situation was completely different in the case of DHZ and DHZR (Fig. 3, lower panel). Until the middle of the exponential growth phase, the levels of DHZ and particularly of its riboside were negligible. However, there was a significant increase in both DHZ-type cytokinins at the end of the exponential phase and during the whole stationary phase. The dynamics of DHZ-type cytokinins were quite different from those of both Z- and iP-type cytokinins in that the former accumulated from a very low level at the beginning of SBI to a very high level at the end, when their levels were at least twofold higher than those of the iP-type cytokinins. At that time, the level of DHZ was three times higher than that of Z, and the level of DHZR was nearly 15-times higher than that of ZR.

This may reflect the different function of DHZ-type cytokinins compared with Z- and iP-type cytokinins. Both Z and iP (and to a lesser extent, their ribosides) represent physiologically active forms of cytokinins (Laloue and Pethe 1982). The DHZ-type cytokinins exhibit lower physiological activities (Skoog and Abdul Ghani 1981) and may be considered to be products of cytokinin inactivation and/or transport forms of cytokinins. The low level of DHZ-type cytokinins at the beginning of SBI and during the exponential growth phase seems to correspond to the very low accumulation of transport forms of cytokinins. In contrast, towards the end of SBI – when the requirement of the cells for active cytokinins decreased – the accumulation of DHZ-type cytokinins increased significantly.

There may be another factor influencing the levels of individual cytokinin forms in the cultivation medium: i.e. cytokinin oxidase. This cytokinin-degrading enzyme is believed to be a key element in cytokinin regulation by down-regulating cytokinin levels inside plant cells. Recent cloning of a cytokinin oxidase gene from maize seeds showed that the gene product contained a signal sequence targeting the enzyme towards secretion (Houba-Herin et al. 1999; Morris et al. 1999). This enzyme activity has since been detected in the cultivation medium of suspension-cultured tobacco cells (Motyka et al. 2000). The affinity of the enzyme is high towards Z- and iP-type cytokinins (both bases and ribosides); DHZ and DHZR, however, are not substrates for it (Motyka and Kamínek 1992; Galuszka et al. 2000). Thus, the possible activity of this enzyme in the cultivation medium might explain both

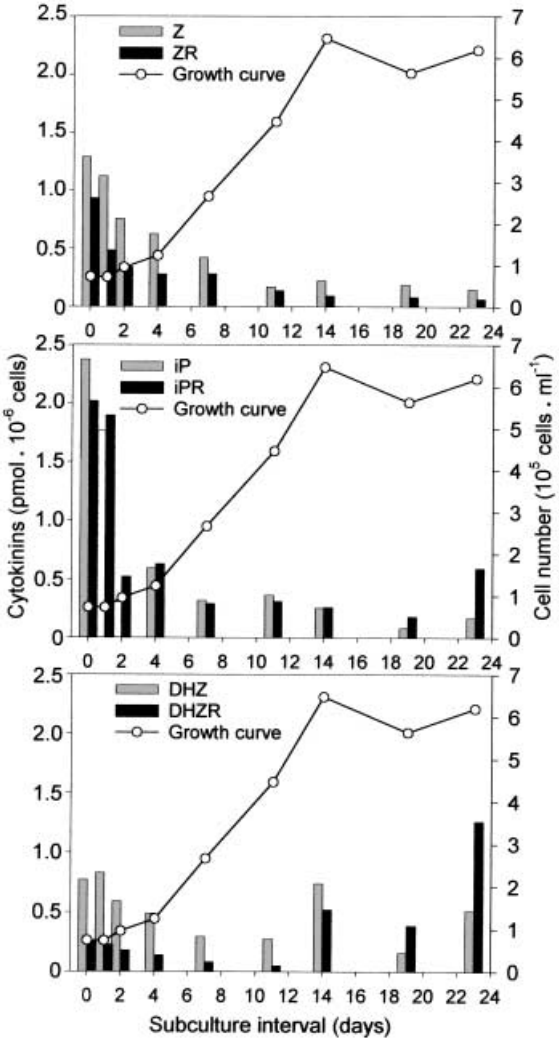

Fig. 4 Dynamics of individual cytokinin levels in the cultivation medium during the SBI of the VBI-0 tobacco cell strain grown in suspension culture, as expressed per equivalent of cell number (i.e. 10^6 cells). Abbreviations as in Fig. 3. Standard deviations of cytokinin determinations were less than 3% of the means (n=3)

the relatively low levels of Z- and iP-type cytokinins and the much higher, and towards the end of SBI still increasing, levels of DHZ and DHZR in the stationary phase.

As already mentioned, in vitro cultured plant cells need cytokinins to control their growth cycle and, in particular, their cell cycle (Redig et al. 1996; Pasternak et al. 2000). The requirements for active forms of cytokinins are especially high at the beginning of SBI and during the exponential growth phase when very intensive cell division occurs. Surprisingly, when expressed per unit volume of cultivation medium (1 ml), the amounts of physiologically active cytokinins – Z-type and iP-type ones – were relatively low at that part of SBI. However, if the amounts of individual cytokinins are calculated per equivalent of cell number (i.e. the measured amounts extracted from medium aliquots divided by the actual number of cells in the aliquots), the complete picture is quite different (Fig. 4). With respect to both Z- and

Table 2 Concentration of cytokinins in the cells (internal cytokinins) and in the cultivation medium (external cytokinins) of the VBI-0 tobacco cell strain grown under standard cultivation conditions (see Materials and methods). Standard deviations of cytokinin determinations were 2.6%–3.1% of the mean (three replications) (*nd* not detected)

	Cells (internal cytokinins) (pmol 10^{-6} cells)				Medium (external cytokinins) (pmol 10^{-6} cells)			
	Day 2	Day 8	Day 16	Day 23	Day 2	Day 8	Day 16	Day 23
Z	4.29	0.20	nd	0.51	0.94	nd	nd	nd
ZR	0.20	nd	0.10	nd	0.20	nd	nd	nd
iP	0.46	0.27	0.18	0.44	1.05	nd	0.06	0.15
iPR	0.88	0.18	0.07	0.56	1.35	0.15	0.15	0.09
DHZ	2.46	1.37	1.41	2.97	6.53	0.66	0.58	0.70
DHZR	4.06	0.45	1.54	8.64	3.31	0.98	0.67	0.66

iP-type cytokinins (Fig. 4, upper and middle panels), their levels at the beginning of SBI were much higher than those of DHZ-type cytokinins (Fig. 4, lower panel), and they significantly decreased during the exponential growth phase. This finding is in accordance with previous measurements of endogenous cytokinins inside the cells of the same strain VBI-0 (Zažimalová et al. 1996), where the highest endogenous concentrations of iP and iPR were found at the beginning of SBI and reached values of the same order of magnitude (picomoles per 10^{-6} cells). However, the momentary endogenous levels of cytokinins and, consequently, also their exogenous concentrations in the medium vary significantly in relation to cell density and to the actual state of the particular subculture development (unpublished data). This implies that a precise quantitative comparison between internal and excreted cytokinins during the growth cycle can be carried out only within one particular subculture where both internal and external cytokinins are analysed in parallel.

We therefore investigated the mutual relationship between internal and external cytokinins in detail. Concurrent extractions and purifications of the internal (inside cells) and external (in the medium) cytokinins were carried out at crucial stages of the growth cycle of VBI-0 cells grown under standard cultivation conditions: in the lag-phase (day 2), in the mid-exponential phase (day 8), at the transition between exponential and stationary phases (day 16) and in the late stationary phase (day 23). The data are summarised in Table 2, where both internal and external cytokinin concentrations are expressed per equivalent of cell number. In general, the results are in agreement with the external cytokinin measurements performed under the large-scale cultivation conditions (see above). In the case of internal cytokinins of the Z- and iP-type, similar trends were observed to those reported earlier (Zažimalová et al. 1996). When measured in parallel in the same subculture, both internal and external Z-type and partly also iP-type cytokinins (expressed per cell number equivalents) were relatively low except at the beginning of subcultivation. On day 2 (end of lag phase) Z, iP and iPR reached their maximum levels and underwent very significant excretion to the cultivation medium. The external concentrations (per cell number equivalents) were even higher than the internal ones (in terms of chemical concentration, they reached values around 40–60 p*M*). At days 8, 16 and 23, the external concentrations of these cytokinins were approximately proportional to their internal concentrations. The DHZ-type cytokinin (DHZ and DHZR) levels were higher than those of Z- and iP-type cytokinins during the whole subcultivation period. Again, these cytokinins were excreted approximately in proportion to their internal levels (except for the reversed ratio for DHZ on day 2, and the very high internal concentration of DHZR on day 23 in contrast to its low external level).

Cell viability during the whole subcultivation period was stable, varying between 80% and 92% living cells in the suspension under large-scale cultivation conditions and between 88% and 95% under standard cultivation conditions. Therefore, any possible release of cytokinins from dead or injured cells is unlikely to have significantly influenced the final data.

The analyses of cytokinins described in this report provide evidence that ‘superfluous’ cytokinins are excreted from the cells into the cultivation medium and that the level of this excretion reflects their actual levels inside the cells. The excretion of cytokinins might represent a supplementary (if not equally important) mechanism of regulation of endogenous cytokinin levels, in addition to metabolic control and, in the case of cytokinin-dependent cell strains, to the uptake of cytokinins from the cultivation medium. On the other hand, once the cytokinins have been excreted from the cells into the external medium, their presence in the medium may influence cell behaviour, even in the case of cytokinin-independent cell lines. Such effects may be mediated through the re-uptake of secreted cytokinins by the cells or through the interactions of excreted cytokinins with cell surface receptors. Thus, the cells, together with the cultivation medium, represent a complex and well-balanced dynamic system, the regulation of which is an important topic for future research.

Acknowledgements This research was supported by grants to E.Z. from the Grant Agency of the Academy of Sciences of the Czech Republic, project no. A6038706, and by the Ministry of Education, Youth and Sports, project no. OK 379/1999. The authors thank Prof. Miroslav Kamínek for his critical comments, and Dipl. Ing. Josef Eder and Dipl. Ing. Petre Dobrev, Institute of Experimental Botany, Prague, for the HPLC separation of cytokinins.

References

Akiyoshi DE, Morris RO, Hinz R, Mischke BS, Kosuge T, Garfinkel DJ, Gordon MP, Nester EW (1983) Cytokinin/auxin balance in crown gall tumors is regulated by specific loci in the T-DNA. Proc Natl Acad Sci USA 80:407–411

Auer C, Motyka V, Březinová A, Kamínek M (1999) Endogenous cytokinin accumulation and cytokinin oxidase activity during shoot organogenesis of *Petunia hybrida*. Physiol Plant 105:141–147

Barea JM, Novarro E, Montoya E (1976) Production of plant growth regulators by rhizosphere phosphate-solibilizing bacteria. J Appl Bacteriol 40:129–136

Black RC, Binns AN, Chang CF, Lynn DG (1994) Cell-autonomous cytokinin-independent growth of tobacco cells transformed by *Agrobacterium-tumefaciens* strains lacking the cytokinin biosynthesis gene. Plant Physiol 105:989–998

Březinová A, Holík J, Chvojka L (1992) Radioimmunoassay of isopentenyladenosine in plants. In: Kamínek M, Mok DWS, Zažimalová E (eds) Physiology and biochemistry of cytokinins in plants. SPB Academic Publishing, The Hague, pp 479–481

Centeno ML, Rodriguez A, Feito I, Fernandez B (1996) Relationship between endogenous auxin and cytokinin levels and morphogenic responses in *Actinidia deliciosa* tissue cultures. Plant Cell Rep 16:58–62

Cvikrová M, Hrubcová M, Meravý L, Pospíšil F (1988) Changes in the content of phenolic substances during the growth of *Nicotiana tabacum* cell suspension culture. Biol Plant 30:185–192

Fosket DE (1993) Plant growth and development. A molecular approach. Academic Press, London, pp 298–393

Galuszka P, Frébort I, Šebela M, Peč P (2000) Degradation of cytokinins by cytokinin oxidases in plants. Plant Growth Regul 32:315-327

Gogala N (1991) Regulation of mycorrhizal infection by hormonal factors produced by hosts and fungi. Experientia 47:331–340

Hansen CE, Meins F Jr, Aebi R (1987) Hormonal regulation of zeatin-riboside accumulation by cultured tobacco cells. Planta 172:520–525

Heller R (1953) Studies on the mineral nutrition of in vitro plant tissue cultures (in French). Ann Sci Nat Bot Biol Veg 14:1–223

Hewelt A, Prinsen E, Schell J, Van Onckelen H, Schmülling T (1994) Promoter tagging with a promoterless *ipt* gene leads to cytokinin-induced phenotypic variability in transgenic tobacco plants: implications of gene dosage effects. Plant J 6:879–891

Houba-Herin N, Pethe C, d'Alayer J, Laloue M (1999) Cytokinin oxidase from *Zea mays*: purification, cDNA cloning and expression in moss protoplasts. Plant J 17:615–626

John PCL, Zhang K, Dong Ch, Diederich L, Wightman F (1993) $p34^{cdc2}$-related proteins in control of cell cycle progression, the switch between division and differentiation in tissue development, and stimulation of division by auxin and cytokinin. Aust J Plant Physiol 20:503–526

Kamínek M (1992) Progress in cytokinin research. Trends Biotechnol 10:159–164

Kamínek M, Motyka V, Vaňková R (1997) Regulation of cytokinin content in plant cells. Physiol Plant 101:689–700

Klee HJ, Romano CP (1994) The roles of phytohormones in development as studied in transgenic plants. Crit Rev Plant Sci 13:311–324

Laloue M, Pethe M (1982) Dynamics of cytokinin metabolism in tobacco cells. In: Wareing PF (ed) Plant growth substances 1982. Academic Press, London, pp 185–195

Leyser HMO, Pickett FB, Dharmasiri S, Estelle M (1996) Mutations in *AXR3* gene of *Arabidopsis* result in altered auxin response including ectopic expression from the SAUR-AC1 promoter. Plant J 10:403–413

Li C-J, Guevara E, Herrera J, Bangerth F (1995) Effect of apex excision and replacement by 1-naphthylacetic acid on cytokinin concentration and apical dominance in pea plants. Physiol Plant 94:465–469

Meins F Jr (1989) Habituation: heritable variation in the requirement of cultured plant cells for hormones. Annu Rev Genet 23:395–408

Morris RO, Bilyeu KD, Laskey JG, Cheikh N (1999) Isolation of gene encoding a glycosylated cytokinin oxidase from maize. Biochem Biophys Res Commun 255: 328–333

Motyka V, Kamínek M (1992) Characterization of cytokinin oxidase from tobacco and poplar callus cultures. In: Kamínek M, Mok DWS, Zažimalová E (eds) Physiology and biochemistry of cytokinins in plants. SPB Academic Publishing, The Hague, pp 33-39

Motyka V, Čapková V, Gaudinová A, Petrášek J, Kamínek M, Schmülling T (2000) Stimulatory effect of cytokinins on cytokinin oxidase activity in tobacco includes changes in enzyme glycosylation and excretion. Plant Physiol Biochem 38[Suppl]:79

Opatrný Z, Opatrná J (1976) The specificity of the effect of 2,4-D and NAA on the growth, micromorphology, and the occurrence of starch in long-term *Nicotiana tabacum* cell strains. Biol Plant 18:381–400

Pasternak T, Miskolczi P, Ayaydin F, Mészáros T, Dudits D, Fehér A (2000) Exogenous auxin and cytokinin dependent activation of CDKs and cell division in leaf protoplast-derived cells of alfalfa. Plant Growth Regul 32:129–141

Petrášek J, Freudenreich A, Heuing A, Opatrný Z, Nick P (1998) Heat-shock protein 90 is associated with microtubules in tobacco cells. Protoplasma 202:161–174

Phillips HJ (1973) Dye exclusion tests for cell viability. In: Kruse PF Jr, Patterson MK (eds.) Tissue cultures: methods and application. Academic Press, London, p 406

Redig P, Shaul O, Inzé D, Van Montagu M, Van Onckelen H (1996) Levels of endogenous cytokinins, indole-3-acetic acid and abscisic acid during the cell cycle of synchronized tobacco BY-2 cells. FEBS Lett 391:175–180

Skoog F, Abdul Ghani AKB (1981) Relative activities of cytokinins and antagonists in releasing lateral buds of *Pisum* from apical dominance compared with their relative activities in the regulation of growth of tobacco callus. In: Guern J, Péaud-Lenoël C (eds) Metabolism and molecular activities of cytokinins. Springer, Berlin Heidelberg New York, pp 140–150

Skoog F, Armstrong DJ (1970) Cytokinins. Annu Rev Plant Physiol 21:359–384

Skoog F, Miller C (1957) Chemical regulation of growth and organ formation in plant tissues cultured in vitro. In: Porter HK (ed) Symp Soc Exp Biol No 11: The biological action of growth substances. Cambridge University Press, London, pp 118–140

Stickens D, Tao W, Verbelen JP (1996) A single cell model system to study hormone signal transduction. Plant Growth Regul 18:149–154

Strzelczyk F, Kampert M, Li CY (1994) Cytokinin-like substances and ethylene production by *Azospirillum* in media with different carbon sources. Microbiol Res 149:55–60

Van Loven K, Beinsberger SEI, Valcke RLM, Van Onckelen HA, Clijsters HMM (1993) Morphometric analysis of the growth of Phsp70-ipt transgenic tobacco plants. J Exp Bot 44:1671–1678

Vaňková R, Kamínek M, Eder J, Vaněk T (1987) Dynamics of production of *trans*-zeatin and *trans*-zeatin riboside by immobilized cytokinin-autonomous and cytokinin-dependent tobacco cells. J Plant Growth Regul 6:147-157

Vaňková R, Gaudinová A, Kamínek M, Eder J (1992) The effect of interaction of synthetic cytokinin and auxin on production of natural cytokinins by immobilized tobacco cells. In: Kamínek M, Mok DWS, Zažimalová E (eds) Physiology and biochemistry of cytokinins in plants. SPB Academic Publishing, The Hague, pp 47–51

Vaňková R, Gaudinová A, Süssenbeková H, Dobrev P, Strnad M, Holík J, Lenfeld J (1998) Comparison of oriented and random immobilization in immunoaffinity chromatography of cytokinins. J Chromatogr A 811:77–84

Weiler EW (1984) Immunoassay of plant growth regulators. Annu Rev Plant Physiol 35:85–95

Zažimalová E, Opatrný Z, Březinová A, Eder J (1995) The effect of auxin starvation on the growth of auxin-dependent tobacco cell culture: dynamics of auxin reception and endogenous free IAA content. J Exp Bot 46:1205–1213

Zažimalová E, Březinová A, Holík J, Opatrný Z (1996) Partial auxin deprivation affects endogenous cytokinins in an auxin-dependent, cytokinin-independent tobacco cells strain. Plant Cell Rep 16:76-79

Zažimalová E, Březinová A, Motyka V, Kamínek M (1999) Control of cytokinin biosynthesis and metabolism. In: Libbenga KR, Hall MA, Hooykaas P (eds) Biochemistry and molecular biology of plant hormones. Series new comprehensive biochemistry. Elsevier, Amsterdam, pp 141–160

Zhang R, Zhang X, Wang J, Letham DS, McKinney SA, Higgins TJV (1995) The effect of auxin on cytokinin levels and metabolism in transgenic tobacco tissue expressing an *ipt* gene. Planta 196:84–94

CHAPTER 2

Auxin efflux carrier activity and auxin accumulation regulate cell division and polarity in tobacco cells

Jan Petrášek, Miroslav Elčkner, David A. Morris, Eva Zažímalová

Planta 216, 302-308, 2002

This chapter describes for the first time at cellular level the effect of 1-N-naphthylphthalamic acid (NPA; an inhibitor of auxin efflux) on cell division polarity. We have shown that the application of NPA to tobacco VBI-0 cells results in increased accumulation of [^{3}H]NAA in cells and temporary and reversible inhibition of cell division activity. Partial loss of cell polarity and disturbed orientation of cell division were observed when cell division activity resumed.

My contribution to this article was in the preparation and cultivation of plant material, determination of all growth characteristics, DIC microscopy, auxin-accumulation assays, processing and interpretation of all measured data and in the writing and editing of the manuscript text and figures.

Miroslav Elčkner participated on auxin-accumulation assays, as well as Eva Zažímalová and David Morris. Eva Zažímalová (corresponding author) and David Morris were involved in writing and editing of the manuscript.

The work was supported by the Grant Agency of the Czech Republic (project No. 206/98/1510), by the EU INCO Copernicus (project No. ERBIC15 CT98 0118) to Eva Zažímalová and by grants to David A. Morris from the UK Royal Society and the Academy of Sciences of the Czech Republic under the European Science Exchange Scheme.

Planta (2002) 216: 302–308
DOI 10.1007/s00425-002-0845-y

ORIGINAL ARTICLE

Jan Petrášek · Miroslav Elčkner · David A. Morris
Eva Zažímalová

Auxin efflux carrier activity and auxin accumulation regulate cell division and polarity in tobacco cells

Received: 19 January 2002 / Accepted: 3 June 2002 / Published online: 14 August 2002

Abstract Division and growth of most types of in vitro-cultured plant cells require an external source of auxin. In such cultures, the ratio of external to internal auxin concentration is crucial for the regulation of the phases of the standard growth cycle. In this report the internal concentration of auxin in suspension-cultured cells of *Nicotiana tabacum* L., strain VBI-0, was manipulated either (i) by increasing 10-fold the normal concentration of 1-naphthaleneacetic acid (NAA) and 2,4-dichlorophenoxyacetic acid in the external medium; or (ii) by addition 1-N-naphthylphthalamic acid (NPA; an inhibitor of auxin efflux and of auxin efflux carrier traffic). Both treatments delayed the onset of cell division for 6–7 days without loss of cell viability. In both cases, cell division activity subsequently resumed coincident with a reduction in the ability of cells to accumulate [^{3}H]NAA from an external medium. Following renewed cell division, a significant proportion of the NPA-treated cells but not those grown at high auxin concentration, exhibited changes in the orientation of new cell divisions and loss of polarity. We conclude that cell division, but not cell elongation, is prevented when the internal auxin concentration rises above a critical threshold value and that the directed traffic of auxin efflux carriers to the plasma membrane may regulate the orientation of cell divisions.

Keywords Auxin carrier · 1-N-Naphthylphthalamic acid · *Nicotiana* (cell culture) · Phytotropin · Polar auxin transport

J. Petrášek · M. Elčkner · D.A. Morris · E. Zažímalová (✉)
Institute of Experimental Botany, Rozvojová 135,
16502 Prague 6 – Lysolaje, Czech Republic
E-mail: eva.zazim@ueb.cas.cz
Fax: +420-2-20390474

Present address: D.A. Morris
Division of Cell Sciences,
School of Biological Sciences, University of Southampton,
Bassett Crescent East, Southampton, SO16 7PX, UK

Abbreviations 2,4-D: 2,4-dichlorophenoxyacetic acid · IAA: indole-3-acetic acid · NAA: 1-naphthaleneacetic acid · NPA: 1-N-naphthylphthalamic acid

Introduction

The polar transport of auxins [indole-3-acetic acid (IAA) and related compounds] plays a key role in the regulation of auxin-dependent growth and developmental processes. Mediated auxin influx into individual cells is catalysed by specific auxin-anion uptake carriers, whilst efflux is catalysed by a different auxin-anion efflux carrier system (Rubery and Sheldrake 1974; Raven 1975; reviewed by Goldsmith 1977). Biochemical, physiological and molecular evidence indicates that the polarity of auxin transport through cells and tissues results from the polarised distribution of auxin efflux carriers in the plasma membrane (reviewed by Bennett et al. 1998; Morris 2000). Available evidence indicates that in contrast to the auxin uptake carrier, the efflux carrier is a much more complex system consisting of the transport catalyst itself and one or more associated regulatory proteins (Morris et al. 1991; Muday 2000). One of these regulatory proteins is believed to be a specific binding protein for phytotropins [1-N-naphthylphthalamic acid (NPA) and related compounds], which may be associated with the actin cytoskeleton (Muday 2000; Muday and DeLong 2001; Muday and Murphy 2002). Phytotropins are potent non-competitive inhibitors of auxin efflux (and, consequently, stimulators of net auxin accumulation) and of polar auxin transport (Rubery 1990).

Cell-suspension cultures provide good model systems in which the effects of growth substances on cell division and growth can be studied directly. In such cultures the rate and intensity of cell division are regulated, among other things, by changes in the external and internal concentrations of two essential phytohormones, auxins and cytokinins. Manipulation of the levels of these hormones in tobacco cell cultures (and, consequently,

the ratio of their momentary concentrations in the cultivation medium) may result in a change of developmental programme from cell elongation to cell division (Hasezawa and Syono 1983; Stickens et al. 1996).

Earlier we described the relationships between internal auxin (IAA) level and auxin-binding activity in relation to cell division intensity in the auxin-dependent and cytokinin-autonomous tobacco cell strain VBI-0 (Zažímalová et al. 1995). During the exponential (rapid cell division) phase, reduction in the external auxin concentration resulted in a substantial decrease of cell division activity but increased the internal level of free IAA in cells and the activity of a membrane-bound auxin-binding site. The strong inhibition of auxin efflux by NPA greatly increases auxin accumulation in NPA-treated tissues (Morris and Robinson 1998). Similarly, increases in the external concentration of auxin also strongly promote total auxin accumulation (Johnson and Morris 1989). To investigate the effects of raised internal auxin levels on cell division activity and cell phenotype in VBI-0 suspension cultures, we have examined the response of VBI-0 cells to the inclusion of NPA in the culture medium, or to increases in the concentration of auxin supplied in the medium. Here we report that whilst both treatments result in a temporary and reversible inhibition of cell division activity, treatment with NPA, but not with high external auxin concentrations, causes partial loss of cell polarity and disturbed orientation of cell division when division activity resumes.

Materials and methods

Plant material

The auxin-dependent and cytokinin-autonomous VBI-0 tobacco cell strain derived from the stem pith of *Nicotiana tabacum* L., cv. Virginia Bright Italia (Opatrný and Opatrná 1976) was cultivated in standard Heller liquid medium (Heller 1953) supplemented with synthetic auxins 1-naphthaleneacetic acid (NAA) and 2,4-dichlorophenoxyacetic acid (2,4-D; 5.4 μM, and 4.5 μM, respectively). Cells were sub-cultured every 2 weeks (inoculation density approx. 5×10^4 cells ml^{-1}) and cultivated at 25 °C in darkness on an orbital shaker (INR-200; Sanyo–Gallenkamp, UK) at 120 rpm (diameter 32 mm).

Determination of cell population density and viability test

Cell densities were determined by counting cells in at least 10 aliquots of each culture sample using a Fuchs-Rosenthal haemocytometer slide. Cell viability was assessed by the Trypan Blue dye exclusion test (Phillips 1973). 0.5 ml of 0.4% Trypan Blue solution (Sigma) was mixed with 0.5 ml of cell suspension and cells were examined microscopically within 5 min. The percentage of viable (unstained) cells was determined from at least 10 optical fields on each of 3 separate slides.

Microscopic examination of cells

Cells were examined with an Olympus Provis AX-70 microscope equipped with Nomarski DIC optics and an automatic photomicrography system. Images were stored on a computer for electronic processing. The frequency of longitudinal and oblique cell divisions in control (no NPA) and NPA-treated cells (expressed as a percentage of the dividing cells) was determined by microscopic examination of 5 separate samples per treatment (500 cells were assessed in each sample).

NPA treatments

NPA was synthesised at the Institute of Experimental Botany, Prague, by the method of Meyer and Wolfsleben (1911), and its quality and purity were checked by melting-point determination, infrared spectroscopy, thin-layer chromatography and HPLC.

In experiments in which NPA was included in the cultivation medium, it was added as a 5 mM filter-sterilised stock solution in 96% ethanol directly to the cultivation medium at the start of the sub-culture interval to a final concentration of 10, 50 and 100 μM. An equivalent volume of 96% ethanol was added to control cultures. In other experiments, NPA was included only during the accumulation assays and was added to the uptake buffer to give the required final concentration. An equivalent volume of 96% ethanol was added to control assays.

Auxin-accumulation assay

The accumulation by the cells of [^{3}H]NAA (specific radioactivity 935 GBq $mmol^{-1}$; synthesised at the Isotope Laboratory, Institute of Experimental Botany, Prague, Czech Republic) was measured in 0.5-ml aliquots of cell suspension (cell density ca. 2×10^5 cells ml^{-1}) by a method modified from the protocol of Delbarre et al. (1996). Briefly, each cell suspension was filtered, re-suspended in uptake buffer (20 mM Mes, 40 mM sucrose, 0.5 mM $CaSO_4$, pH adjusted to 5.7 by KOH) and equilibrated for 45 min with continuous orbital shaking. Equilibrated cells were collected by filtration, re-suspended in fresh uptake buffer and incubated on the orbital shaker for 1.5 h in darkness at 25 °C. [^{3}H]NAA was added to the cell suspension to give a final concentration of 2 nM. At timed intervals (6 or 20 min according to experiment), 0.5-ml aliquots of suspension were withdrawn and accumulation of label was terminated by rapid filtration under reduced pressure on 22-mm-diameter cellulose filters. The cell cakes and filters were transferred to scintillation vials, extracted in 0.5 ml ethanol for 30 min and radioactivity was determined by liquid scintillation counting. Counts were corrected for surface radioactivity by subtracting counts obtained for aliquots of cells withdrawn immediately after the addition of [^{3}H]NAA. Treatments were replicated at least three times and averaged values (± standard errors), expressed as pmol NAA accumulated per 10^6 cells, are shown below.

Results

Cell division in VBI-0

VBI-0 cells inoculated into media containing 50 μM NPA showed a remarkably different behaviour from control cells (Figs. 1, 2a). NPA treatment resulted in an almost complete cessation of cell division for the first 6 days of cultivation, accompanied by a stimulation of cell elongation (cf. Fig. 1b and Fig. 1e). The cessation of cell division was only temporary, however, and after several days (usually 6–9) the cells started to divide again (Fig. 1f, g). As revealed by the Trypan Blue test, cell viability was not affected by NPA treatment and was between 79 and 89% for control cells and between 81 and 93% for NPA-treated cells. Standard deviations of

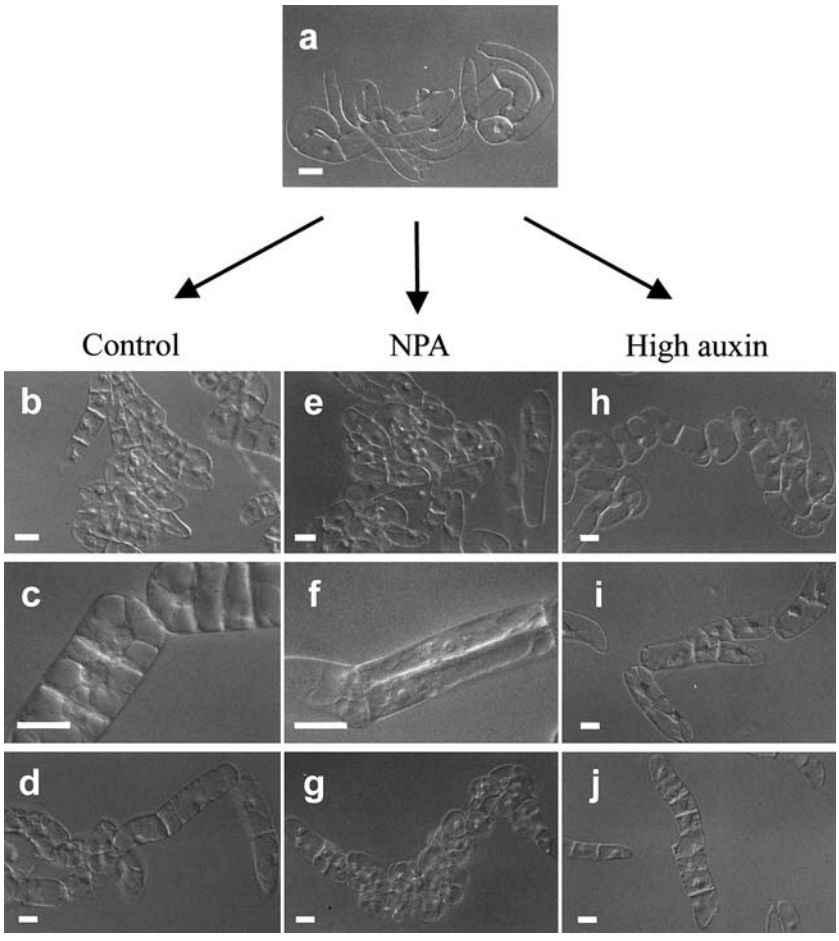

Fig. 1a–j Effects of NPA and of high external auxin concentration on cell division activity and phenotypic characters of suspension-cultured cells of tobacco (*Nicotiana tabacum*, line VBI-0). **a** Two-week-old inoculum consisting of individual elongated cells. **b–d** Cells grown in control medium (5.4 μM NAA plus 4.5 μM 2,4-D; no NPA) for 3, 6 and 9 days, respectively. **e–g** Cells grown for 3, 6 and 9 days, respectively, in control medium (as above) supplemented with NPA (50 μM). **e** Inhibition of cell division is apparent after 3 days. **f** Axial (longitudinal) divisions in 6-day-old cells. **g** Renewal of cell division activity and formation of non-polarised cell clusters 9 days after start of NPA treatment. **h–j** Cells grown for 3, 6 and 9 days, respectively, in the presence of high external auxin concentrations (54 μM NAA plus 45 μM 2,4-D; no NPA). **h** 3-day-old cells in which cell division has been inhibited. **i, j** Cells grown for 6 and 9 days, respectively, at high external auxin concentration showing renewed cell division activity and the development of polarised, one-cell wide filaments as a result of regular transverse divisions. Bars = 50 μm

cell viability determinations were between 4 and 6% of the means for both control and treated cells.

Similar effects on cell division and cell elongation were observed in cells cultured in media containing 10 times the normal concentrations of NAA and 2,4-D (Figs. 1h–j, 2b). Cell division activity was suppressed by the high auxin concentration but, as with NPA, the rate of cell division began to increase again after about 6 days (Fig. 1i, j). Similar to the NPA treatment, cell growth continued during the period of suppressed division activity (Fig. 1h). Like treatment with NPA, raising the external auxin concentration 10-fold did not affect cell viability (data not shown).

Accumulation of [^{3}H]NAA

To check whether high NPA concentrations might have damaging effects on cells, the effects of [^{3}H]NAA accumulation by VBI-0 cells were tested by exposing cells to a range of NPA concentrations between 1 and 100 μM (Fig. 3). Inhibition of [^{3}H]NAA efflux (i.e. stimulation of NAA accumulation) by NPA in VBI-0 cells was saturated between 1 and 30 μM. Since 50 μM NPA had a maximal and consistent effect on auxin accumulation with no obvious signs of cell damage, this concentration was chosen as a standard for the present study.

To confirm that NPA treatment caused an increase in auxin accumulation, we measured net accumulation of [^{3}H]NAA (2.0 nM) by cells cultured in standard medium and in medium supplemented with 50 μM NPA from the start of the sub-culture period. Accumulation was measured over a 6-min uptake period. In these experiments, NPA was not included in the uptake buffer. Previous results have demonstrated that no substantial metabolism of [^{3}H]NAA occurs over this time interval (Delbarre et al. 1996). As expected, inclusion of NPA in the cultivation medium substantially increased the abil-

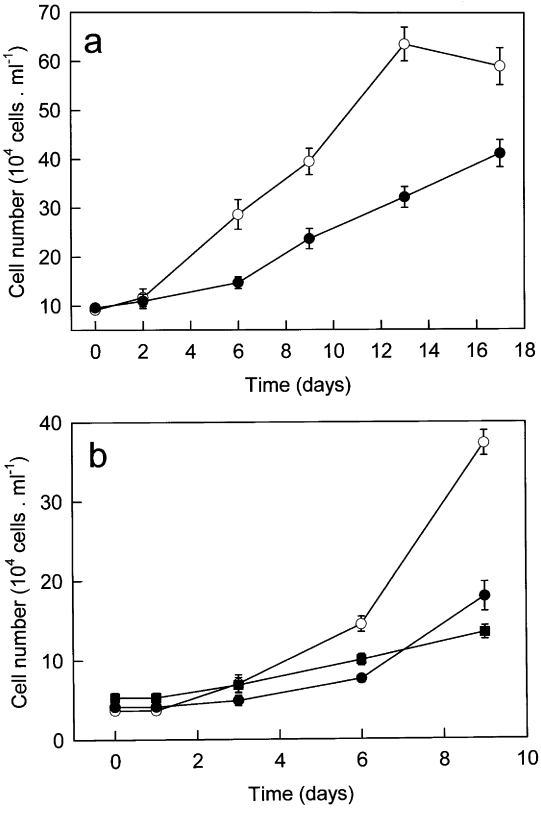

Fig. 2a, b Changes with time in cell densities during the suspension culture of tobacco VBI-0 cells. **a** Delay in the onset of the exponential cell division phase in cells cultured in the presence (*filled circles*) or absence (*open circles*) of NPA (50 μM). **b** Inhibition of cell division in VBI-0 cells grown in the presence of high (*filled circles*; 54 μM NAA plus 45 μM 2,4-D) or normal (*open circles*; 5.4 μM NAA plus 4.5 μM 2,4-D) external auxin concentrations. The effects of NPA (50 μM), also included in this experiment, are shown for comparison (*filled squares*). Values represent arithmetic means ± SE ($n=10$)

ity of the cells to accumulate [^{3}H]NAA (Table 1). However, both accumulation by control cells (no NPA) and the magnitude of the response to NPA changed dramatically with progress of the culture cycle (Fig. 4, Table 1). Maximum levels of accumulation and greatest responses to NPA both occurred in the period 2–5 days after the initiation of the cultures, corresponding to the start of the exponential phase in control cells and the time when NPA had its greatest effect on cell division activity (Fig. 4, Table 1).

Phenotypic effects of NPA

Despite their similar effects in delaying the exponential phase of cell division, the responses to high external auxin concentrations and to NPA treatment differed in an important respect following the resumption of cell division. Following renewed cell division activity, cells exposed to high auxin concentrations gave rise to a normal polar filamentous phenotype by repeated

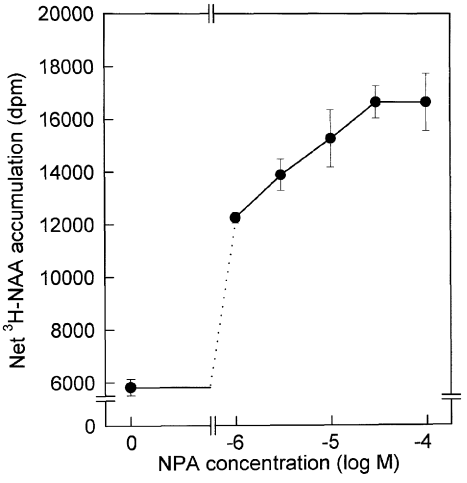

Fig. 3 Effect of concentration of NPA on the net accumulation of [^{3}H]NAA (2 nM) by exponential (6-day-old) suspension-cultured tobacco VBI-0 cells (20 min uptake period). Values represent arithmetic means ± SE ($n=8$)

transverse cell divisions (cf. Fig. 1c, d and Fig. 1i, j). In a substantial proportion of the cells treated with NPA (50 μM), however, the orientation of cell division following recovery was frequently oblique or even longitudinal (Fig. 1f). This sometimes resulted in the formation of cell clumps rather than linear filaments (Fig. 1g).

We have compared the occurrence of longitudinal or oblique cell divisions at a range of NPA concentrations between 0 and 100 μM (Fig. 5). There were no qualitative differences in the appearance of cell clumps arising from abnormal divisions at 10 μM NPA (Fig. 5b), 50 μM NPA (Fig. 1g), and 100 μM NPA. However, the proportion of abnormally aligned cell division axes was lower at 10 μM NPA and increased with increasing NPA concentration (Fig. 5c).

The percentage of occurrence of abnormal cell divisions varied depending on the inoculum density: the proportion of longitudinal or oblique cell divisions was higher at lower inoculum densities (1×10^4–2×10^4 cells ml^{-1}). There was no effect on the phenotype when NPA was applied at the end of the exponential growth phase, i.e. the late NPA application did not influence either cell elongation or the establishment of cell polarity (data not shown).

Discussion

The tobacco cell line VBI-0 possesses several unique characteristics which, together with its good phenotypic stability, makes it an excellent model system for cytological and biochemical studies. These characteristics include a high spontaneous friability (which reduces the tendency of the cells to form clumps in suspension cultures), a filamentous phenotype, polar growth of cells and filaments, and a well-defined temporal separation of cell division and cell elongation phases (Zažímalová et al.

Table 1 Effects of cultivation of VBI-0 cells in the presence of 50 μM NPA on the changes with time in net [^{3}H]NAA accumulation (6 min uptake period in sub-samples of cells collected on the days shown) and on cell densities during the early stages of growth of VBI-0 suspension cultures. Values are arithmetic means ± SE ($n = 10$ for cell densities and $n = 3$ for auxin accumulation). *n.d.* Not detected

Day	Net [^{3}H]NAA accumulation (pmol 10^{-6} cells)			Cell number (10^4 cells ml^{-1})		
	Control	50 μM NPA	Response to NPA (% of control)	Control	50 μM NPA	Response to NPA (% of control)
0	0.16 ± 0.02	0.16 ± 0.02	0	5.18 ± 0.50	5.18 ± 0.50	0
3	5.10 ± 0.32	12.82 ± 0.26	151.4	8.17 ± 0.65	5.52 ± 0.46	67.6
5	0.59 ± 0.26	4.89 ± 0.26	728.8	12.27 ± 1.40	7.71 ± 0.53	62.8
9	n.d.	n.d.	–	37.51 ± 1.90	12.12 ± 0.56	32.3

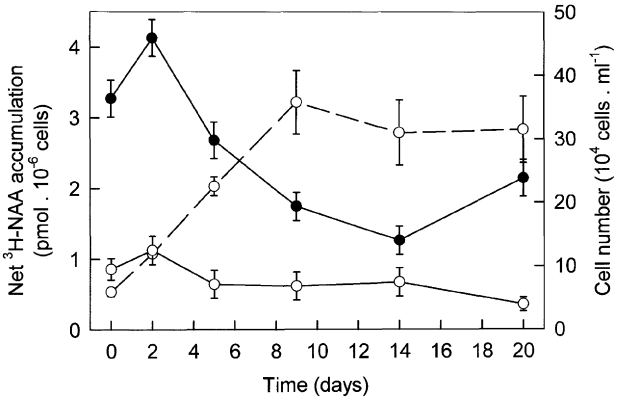

Fig. 4 Changes in rate of accumulation of [^{3}H]NAA (2 nM; 6 min uptake period) during the growth cycle of suspension-cultured tobacco VBI-0 cells, measured in the presence (*filled circles*) or absence (*open circles*) of NPA (50 μM; *unbroken line*). Changes with time in the cell density of control cultures (*open circles*; *broken line*) are shown. Values represent arithmetic means ± SE ($n = 10$ for cell densities and $n = 3$ for auxin accumulation)

1995, 1996; Petrášek et al. 1998). The strain is auxin-dependent and the progress of its growth cycle, including duration of the lag phase, rate of cell division, and duration of the exponential phase, is closely correlated with the particular concentration of auxin in the cultivation medium. The external auxin concentration also has been shown to regulate the concentration of native auxin (IAA) inside the cells (Zažímalová et al. 1995).

In the present study we investigated the effects on cell division and on cell elongation in suspension-cultured VBI-0 cells of manipulating internal auxin concentration by two contrasting methods: firstly, by changing the auxin concentration in the medium in which the cells were cultured (Zažímalová et al. 1995); and secondly, by inhibiting auxin efflux (thereby stimulating net auxin accumulation) by exposing the cells to NPA, a compound which strongly inhibits auxin efflux carrier activity (Rubery 1990; see also Delbarre et al. 1996).

Taken together, the results presented here indicate that there is a critical threshold concentration of internal auxin above which cell division cannot proceed but above which cell elongation can continue or may even be promoted. Thus factors regulating internal auxin concentration, including auxin influx from and efflux to the external medium, may differentially regulate cell elongation and cell division. Furthermore, the data presented in Fig. 4 and Table 1 demonstrate that substantial temporal changes in auxin efflux carrier activity occur during the normal course of the growth cycle in cultured VBI-0 cells. Thus the onset and duration of the exponential and stationary phases of growth in vitro normally may be controlled by the regulation of the activity of auxin carrier systems.

Of particular significance was the observation that treatment of the cells with NPA caused a marked change in their phenotypic behaviour after competency to divide recovered. On the other hand, cells cultured at high external auxin concentrations recovered to produce normal, linear cell filaments. The reasons for these different responses may reside in the mechanism by which NPA inhibits auxin efflux. It is now well established that the half-life of auxin carriers in the plasma membrane is very short (Delbarre et al. 1998; Morris and Robinson 1998; Robinson et al. 1999; Steinman et al. 1999) and that they may cycle rapidly between the plasma membrane and an as yet unidentified endomembrane compartment (Robinson et al. 1999; Geldner et al. 2001, and references therein). Recently it has been reported that the inhibitor of polar auxin transport 2,3,5-triiodobenzoic acid (TIBA; and possibly also NPA – although no details of the latter were presented) prevents the traffic of PIN1 (a putative auxin efflux catalyst) and other rapidly cycled proteins to and from the plasma membrane in *Arabidopsis* root cells (Geldner et al. 2001). Consequently, the inhibition of auxin efflux by auxin transport inhibitors conceivably might be caused by net loss of functional efflux carriers from the plasma membrane, or by other non-specific effects of these compounds on protein traffic, rather than by inhibition of the transport catalytic activity of plasma membrane-located efflux carriers per se. This also might explain why NPA and brefeldin A (an inhibitor of vesicle traffic) mimic each other in their effects on auxin transport (Robinson et al. 1999; Geldner et al. 2001). However, it should be noted that despite the potential importance of the claimed role for

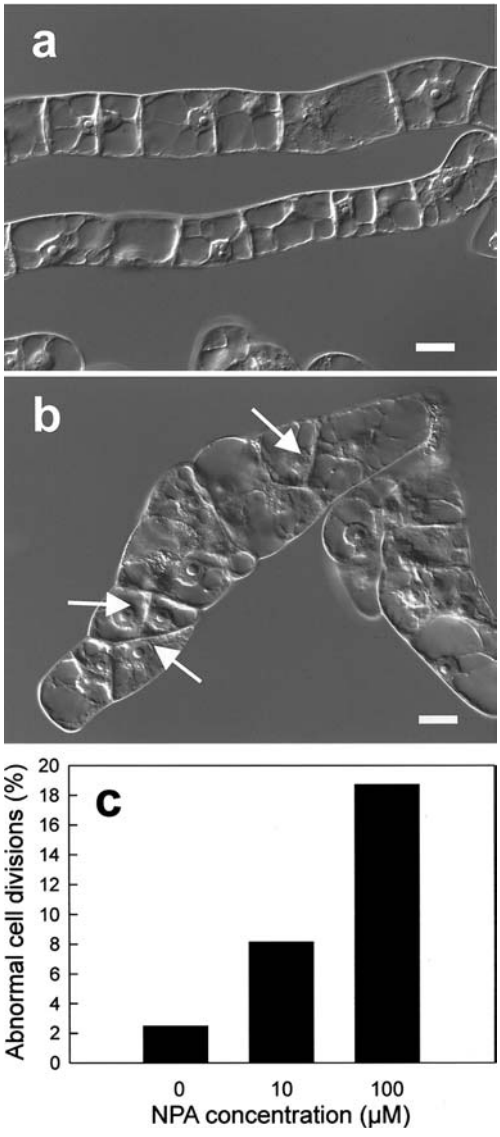

Fig. 5a–c Effects of NPA (10 μM) on phenotype of suspension-cultured tobacco VBI-0 cells. **a** Cells grown in control medium, day 9. **b** Cells grown in control medium supplemented with NPA (10 μM), day 9. Note abnormal cell division planes (*arrows*). Bars in **a** and **b** = 50 μm. **c** Effect of concentration of NPA on the occurrence of abnormal cell divisions at day 9. Standard deviations of the means were less than 10 and 12% of the mean values for control and NPA-treated cells, respectively ($n = 5$; 500 cells per sample)

NPA in inhibiting protein traffic, no experimental data on NPA were shown in the paper by Geldner et al. (2001). Furthermore, the concentration of NPA (200 μM) reported by these authors to be necessary to cause a general perturbation of protein trafficking to and from the plasma membrane is some 2 orders of magnitude greater than that commonly reported to be effective in inhibiting auxin efflux. In the VBI-0 cell line used in our experiments as little as 10^{-6} M NPA caused a substantial (more than 2-fold) increase in the net accumulation of [^{3}H]NAA (Fig. 3). Indeed, given these very high concentrations of NPA, the possibility cannot be excluded that the reported effects of NPA on protein traffic (Geldner et al. 2001) are side effects of high NPA concentrations that are unrelated to the effects of NPA on auxin efflux.

We reported elsewhere (Černá et al. 2002) that whilst treatment with either brefeldin A (20 μM) or NPA (50 μM) results in a very rapid and substantial increase in the rate of [^{3}H]NAA accumulation by suspension-cultured BY-2 tobacco cells, consistent with disruption of efflux carrier activity at the plasma membrane, only brefeldin A affected the arrangement of the actin cytoskeleton, which is believed to be involved in auxin efflux carrier traffic to the plasma membrane (reviewed by Muday and Murphy 2002). Thus, in contrast to the results reported by Geldner et al. (2001), in our hands the concentrations of NPA that induce a marked increase in NAA accumulation by tobacco cells appear not to disrupt actin-dependent efflux carrier protein traffic.

As pointed out by Muday and DeLong (2001), the mechanism of action of NPA on membrane protein cycling remains completely unknown. Thus, the possibility cannot completely be excluded that the changes in cell polarity following NPA treatment may result from more general, but as yet unsubstantiated, effects of NPA on the targeting of rapidly turned-over proteins. However, it is more likely that the observed abnormalities in the planes of cell division and developmental polarity following the NPA treatment resulted from misdirected targeting of auxin efflux carriers themselves to the plasma membrane during the recovery period. If this is true, then it follows that the site-directed traffic of auxin carriers to the plasma membrane may play a crucial role in the regulation of both cell division activity and the establishment of cellular polarity.

Acknowledgements The work was supported by the Grant Agency of the Czech Republic (project No. 206/98/1510), by the EU INCO Copernicus (project No. ERBIC15 CT98 0118) to E.Z. and by grants to D.A.M. from the UK Royal Society and the Academy of Sciences of the Czech Republic under the European Science Exchange Scheme. The authors thank Andrea Hourová for her excellent technical assistance.

References

Bennett MJ, Marchant A, May ST, Swarup R (1998) Going the distance with auxin: unravelling the molecular basis of auxin transport. Philos Trans R Soc Lond Ser B 353:1511–1515

Černá A, Elčkner M, Petrášek J, Schwarzerová K, Opatrný Z, Morris DA, Zažímalová E (2002) Correlated effects of the auxin transport inhibitor NPA and the vesicle-trafficking inhibitor BFA on auxin transport and arrangement of the cytoskeleton in suspension-cultured tobacco cells. In: Abstracts of the Keystone symposium, Specificity and crosstalk in plant signal transduction, Granlibakken resort, Tahoe City, Calif., USA, January 22–27 2002

Delbarre A, Muller P, Imhoff V, Guern, J (1996) Comparison of mechanisms controlling uptake and accumulation of 2,4-dichlorophenoxy acetic acid, naphthalene-1-acetic acid, and indole-3-acetic acid in suspension-cultured tobacco cells. Planta 198:532–541

Delbarre A, Muller P, Guern J (1998) Short-lived and phosphorylated proteins contribute to carrier-mediated efflux, but not influx, of auxin in suspension-cultured tobacco cells. Plant Physiol 116:833–844

Geldner N, Friml J, Stierhof Y-D, Jürgens G, Palme K (2001) Auxin transport inhibitors block PIN1 cycling and vesicle trafficking. Nature 413:425–428

Goldsmith MHM (1977) The polar transport of auxin. Annu Rev Plant Physiol 28:439–478

Hasezawa S, Syono K (1983) Hormonal control of elongation of tobacco cells derived from protoplasts. Plant Cell Physiol 24:127–132

Heller R (1953) Studies on the mineral nutrition of in vitro plant tissue cultures (in French). Ann Sci Nat Bot Biol Veg 14:1–223

Johnson CF, Morris DA (1989) Applicability of the chemiosmotic polar diffusion theory to the transport of indol-3yl-acetic acid in the intact pea plant (*Pisum sativum* L.). Planta 178:242–248

Meyer R, Wolfsleben K (1911) Zur Kenntnis des Naphthoresorcins und des 1.3-Amino-naphthols. Ber Dtsch Chem Ges 44:1958–1966

Morris DA (2000) Transmembrane auxin carrier systems – dynamic regulators of polar auxin transport. Plant Growth Regul 32:161–172

Morris DA, Robinson JS (1998) Targeting of auxin carriers to the plasma membrane: differential effects of brefeldin A on the traffic of auxin uptake and auxin efflux carriers. Planta 205:606–612

Morris DA, Rubery PH, Jarman J, Sabater M (1991) Effects of inhibitors of protein synthesis on transmembrane auxin transport in *Cucurbita pepo* L. hypocotyl segments. J Exp Bot 42:773–783

Muday GK (2000) Interactions between the actin cytoskeleton and an auxin transport protein. In: Staiger CJ, Baluska F, Volkmann D, Barlow P (eds) Actin: a dynamic framework for multiple plant cell functions. Kluwer, Dordrecht, pp 541–556

Muday GK, DeLong A (2001) Polar auxin transport: controlling where and how much. Trends Plant Sci 6:535–542

Muday GK, Murphy AS (2002) An emerging model of auxin transport regulation. Plant Cell 14:293–299

Opatrný Z, Opatrná J (1976) The specificity of the effect of 2,4-D and NAA on the growth, micromorphology, and the occurrence of starch in long-term *Nicotiana tabacum* cell strains. Biol Plant 18:381–400

Petrášek J, Freudenreich A, Heuing A, Opatrný Z, Nick P (1998) Heat-shock protein 90 is associated with microtubules in tobacco cells. Protoplasma 202:161–174

Phillips HJ (1973) Dye exclusion tests for cell viability. In: Kruse PF, Patterson MK (eds) Tissue cultures: methods and application. Chapter 3, Section VIII – Evaluation of culture dynamics. Academic Press, New York, p 406

Raven JA (1975) Transport of indole-3-acetic acid in plant cells in relation to pH and electrical potential gradients, and its significance for polar IAA transport. New Phytol 74:163–172

Robinson JS, Albert AC, Morris DA (1999) Differential effects of brefeldin A and cycloheximide on the activity of auxin efflux carriers in *Cucurbita pepo* L. J Plant Physiol 155:678–684

Rubery PH (1990) Phytotropins: receptors and endogenous ligands. In: Roberts J, Kirk C, Venis M (eds) Hormone perception and signal transduction in animals and plants. Company of Biologists, Cambridge, pp 119–146

Rubery PH, Sheldrake AR (1974) Carrier-mediated auxin transport. Planta 188:101–121

Steinman T, Geldner N, Grebe M, Mangold S, Jackson CL, Paris S, Gälweiler L, Palme K, Jürgens G (1999) Coordinated polar localization of auxin efflux carrier PIN1 by GNOM ARF GEF. Science 286:316–318

Stickens D, Tao W, Verbelen JP (1996) A single cell model system to study hormone signal transduction. Plant Growth Regul 18:149–154

Zažímalová E, Opatrný Z, Březinová A, Eder J (1995) The effect of auxin starvation on the growth of auxin-dependent tobacco cell culture: dynamics of auxin-binding activity and endogenous free IAA content. J Exp Bot 46:1205–1213

Zažímalová E, Březinová A, Holík J, Opatrný Z (1996) Partial auxin deprivation affects endogenous cytokinins in an auxin-dependent, cytokinin-independent tobacco cell strain. Plant Cell Rep 16:76–79

CHAPTER 3

Do Phytotropins Inhibit Auxin Efflux by Impairing Vesicle Traffic?

Jan Petrášek, Adriana Černá, Kateřina Schwarzerová, Miroslav Elčkner, David A. Morris, Eva Zažímalová

Plant Physiology 131, 254-263, 2003

This chapter is the continuation of our work aiming to explain the mechanism of action of phytotropins and how they regulate cell division polarity. We have compared the effect of phytotropin 1-*N*-naphthylphthalamic acid (NPA) and vesicle trafficking inhibitor brefeldin A (BFA) on both auxin transport and cellular structures (cytoskeleton, endoplasmic reticulum) in tobacco BY-2 cells. Both these compounds strongly decreased auxin efflux, but BFA in contrast to NPA had substantial structural impact on actin cytoskeleton and membranes of endoplasmic reticulum. This, together with concentration relationships, suggests that NPA and perhaps other phytotropins have very specific effect on putative auxin efflux carrier activity rather than they generally inhibit vesicle-mediated protein traffic to the plasma membrane.

My contribution to this article was in the preparation and cultivation of plant material, determination of its growth characteristics, image analysis, *in vivo* time-lapse microscopy, auxin-accumulation assays, processing and interpretation of all measured data and in the writing and editing of the manuscript text and figures.

Adriana Černá as a diploma student of Eva Zažímalová was included under my co-supervision in the visualization of actin filaments and microtubules and drug treatments. Kateřina Schwarzerová transformed BY-2 cells and Miroslav Elčkner participated on auxin-accumulation assays and preparation of experimental material. Eva Zažímalová (corresponding author) and David Morris were involved in auxin-accumulation experiments, performed thin layer chromatography of labelled compounds and wrote and edited the manuscript.

This work was supported by the European Union, International Cooperation Copernicus (grant no. ERBIC15 CT98 0118 to Eva Zažímalová), by the Ministry of Education, Youth, and Sports of the Czech Republic (project no. LN00A081) and by the UK Royal Society and the Academy of Sciences of the Czech Republic under the European Science Exchange Scheme (grant to David A. Morris).

Do Phytotropins Inhibit Auxin Efflux by Impairing Vesicle Traffic?[1]

Jan Petrášek, Adriana Černá, Kateřina Schwarzerová, Miroslav Elčkner, David A. Morris[2], and Eva Zažímalová*

Institute of Experimental Botany, The Academy of Sciences of the Czech Republic, Rozvojová 135, CZ–16502 Prague 6, Czech Republic (J.P., M.E., D.A.M., E.Z.); and Department of Plant Physiology, Faculty of Science, Charles University, Viničná, CZ–12844 Prague 2, Czech Republic (J.P., A.Č., K.S.)

Phytotropins such as 1-*N*-naphthylphthalamic acid (NPA) strongly inhibit auxin efflux, but the mechanism of this inhibition remains unknown. Auxin efflux is also strongly decreased by the vesicle trafficking inhibitor brefeldin A (BFA). Using suspension-cultured interphase cells of the BY-2 tobacco (*Nicotiana tabacum* L. cv Bright-Yellow 2) cell line, we compared the effects of NPA and BFA on auxin accumulation and on the arrangement of the cytoskeleton and endoplasmic reticulum (ER). The inhibition of auxin efflux (stimulation of net accumulation) by both NPA and BFA occurred rapidly with no measurable lag. NPA had no observable effect on the arrangement of microtubules, actin filaments, or ER. Thus, its inhibitory effect on auxin efflux was not mediated by perturbation of the cytoskeletal system and ER. BFA, however, caused substantial alterations to the arrangement of actin filaments and ER, including a characteristic accumulation of actin in the perinuclear cytoplasm. Even at saturating concentrations, NPA inhibited net auxin efflux far more effectively than did BFA. Therefore, a proportion of the NPA-sensitive auxin efflux carriers may be protected from the action of BFA. Maximum inhibition of auxin efflux occurred at concentrations of NPA substantially below those previously reported to be necessary to perturb vesicle trafficking. We found no evidence to support recent suggestions that the action of auxin transport inhibitors is mediated by a general inhibition of vesicle-mediated protein traffic to the plasma membrane.

The polar transport of auxins (such as indole-3-acetic acid [IAA]) plays a crucial role in the regulation of growth and development in plants (Davies, 1995). Much experimental evidence supports the proposal by Rubery and Sheldrake (1974) and Raven (1975) that auxin transport polarity results from the differential permeabilities of each end of transporting cells to auxin anions (IAA^-) and undissociated auxin molecules (IAA; for review, see Goldsmith, 1977). IAA (a weak organic acid) is relatively lipophilic and can readily enter cells by diffusion from the more acidic extracellular space; the IAA^- anion, on the other hand, is hydrophilic and does not cross membranes easily. As a consequence, auxins tend to accumulate in plant cells by a process of "anion trapping" and exit the symplast with the intervention of transmembrane auxin anion efflux carriers (Goldsmith, 1977). There is now overwhelming evidence that the differential efflux of IAA^- anions from the two ends of auxin-transporting cells results from an asymmetric (polar) distribution of such carriers (Goldsmith, 1977; Lomax et al., 1995). Genes encoding putative auxin influx and efflux carriers have been identified from Arabidopsis and other species (for review, see Morris, 2000; Muday and DeLong, 2001; Friml and Palme, 2002). It has been shown that efflux carrier proteins, encoded by members of the *PIN* (*PIN-FORMED*) gene family, and possibly influx carriers (encoded by *AUX1*), are targeted to specific regions of the plasma membrane (PM) in auxin-transporting cells (Bennett et al., 1996; Gälweiler et al., 1998; Müller et al., 1998; Swarup et al., 2001; for review, see Friml and Palme, 2002).

Studies employing specific inhibitors of components of the polar auxin transport process have played a major role in shaping our understanding of the polar auxin transport machinery. The most widely used inhibitor of auxin efflux is 1-*N*-naphthylphthalamic acid (NPA), a well-characterized member of a group of inhibitors known as phytotropins (Katekar and Geissler, 1980; Rubery, 1990). The application of NPA to various plant tissues results in the inhibition of auxin efflux carrier activity and, as a consequence, increases auxin accumulation in cells (for review, see Morris, 2000). Although the mechanism of its inhibitory action on polar auxin transport remains obscure, it seems to be mediated by a specific, high affinity, NPA-binding protein (NBP; Sussman and Gardner, 1980; Rubery, 1990). Observations on zuc-

[1] This work was supported by the European Union, International Cooperation Copernicus (grant no. ERBIC15 CT98 0118 to E.Z.); by the Ministry of Education, Youth, and Sports of the Czech Republic (project no. LN00A081); and by the UK Royal Society and the Academy of Sciences of the Czech Republic under the European Science Exchange Scheme (grant to D.A.M.).

[2] Present address: Division of Cell Sciences, School of Biological Sciences, University of Southampton, Bassett Crescent East, Southampton SO16 7PX, UK.

* Corresponding author; e-mail eva.zazim@ueb.cas.cz; fax 420–220390–474.

Article, publication date, and citation information can be found at www.plantphysiol.org/cgi/doi/10.1104/pp.012740.

chini (*Cucurbita pepo*) hypocotyl cells have shown that the NBP is probably a peripheral membrane protein located on the cytoplasmic face of the PM and associated with the cytoskeleton (Cox and Muday, 1994; Dixon et al., 1996; Butler et al., 1998; but compare with Bernasconi et al., 1996). Protein synthesis inhibitors such as cycloheximide (CH) rapidly uncouple carrier-mediated auxin efflux and the inhibition of efflux by NPA (Morris et al., 1991). In the short term, however, CH has no effect on either the specific and saturable binding of NPA or on auxin efflux itself, suggesting that the NBP and the efflux catalyst may interact through a third, rapidly turned over protein (Morris et al., 1991; for discussion, see Morris, 2000; Luschnig, 2001). Although the identity of the NBP and its mechanism of action on auxin efflux carriers remain unknown, the Arabidopsis *tir3* (*transport inhibitor response 3*) mutant exhibits a reduced number of NPA-binding sites and a reduction in polar auxin transport (Ruegger et al., 1997). Thus, *TIR3* (renamed *BIG* by Gil et al., 2001, to reflect the unusually large size—566 kD—of the protein it encodes) may code for an NBP or may be required for NBP expression, localization, or stabilization (for discussion see Gil et al., 2001; Luschnig, 2001).

In addition to polar auxin transport inhibitors, drugs that inhibit Golgi-mediated vesicle traffic, such as brefeldin A (BFA) and monensin, also very rapidly inhibit auxin efflux carrier activity in zucchini hypocotyl tissue (Wilkinson and Morris, 1994; Morris and Robinson, 1998), and in suspension-cultured tobacco (*Nicotiana tabacum* L. cv Xanthi XHFD8) cells (Delbarre et al., 1998). They also inhibit polar auxin transport through tissue (Robinson et al., 1999). However, the time lag for inhibition of efflux carrier activity by BFA (minutes) is considerably shorter than the lag for inhibition of efflux activity by protein synthesis inhibitors (up to 2 h; Morris et al., 1991). This implies that efflux catalysts turn over very rapidly in the PM without a requirement for concurrent protein synthesis, a situation that contrasts sharply with the inhibitory action of NPA on auxin efflux, which does require concurrent protein synthesis (see above). Results of a detailed comparison of the effects of CH and BFA on efflux carrier activity revealed that efflux carrier proteins probably cycle between the PM and an unidentified intracellular compartment (Robinson et al., 1999; compare with Delbarre et al., 1998). This possibility has been strongly supported by the observation that AtPIN1, a member of a family of putative Arabidopsis auxin efflux carrier proteins (see Friml and Palme, 2002), is rapidly and reversibly internalized after BFA treatment of Arabidopsis roots (Geldner et al., 2001).

A link has been suggested recently between the inhibitory action of polar auxin transport inhibitors on auxin efflux and their inhibitory effects on the actin-dependent vesicle trafficking and cycling of efflux carrier proteins (Geldner et al., 2001). Treatment of Arabidopsis roots with the auxin transport inhibitor 2,3,5-triiodobenzoic acid (TIBA) prevented the BFA-induced internalization of the putative auxin efflux carrier AtPIN1 and prevented the traffic of internalized PIN1 to the PM after BFA washout. This would have the effect of reducing the density of carriers in the PM available for auxin efflux. The authors found similar effects of TIBA on a rapidly turned-over PM-ATPase and the *KNOLLE* gene product (a syntaxin involved in vesicle docking; see Muday and Murphy, 2002). As a consequence, a rather general action of auxin transport inhibitors on membrane-trafficking processes was suggested, rather than a specific effect on auxin efflux carriers (Geldner et al., 2001).

The site-directed traffic of auxin efflux carrier proteins involves not only the Golgi-mediated secretory system itself, but also the participation of components of the cytoskeletal system. The application of cytochalasin (an actin-depolymerizing agent) reduced polar auxin transport in maize (*Zea mays*) coleoptiles (Cande et al., 1973) and in zucchini hypocotyls (Butler et al., 1998). Moreover, cytochalasin D has been shown recently to block the cycling of PIN1 between endosomal compartments and the PM in Arabidopsis roots (Geldner et al., 2001). These observations are consistent with an important role for actin filaments (AFs) in the proper localization and function of components of the auxin efflux carrier complex (for review, see Muday, 2000; Muday and Murphy, 2002). Evidence from a careful in vitro biochemical analysis of the association between the NBP and the cytoskeleton in membrane preparations from zucchini hypocotyls indicates a strong link between NPA action and the actin cytoskeleton (Butler et al., 1998). Only treatments that stabilized F-actin (phalloidin), but not those that stabilized microtubules (MTs; taxol), increased NPA-binding activity. Furthermore, direct interaction between the high-affinity NBP and F-actin was proven by F-actin affinity chromatography in the same system (Hu et al., 2000).

The processes that regulate the cycling of the efflux carrier proteins and that direct their traffic to specific areas of the PM remain unknown, although recent observations are beginning to provide insights into possible mechanisms. Gil et al. (2001) have reported that *tir3* (see above) and *doc1* (*dark overexpression of CAB*; Li et al., 1994) are allelic mutants of a gene (*BIG*) that has significant identity with the *CAL/O* (*CALOSSIN/PUSHOVER*) gene. The product of *CAL/O* is involved in the regulation of synaptic vesicle cycling in *Drosophila melanogaster* (Richards et al., 1996). BIG (TIR3) is required for normal auxin transport in plants and is probably associated with the actin cytoskeleton (Cox and Muday, 1994; Butler et al., 1998). Because the cycling of putative auxin efflux carrier proteins involves BFA-sensitive and actin-dependent vesicle traffic to the PM (Geldner et al., 2001), BIG

may play a similar role in plants to that of CAL/O in *D. melanogaster*, and regulate this directed vesicle traffic.

The observations discussed above associate the inhibition of auxin efflux carrier activity by NPA with effects of the compound on actin-dependent and Golgi vesicle-mediated targeting of efflux carrier protein to the PM. Nevertheless, almost nothing is known about the effects (if any) of NPA or other phytotropins on the organization of components of the cytoskeleton or on the vesicle secretory system. Given the possibility that phytotropins might have a general effect on vesicle traffic to the PM and on the cycling of proteins between the PM and endosomal compartments (as suggested by Geldner et al., 2001; but see "Discussion"), some physical disruption of the secretory pathway and/or cytoskeleton might be expected to occur after the application of these compounds. However, to the best of our knowledge, no such disruption has been reported so far.

Here, we report an investigation to compare the action of BFA and NPA on both auxin accumulation and on the arrangement and structure of components of the secretory pathway and the cytoskeleton (AFs, MTs, and endoplasmic reticulum [ER]) in suspension-cultured BY-2 tobacco cells. Using a new quantitative method to study the rearrangement of AFs and the formation of actin clusters in the perinuclear region of cells, we show that although both of these compounds increase auxin accumulation by inhibiting auxin efflux, only BFA has an effect on the structure of AFs and the ER. Our observations lead us to suggest that although radial and perinuclear (but possibly not cortical) AFs and ER are required for normal auxin efflux, the inhibitory action of NPA on efflux does not involve any changes in the cytoskeleton and ER.

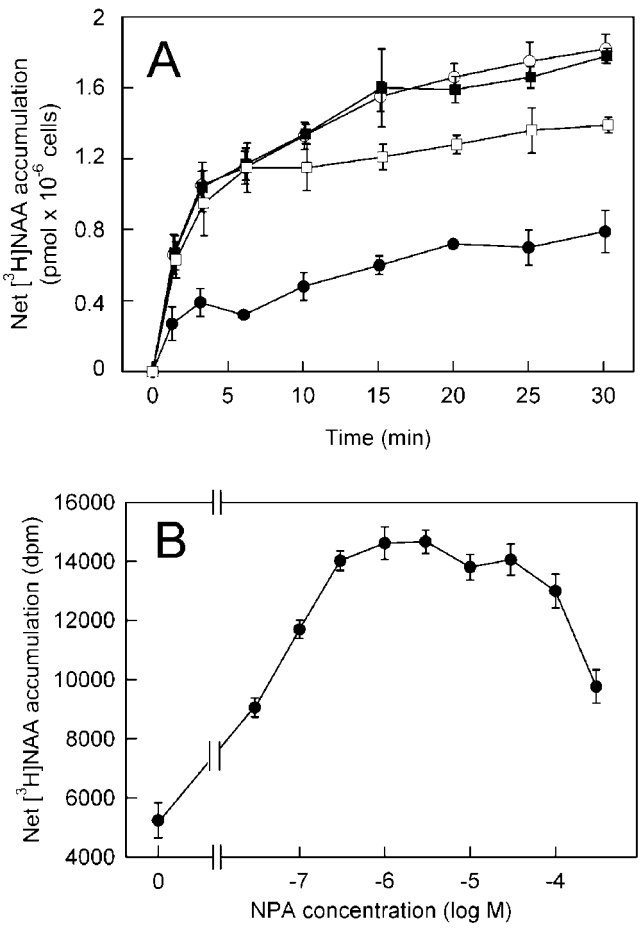

Figure 1. The effect of NPA on the net accumulation of [^{3}H]NAA (2 nM) in 2-d-old BY-2 cells. A, Time course of net [^{3}H]NAA accumulation in the absence (●, control) and in the presence of 10 μM (○), 50 μM (■), and 200 μM (□) NPA. Error bars = SEs of the mean (n = 3). B, The effect of concentration of NPA on net [^{3}H]NAA accumulation, measured over 20 min, by 2-d-old BY-2 cells. Results expressed as mean radioactivity per 0.5 mL of cell suspension (cell density 7×10^5 cells mL^{-1}). Error bars = SEs of the mean (n = 4).

RESULTS

Effects of NPA and BFA on the Accumulation of Auxin

The rate of [^{3}H]-labeled naphthalene-1-acetic acid ([^{3}H]NAA) accumulation by BY-2 cells is shown in Figures 1A and 2A. After an initial period of rapid uptake lasting 3 to 10 min depending on experiment, uptake settled to a slower, steady rate that was maintained for up to 40 min. Accumulation was extremely sensitive to NPA and was stimulated approximately 3-fold in the presence of 10 or 50 μM NPA (Fig. 1A). An NPA concentration dependence study indicated that [^{3}H]NAA accumulation was maximally stimulated by as little as 1.0 μM NPA and that the stimulatory effect of NPA began to decline rapidly at concentrations around or greater than 100 μM (Fig. 1B). Because of the greatly reduced stimulation of [^{3}H]NAA accumulation at high concentrations of NPA, possibly caused by toxic side effects not directly related to auxin efflux, the maximum concentration of NPA employed in subsequent cytological observations was restricted to 50 μM.

A similar picture emerged in the case of BFA (Fig. 2), although the maximum stimulation of [^{3}H]NAA accumulation (at between 10 and 40 μM BFA) was lower than that caused by NPA (compare Figs. 1A with 2A, and 1B with 2B). As with NPA, high concentrations of BFA (100 μM) reduced the stimulation of [^{3}H]NAA accumulation (Fig. 2B).

Over the uptake period used here, no significant metabolism of [^{3}H]NAA by BY-2 cells was detected. Apart from a small amount of label that remained at the origin in all chromatography solvents used (less than 10% of the total label recovered), the recovered ethanol-soluble radioactivity migrated as a single spot that had the same mobility on cellulose thin-layer plates as authentic [^{3}H]NAA (data not shown).

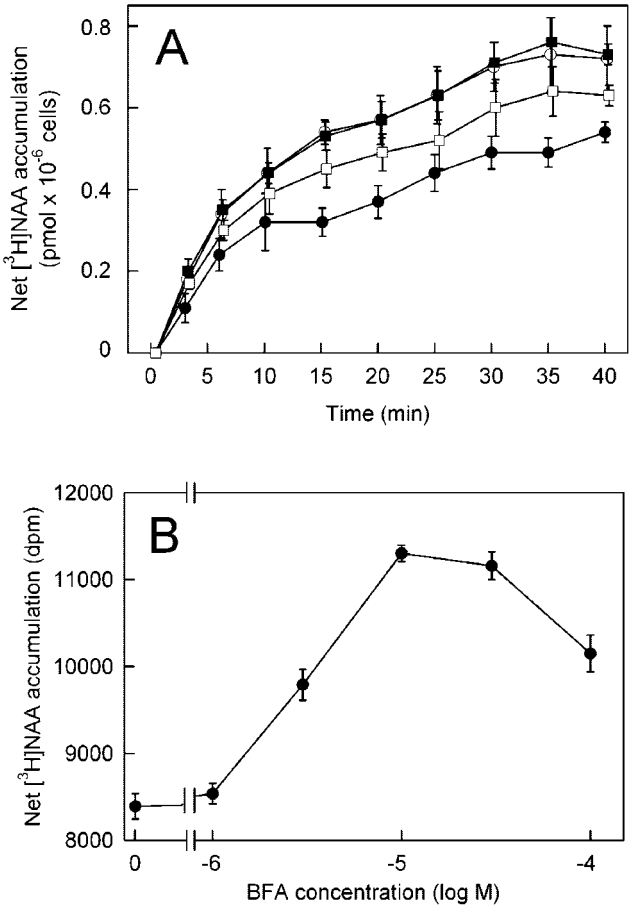

Figure 2. The effect of BFA on the net accumulation of [^{3}H]NAA (2 nM) in 2-d-old BY-2 cells. A, Time course of net [^{3}H]NAA accumulation in the absence (●, control) and in the presence of 20 μM (○), 40 μM (■), and 100 μM (□) BFA. Error bars = SEs of the mean (n = 3). B, The effect of concentration of BFA on net [^{3}H]NAA accumulation, measured over 20 min, by 2-d-old BY-2 cells. Results expressed as mean radioactivity per 0.5 mL of cell suspension (cell density 7×10^5 cells mL^{-1}). Error bars = SEs of the mean (n = 4).

Effects of BFA and NPA on AFs and MTs

To test the reaction of the cytoskeleton to the application of agents that modify polar auxin transport, the arrangement of both AFs and MTs in BFA- and NPA-treated cells was studied during a 30-min incubation period in parallel with the auxin accumulation measurements described above. Because the cell populations used to measure auxin accumulation were predominantly in interphase, we investigated the arrangement of the interphase cytoskeleton (MTs and AFs in the cortical cytoplasm and AFs in the transvacuolar strands and perinuclear region). Typical interphase BY-2 tobacco cells contained fine and transversally oriented AFs (Fig. 3A) and MTs (Fig. 3G) in the cortical cytoplasm, together with radially oriented AFs in transvacuolar strands and in the perinuclear region (Fig. 3D). There were no MTs in transvacuolar strands and around the nucleus in interphase cells (Fig. 3G). Although both NPA and BFA significantly increased auxin accumulation (Figs. 1 and 2), their effects on cytoskeleton arrangement differed considerably. Although the fine cortical AFs and MTs retained their transverse orientation after a 30-min treatment with 20 μM BFA (Fig. 3, B and H), BFA had a dramatic effect on the arrangement of the radial and perinuclear AFs (Fig. 3E). Fine AFs in the transvacuolar strands collapsed and actin became concentrated in clusters around the nucleus (Fig. 3E).

We have developed a simple procedure for the evaluation of quantitative changes in actin aggregation in the perinuclear region, utilizing image analysis software. This method is based on the fact that relative fluorescence intensities of regions with aggregated actin are very different from the background fluorescence intensities. Thus, aggregation of actin increases the degree of variation in fluorescence intensities of individual pixels in the area of interest. Full details of the procedure are described in "Materials and Methods" (see also Fig. 4). This procedure was used to evaluate the effects of BFA and it was shown that the degree of actin aggregation noticeably increased with duration of treatment (Fig. 4E). The highest BFA concentration tested (100 μM) was shown to be inhibitory for actin aggregation in the same way that it was inhibitory for auxin accumula-

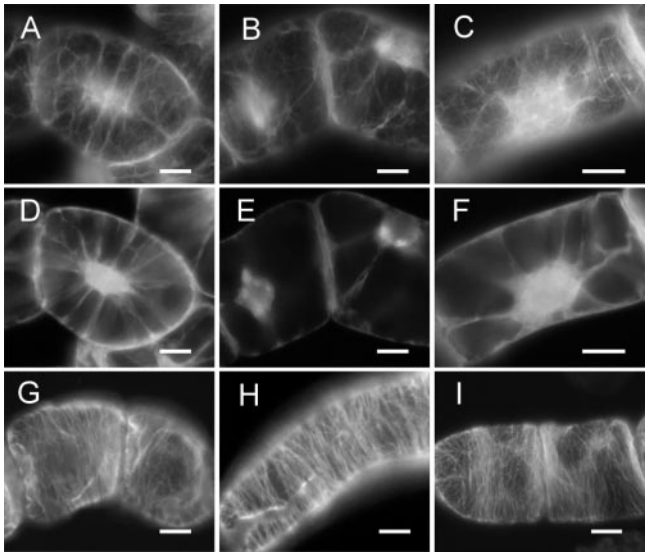

Figure 3. The effect of BFA and NPA on the arrangement of AFs and MTs in 2-d-old BY-2 cells. Control cells with fine AFs in the cortical region (A), radially oriented AFs in transvacuolar strands (D), and transversely oriented cortical MTs (G). B, E, and H, AFs and cortical MTs after 30-min incubation in 20 μM BFA. Modification of AFs staining pattern in cortical (B) and perinuclear region (E), where AFs in transvacuolar strands are "pulled down," forming clusters around the nucleus. H, Unaffected arrangement of cortical MTs. C, F, and I, AFs and cortical MTs after 30-min incubation in 50 μM NPA. Unaltered AFs staining pattern in the cortical (C) and perinuclear region (F). I, Transversally oriented cortical MTs with no obvious changes. Each image is representative of cells in the treatment specified. Approximately 1,000 cells per treatment were examined. Scale bars = 10 μm.

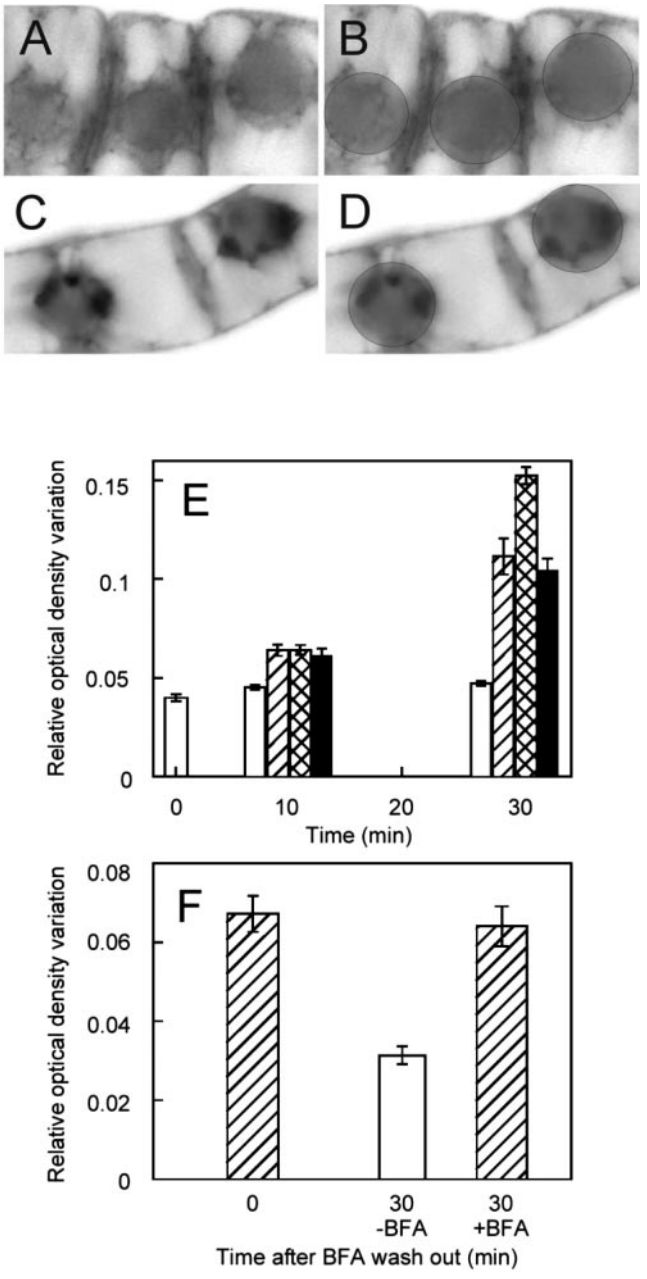

Figure 4. The quantification of BFA effect on AFs. Grabbed images of tetramethylrhodamine B isothiocyanate (TRITC)-phalloidin-stained control (A) and BFA-treated cells (C) after transformation to complementary colors. B and D, Interactively applied circular measuring frame over the perinuclear region for the measurement of the relative optical density variation (ODV) parameter. See "Materials and Methods" for details. E, Relative ODV in control (white columns) and in the presence of 20 μM (shaded columns), 40 μM (checked columns), and 100 μM (black columns) BFA. F, Relative ODV after 30-min incubation in 20 μM BFA (time 0 min, shaded column) and after washout and subsequent 30-min incubation in fresh medium without BFA (time 30 min, white column) and in the presence of 20 μM BFA in the medium (time 30 min, shaded column). Error bars = SES of the mean (n = 10 optical fields, 30 cells assessed in each).

tion (compare Fig. 4E with 2B). The effect of BFA on AFs was reversible and 30 min after washout of BFA with fresh medium, the actin clusters disappeared and the ODV parameter decreased again to control values (Fig. 4F).

In contrast to BFA, 30 min of incubation in 50 μM NPA did not cause any changes in the arrangement of AFs in cortical region (Fig. 3C; compare with Fig. 3, A and B) as well as around the nucleus and in the transvacuolar strands (Fig. 3F; compare with Fig. 3, D and E). Correspondingly, cortical MTs were also unaffected after 30 min in 50 μM NPA (Fig. 3I; compare with Fig. 3, G and H).

The Effect of BFA and NPA on the ER

In addition to the Golgi apparatus, the plant ER has also been shown to be sensitive to BFA treatment (Henderson et al., 1994). Therefore, we investigated if the ER was also affected in cells in which BFA or NPA stimulated the accumulation of auxin. The behavior of ER in interphase cells of BY-2 after NPA or BFA treatment was followed in vivo using cells transformed with the pBIN *m-gfp5*-ER plant binary vector coding for the ER-localized fusion protein (mGFP5-ER). In exponentially growing control interphase cells, ER was present in the form of a tubular network penetrating not only the cortical layer of cytoplasm (Fig. 5A), but also the transvacuolar strands and perinuclear region (Fig. 5D). Within this network, small motile bodies were observed (video sequence can be seen at http://www.ueb.cas.cz/laboratory_of_hormonal_regulations/BFAmovies.htm). The movement of these bodies was observed over the surface of the network of ER tubules that constantly changed its orientation and pattern. Treatment of cells with 20 μM BFA for 30 min resulted in disintegration of the fine tubular network of ER, the formation of large sheets of ER, and the aggregation of the signal into a large number of bright fluorescent spots (Fig. 5B; video sequence can be seen at http://www.ueb.cas.cz/laboratory_of_hormonal_regulations/BFAmovies.htm). However, the first observable effects of BFA were clear after only 5 min (data not shown), when disintegration of the tubular network and formation of fluorescent spots started. On the other hand, even after 30 min of 20 μM BFA treatment, there were still cells with no obvious damage of ER. The accumulation of GFP fluorescence was also observed in the perinuclear region (Fig. 5E). Moreover, the movement of small motile bodies inside ER tubules decreased during a 30-min incubation in 20 μM BFA and had almost stopped by the end of that time period. Longer treatment with 20 μM BFA (7 h) resulted in the formation of large sheets of ER and intensively fluorescing bodies of irregular shape and size (data not shown).

In contrast to BFA, a 30-min incubation in 50 μM NPA had no observable effects on either ER structure

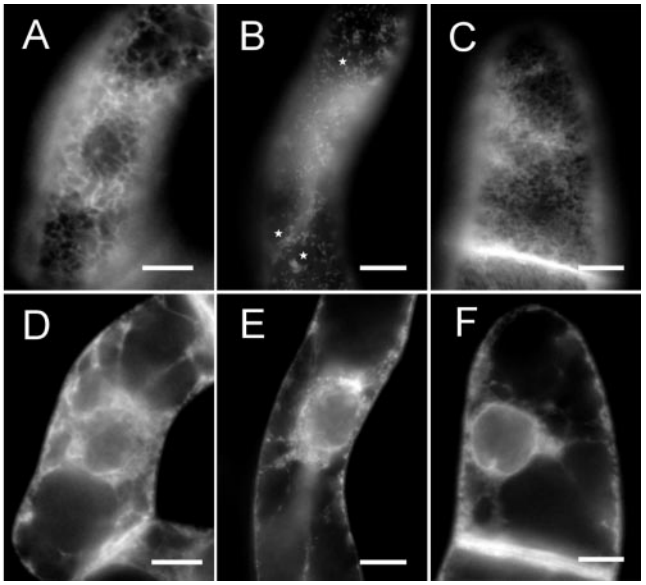

Figure 5. The effect of BFA and NPA on the arrangement of ER in 2-d-old BY-2 cells expressing mGFP5-ER. A and D, Green fluorescent protein (GFP) fluorescence in control cells. Optical cuts through cortical region (A) and perinuclear region (D). B and E, GFP fluorescence in cells after 30-min incubation in 20 μM BFA. The formation of bright fluorescent spots (B) and large sheets (B, asterisks) in the cortical layer are shown. Bright fluorescent spots in transvacuolar strands and in the perinuclear region (E). Video files showing control cells and the effect of 30-min incubation in 20 μM BFA can be seen at http://www.ueb.cas.cz/laboratory_of_hormonal_regulations/BFAmovies.htm. C and F, GFP fluorescence in cells after 30-min incubation in 50 μM NPA. Unaltered ER in the cortical (C) and perinuclear region (F). Bars = 10 μm.

or arrangement (Fig. 5, C and F); furthermore, no changes in the movement of small bodies were found.

The effects of both NPA and BFA on the cell structures examined and on auxin accumulation are summarized in Table I.

DISCUSSION

The Actions of NPA and BFA on Auxin Accumulation Differ

In suspension-cultured tobacco cells, NAA accumulation (inhibition of efflux) is controlled predominantly by the activity of NPA-sensitive auxin efflux carriers (Delbarre et al., 1996). Our results reveal a major discrepancy between the concentration of NPA required to saturate the inhibition of auxin efflux (1 μM) and those reported to be necessary to inhibit either the BFA-sensitive cycling of PIN1 between the PM and an internal compartment (200 μM; Geldner et al., 2001), or PIN1 internalization in the *tir3* mutant of *BIG* (150 μM; Gil et al., 2001). These observations suggest that the stimulation of NAA accumulation in tobacco cells by NPA (Delbarre et al., 1996; Petrášek et al., 2002; this report) is unlikely to have resulted from perturbation of efflux carrier cycling. We show here that in suspension-cultured cells of BY-2 tobacco, the stimulation of NAA accumulation by NPA was markedly reversed at concentrations of NPA around 10 to 30 μM. In another tobacco cell line (VBI-0), although high concentrations of NPA (up to at least 100 μM) did not cause such a reversal, abnormalities in cell division and loss of cell polarity occurred at concentrations of NPA even as low as 10 μM (Petrášek et al., 2002). Therefore, at concentrations of NPA not much greater than those necessary to saturate auxin accumulation, both cell behavior and auxin transport may be perturbed by mechanisms that have nothing to do with the specific effects of NPA on the auxin efflux machinery.

The inhibitory effect of NPA on auxin efflux is extremely rapid. In the suspension-cultured tobacco cells used in our experiments, the stimulation of NAA accumulation by NPA occurred without measurable time lag. This indicates that in cell suspensions, in which NPA would be expected to reach binding sites very rapidly, the inhibitory effect of the compound on auxin efflux carrier activity is very fast. This rapid response contrasts with the rather long treatment periods used in the experiments of Geldner et al. (2001; 2 h) and of Gil et al. (2001; 3 h) to study the effects of NPA and BFA on PIN1 cycling and localization. Unfortunately, no information on the kinetics of the inhibitory effect of NPA on efflux carrier cycling was provided.

Consistent with its reported inhibitory effect on efflux carrier traffic to the PM (Delbarre et al., 1998; Morris and Robinson, 1998; Robinson et al., 1999; Geldner et al., 2001; see introduction), BFA also strongly promoted NAA accumulation by BY-2 cells in a concentration-dependent manner. However, as with NPA, high concentrations of BFA (above 30 μM) reversed the stimulation of auxin accumulation. This biphasic response is correlated with the action of BFA on the actin cytoskeleton (discussed below). In the cell suspensions used in our experiments, the maximum stimulation of NAA accumulation observed (22.7% after 20 min at 10 μM BFA) was substantially less than the maximum stimulation caused by NPA treatment (130.2% after 20 min at 1 μM). These results imply that although BFA may be effective in inhibiting membrane vesicle cycling, even under conditions where the response to BFA is maximal, a small proportion of carrier proteins continues to catalyze auxin efflux across the PM. Evidence for this possibility comes from the results of Geldner et al. (2001). These

Table I. *Summary of the effects of NPA (10–200 μM) and BFA (20–100 μM) on cell structures and auxin accumulation in suspension-cultured 2-d-old BY-2 tobacco cells*

Compound	Microtubules	Actin Filaments	Endoplasmic Reticulum	Auxin Accumulation
NPA	–[a]	–	–	+[b]
BFA	–	+	+	+

[a]–, No differences from control observed. [b]+, Structure affected and/or auxin accumulation increased.

authors demonstrated that treatment of Arabidopsis seedling roots with 50 μM BFA for 2 h resulted in internalization of PIN1. However, close examination of their Figure 1B illustrating this result (Geldner et al., 2001) suggests appreciable residual fluorescence in the PM from PIN1 markers.

BFA But Not NPA Affects the Cytoskeleton

Although a role for the cytoskeleton in polar auxin transport has been established (for review, see Muday, 2000), only few data are available on the state of AFs and MTs after disruption of polar auxin transport with inhibitors. Thus, we compared the effects of NPA and BFA on the arrangement and structure of the cytoskeleton under the same conditions as those used to study the effects of these compounds on NAA accumulation. In agreement with Saint-Jore et al. (2002), who reported that treatment of BY-2 cells with BFA did not affect cortical MTs and AFs, we also found no effect of BFA on cortical cytoskeletal components. However, in the perinuclear region we found that BFA caused actin to form prominent clusters. To our knowledge, this is the first report of this phenomenon in plants.

The lack of information about perinuclear actin possibly stems from the fact that most previous studies have concentrated on AFs in the cortical layer of cytoplasm, and the perinuclear region has largely been overlooked (compare with Satiat-Jeunemaitre et al., 1996; Saint-Jore et al., 2002). Recently, Waller et al. (2002) reported an increased membrane association of cortical actin and bundling of cortical AFs in maize epidermal cells after BFA treatment. This suggests that under some circumstances, even cortical actin can be modified by treatment with BFA. Because phalloidin (used here for actin cytoskeleton visualization) binds preferentially to F-actin, it is likely that the newly formed actin clusters produced in the perinuclear region consist of the filamentous form of actin. A possible explanation for the formation of the perinuclear actin clusters is that actin may play a role in the process of ER-Golgi apparatus fusion after BFA treatment (compare with Ritzenthaler et al., 2002).

The quantitative image analysis showed that perinuclear actin cluster formation increased with increasing concentrations of BFA up to 40 μM but declined substantially with further increase in BFA concentrations to 100 μM. A possible interpretation is that at high concentrations of BFA, the ER-Golgi hybrid compartment (Ritzenthaler et al., 2002) is not formed. As a consequence, AFs are unable to reorganize into clusters. The reduction in actin cluster formation at high BFA concentrations correlates with the reduced stimulation of NAA accumulation under the same conditions. One possibility is that the two processes are functionally connected.

In contrast to BFA, the phytotropin NPA did not cause any changes in the arrangement of either MTs or AFs at concentrations that clearly inhibit NAA transport. The lack of effect on the arrangement of MTs is consistent with similar observations by Hasenstein et al. (1999) on maize root cells, who found that the inhibition of auxin transport by NPA was not accompanied by changes in the orientation of cortical MTs. Several reports strongly point to an association of the NBP and F-AFs (Cox and Muday, 1994; Butler et al., 1998; Hu et al., 2000). Although this association seems essential for the inhibitory action of NPA on auxin efflux, the binding of NPA to the NBP appears not to disrupt the association of the NBP with the actin cytoskeleton (Hu et al., 2000; this report). Thus, we conclude that the inhibitory action of NPA on auxin efflux from plant cells is not associated with disruption of the cytoskeletal system.

BFA But Not NPA Affects the ER

To follow possible mechanisms underlying the changes in perinuclear actin organization, we also investigated the structure of ER in interphase BY-2 cells. Using cells expressing a fusion protein containing GFP and ER-signaling and ER-retention amino acid (His-Asp-Glu-Leu, HDEL) sequences, both mobile particles and a static polygonal network of tubules were observed as reported for other fusion proteins containing an HDEL retention signal (Boevink et al., 1996; Haseloff et al., 1997). Because proteins containing an HDEL retention sequence might occasionally escape from the ER to the cis-Golgi apparatus, where HDEL binds to a specific receptor (Boevink et al., 1998), the possibility cannot be excluded that the fluorescence signal could also be observed in the structure of the cis-Golgi. However, it is unlikely that the mobile particles seen in control cells in this study are Golgi stacks because they did not move in the stop and go fashion characteristic of Golgi stacks (Nebenführ et al., 1999). One possibility is that they are the small, dilated cisternae of ER described previously in Brassicaceae and tobacco guard cells by Hawes et al. (2001). Treatment of cells with BFA resulted in the appearance of brightly fluorescing static spots at the surface of the ER sheets. Similar results were reported by Boevink et al. (1999) and Batoko et al. (2000) for the transient expression of a GFP-HDEL-containing protein. These fluorescing spots may be accumulations of GFP in the ER, but a positive identification has not yet been made (C. Hawes, personal communication). The disintegration of the ER that was observed in our experiments is in agreement with results of Henderson et al. (1994), who showed disruption of ER after 3 h of treatment with BFA in maize root cells by immunofluorescence microscopy with anti-HDEL antibody. Ritzenthaler et al. (2002) reported that up to 20 min, treatment with BFA caused no visible alteration in ER morphology in BY-2 cells. Our results indicated that the first observable changes in ER-targeted GFP distribution

in BY-2 cells can be seen in as little as 5 min after BFA application, when disintegration of the tubular network and formation of fluorescent spots started.

In contrast to BFA treatments, NPA had no effect on ER-targeted GFP distribution in BY-2 cells. To our knowledge, no other data about phytotropin effects on ER are yet available.

The NPA Enigma

Geldner et al. (2001) reported that TIBA (and possibly also other auxin transport inhibitors) prevented the BFA-induced internalization of PIN1 and the traffic of internalized PIN1 to the PM after the BFA washout. Because similar effects of TIBA were observed on the cycling of a PM-ATPase and of the syntaxin KNOLLE, these authors suggested that auxin transport inhibitors affect auxin efflux by generally interfering with membrane trafficking processes. To generalize from these findings, however, may be premature, not least because TIBA is not a good representative of auxin transport inhibitors. First, TIBA does not fulfill the structural requirements of typical phytotropins and acts as a weak auxin antagonist (Katekar and Geissler, 1980). Although it inhibits auxin transport (Katekar and Geissler, 1980; Rubery, 1990), its high-affinity binding to maize microsomal preparations is only partially displaced by NPA (Depta et al., 1983), suggesting different loci of action of TIBA and phytotropins. Second, it has long been established that TIBA is itself a weak auxin, which unlike NPA, undergoes carrier-mediated polar transport on carriers that can be competed by IAA, 2,4-dichlorophenoxyacetic acid, and NAA (Depta and Rubery, 1984). Third, work in our laboratory has shown that in BY-2 tobacco cells, the stimulation of NAA accumulation (2 nM) is saturated by as little as 1 μM TIBA (H. Slizowska, M. Elčkner, and E. Zažímalová, unpublished data). Last, and more importantly, unlike NPA and IAA, at the concentration of 25 μM used by Geldner et al. (2001), TIBA causes substantial cytoplasmic acidification (Depta and Rubery, 1984). This, in turn, is likely to have nonspecific side effects on many cellular processes, possibly including secretory mechanisms.

We believe that there are other good reasons to be cautious in accepting the suggestion that auxin transport inhibitors act by generally interfering with vesicle traffic and turnover. The concentration of NPA stated to be necessary to bring about a similar reduction in PIN1 cycling to that caused by 25 μM TIBA (200 μM NPA; Geldner et al., 2001) is about two orders of magnitude greater than the concentration of NPA required to saturate inhibition of auxin efflux (1–3 μM; Petrášek et al., 2002; this report). Also, in suspension-cultured tobacco cells, concentrations of NPA exceeding about 50 μM reduce the stimulation of NAA accumulation substantially, possibly as a result of nonspecific side effects on the cells unrelated to the specific regulation of auxin efflux (Petrášek et al., 2002; this report). Finally, as discussed above, NPA has no effect on the arrangement of the cytoskeleton or ER in BY-2 cells, even at concentrations well above those that saturate the inhibition of auxin efflux. Therefore, NPA cannot inhibit actin-dependent vesicle traffic in general by an indirect action on the structure of the cytoskeleton and ER.

In conclusion, although the vesicle trafficking inhibitor BFA mimics some of the physiological effects of the phytotropin NPA, particularly insofar as they both inhibit carrier-mediated auxin efflux across the PM, our results clearly suggest that they do so by affecting different cellular mechanisms.

MATERIALS AND METHODS

Plant Material

Cells of tobacco (*Nicotiana tabacum* L. cv Bright-Yellow 2) line BY-2 (Nagata et al., 1992) were cultivated in darkness at 26°C on an orbital incubator (IKA KS501, IKA Labortechnik, Staufen, Germany; 120 rpm, orbital diameter 30 mm) in liquid medium (3% [w/v] Suc, 4.3 g L^{-1} Murashige and Skoog salts, 100 mg L^{-1} inositol, 1 mg L^{-1} thiamin, 0.2 mg L^{-1} 2,4-dichlorophenoxyacetic acid, and 200 mg L^{-1} KH_2PO_4 [pH 5.8]) and subcultured weekly. Stock BY-2 calli were maintained on media solidified with 0.6% (w/v) agar and subcultured monthly. Transgenic cells and calli were maintained on the same media supplemented with 100 μg mL^{-1} kanamycin and 100 μg mL^{-1} cefotaxim. All chemicals were obtained from Sigma (St. Louis) unless otherwise stated.

Transformation of BY-2 Cells

The basic transformation protocol of An (1985) was used. A 2-mL aliquot of 3-d-old BY-2 cells was co-incubated for 3 d with 100 μL of an overnight culture of *Agrobacterium tumefaciens* strain C58C1 carrying pBIN *m-gfp5*-ER plant binary vector (gift of Dr. Jim Haseloff, University of Cambridge, UK). It codes for ER-localized GFP variant mGFP5-ER, a thermotolerant derivative of mGFP4-ER (Haseloff et al., 1997), and contains a C-terminal ER retention signal sequence (HDEL). Incubated cells were then washed three times in 50 mL of liquid medium containing 100 μg mL^{-1} cefotaxim and plated onto solid medium containing 100 μg mL^{-1} kanamycin and 100 μg mL^{-1} cefotaxim. Kanamycin-resistant colonies appeared after 3 to 4 weeks of incubation in darkness at 27°C. Cell suspension cultures established from these were maintained as described above, with the addition of 100 μg mL^{-1} kanamycin and 100 μg mL^{-1} cefotaxim to the cultivation medium.

Effects of NPA and BFA on Cytoskeleton Arrangement

Appropriate volumes of a 25 mM stock solution of BFA in 96% (w/v) ethanol were added to cell cultures to give final concentrations of 20, 40, and 100 μM. NPA (synthesized in the Institute of Experimental Botany, Prague; compare with Petrášek et al., 2002) was added to cell cultures from 5 mM stock solution in 96% (w/v) ethanol to a final concentration of 50 μM (determined by reference to NPA concentration studies; see above). Equivalent volumes of 96% (w/v) ethanol were added to all control cultures.

Cell cultures were treated with BFA or NPA for 30 min with continuous shaking at room temperature (approximately 25°C) before microscopic examination (see below). When required, washout of BFA was performed with fresh cultivation medium after filtration of treated suspensions on 50-mm-diameter cellulose filter paper discs on a Nalgene filter holder (Nalge Company, Rochester, NY). Aliquots of 10 mL of cell suspension were washed three times (10 min each time) in 50 mL of fresh cultivation medium, and cells were examined immediately.

Visualization of AFs

AFs were visualized by the method of Kakimoto and Shibaoka (1987) modified according to Olyslaegers and Verbelen (1998). Filtered cells were fixed for 10 min in 1.8% (w/v) paraformaldehyde (PFA) in standard buffer (50 mM PIPES [pH 7.0], supplemented with 5 mM $MgCl_2$, and 10 mM EGTA). After a subsequent 10-min fixation in standard buffer containing 1% (v/v) glycerol, cells were rinsed twice for 10 min with standard buffer. Then, 0.5 mL of the resuspended cells were incubated for 35 min with the same volume of 0.66 μM TRITC-phalloidin prepared freshly from 6.6 μM stock solution in 96% (w/v) ethanol by dilution (1:10 [v/v]) in phosphate-buffered saline (PBS; 0.15 M NaCl, 2.7 mM KCl, 1.2 mM KH_2PO_4, and 6.5 mM Na_2HPO_4 [pH 7.2]). Cells were than washed three times for 10 min in PBS and observed immediately.

Visualization of MTs

MTs were visualized as described by Wick et al. (1981) with the modifications described by Mizuno (1992). After 30 min of prefixation in 3.7% (w/v) PFA in MT-stabilizing buffer consisting of 50 mM PIPES, 2 mM EGTA, and 2 mM $MgSO_4$ (pH 6.9) at 25°C, the cells were subsequently fixed in 3.7% (w/v) PFA and 1% (w/v) Triton X-100 in MT-stabilizing buffer for 20 min. After treatment with an enzyme solution (1% [w/v] macerozyme and 0.2% [w/v] pectinase) for 7 min at 25°C, the cells were attached to poly-L-Lys-coated coverslips and treated with 1% (w/v) Triton X-100 in MT-stabilizing buffer for 20 min. Subsequently, the cells were treated with 0.5% (w/v) bovine serum albumin in PBS and incubated with a monoclonal mouse antibody against α-tubulin (DM 1A, Sigma) for 45 min at 25°C (dilution 1:500 [v/v] in PBS). After washing with PBS, a secondary fluorescein isothiocyanate (FITC)-conjugated anti-mouse antibody (Sigma), diluted 1:80 (v/v) in PBS, was applied for 1 h at 25°C. Coverslips with cells were carefully washed in PBS, rinsed with water, and embedded in Mowiol solution (Polysciences, Warrington, PA).

Microscopy and Image Analysis

Both fixed and live preparations were observed with an epifluorescence microscope (Eclipse E600, Nikon, Tokyo) equipped with appropriate filter sets for FITC and TRITC fluorescence detection. mGFP5-ER fluorescence was observed using the FITC filter set. Images and time lapse scans were grabbed with a monochrome integrating CCD camera (COHU 4910, COHU Inc., San Diego) and digitally stored. The organization of both the cytoskeleton and ER were studied microscopically in at least 10 independent experiments. Representative images in Figures 3 and 5 show an arrangement typical for around 1,000 cells evaluated in each treatment. Subtle differences reflect the variability of staining pattern and appearance of cells.

After this careful microscopic examination, LUCIA image analysis software (Laboratory Imaging, Prague) was used for the evaluation of the effect of BFA on perinuclear actin aggregation. Images of TRITC-phalloidin-stained AFs were transformed to complementary colors (Fig. 4, A and C) and a circular measuring frame was applied interactively over the perinuclear region (Fig. 4, B and D). The ODV parameter was measured. The ODV parameter is the SD of optical density values under the circular measuring frame, where the bigger the ODV, the higher the aggregation of actin. These optical density values reflect the relative fluorescence intensities of individual pixels. The method measures the "coherency" of the fluorescent signal in the perinuclear region; the less coherent the signal, the greater the extent of actin aggregation. Approximately 300 cells in 10 optical fields were assessed for each sample.

Auxin Accumulation Measurement

Auxin accumulation by cells was measured according to the method of Delbarre et al. (1996), modified by Petrášek et al. (2002). The accumulation by the cells of [^{3}H]NAA (specific radioactivity 935 GBq $mmol^{-1}$, synthesized at the Isotope Laboratory, Institute of Experimental Botany, Prague), was measured in 0.5-mL aliquots of cell suspension (cell density about 7×10^5 cells mL^{-1}, as determined by counting cells in Fuchs-Rosenthal hemocytometer). Each cell suspension was filtered, resuspended in uptake buffer (20 mM MES, 40 mM Suc, and 0.5 mM $CaSO_4$, pH adjusted to 5.7 with KOH), and equilibrated for 45 min with continuous orbital shaking. Equilibrated cells were collected by filtration, resuspended in fresh uptake buffer, and incubated on the orbital shaker for 1.5 h in darkness at 25°C. [^{3}H]NAA was added to the cell suspension to give a final concentration of 2 nM. After a timed uptake period (depending on experiment, see above), 0.5-mL aliquots of suspension were withdrawn and accumulation of label was terminated by rapid filtration under reduced pressure on 22-mm-diameter cellulose filters. The cell cakes and filters were transferred to scintillation vials, extracted in ethanol for 30 min, and radioactivity was determined by liquid scintillation counting (Packard Tri-Carb 2900TR scintillation counter, Packard Instrument Co., Meriden, CT). Counts were corrected for surface radioactivity by subtracting counts obtained for aliquots of cells collected immediately after the addition of [^{3}H]NAA. Counting efficiency was determined by automatic external standardization, and counts were corrected automatically. NPA or BFA were added as required from ethanolic stock solutions to give the appropriate final concentration (see above). In time course experiments, aliquots of cell suspension were removed at timed intervals varying from 0 to 40 min from the start of experiments; the concentration dependence of auxin accumulation in response to NPA or BFA was determined after a 20-min uptake period.

Metabolism of Labeled Compounds

Possible distortion of the results of auxin accumulation studies by metabolism of the [^{3}H]NAA taken up by the cells was checked. Cells of BY-2 were incubated for 30 min as described in the presence of 2 nM [^{3}H]NAA. At the end of the incubation period, 10-mL aliquots of the incubated suspensions were quickly filtered on paper with gentle suction, washed rapidly with 5 mL of uptake buffer, and the cell cake was transferred to 2 mL of prechilled ethanol and stored at −80°C until required. Cell debris was removed by filtration under gentle pressure through cellulose filters. Radioactive compounds in the extracts were separated by chromatography on cellulose thin-layer plates (POLYGRAM CEL 300 UV_{254}, Macherey-Nagel, Düren, Germany), together with samples of the labeled auxins. The plates were developed in three independent solvent systems: (a) *iso*propanol:26% (v/v) ammonia:water (10:1:1 [v/v]), (b) chloroform:ethanol:glacial acetic acid (95:1:5 [v/v]), and (c) chloroform:ethanol:glacial acetic acid (75:20:5 [v/v]). Each chromatogram strip was cut into 20 sequential segments, eluted in ethanol, and counted by liquid scintillation counting.

ACKNOWLEDGMENTS

The authors thank Dr. Jim Haseloff (University of Cambridge, UK) for the pBIN *m-gfp5*-ER binary vector, and Miss Andrea Hourová (Institute of Experimental Botany, Prague) for her excellent technical assistance.

Received August 9, 2002; returned for revision September 10, 2002; accepted October 12, 2002.

LITERATURE CITED

An G (1985) High efficiency transformation of cultured tobacco cells. Plant Physiol **79:** 568–570

Batoko H, Zheng HQ, Hawes C, Moore I (2000) A Rab1 GTPase is required for transport between the endoplasmic reticulum and Golgi apparatus and for normal Golgi movement in plants. Plant Cell **12:** 2201–2217

Bennett MJ, Marchant A, Green HG, May ST, Ward SP, Millner PA, Walker AR, Schulz B, Feldmann KA (1996) *Arabidopsis AUX1* gene: a permease-like regulator of root gravitropism. Science **273:** 948–950

Bernasconi P, Patel BC, Reagan JD, Subramanian MV (1996) The *N*-1-naphthylphthalamic acid-binding protein is an integral membrane protein. Plant Physiol **111:** 427–432

Boevink P, Martin B, Oparka K, Santa Cruz S, Hawes C (1999) Transport of virally expressed green fluorescent protein through the secretory pathway in tobacco leaves is inhibited by cold shock and brefeldin A. Planta **208:** 392–400

Boevink P, Oparka K, Santa Cruz S, Martin B, Betteridge A, Hawes C (1998) Stacks on tracks: The plant Golgi apparatus traffics on an actin/ER network. Plant J **15:** 441–447

Boevink P, Santa Cruz S, Hawes C, Harris N, Oparka KJ (1996) Virus-mediated delivery of the green fluorescent protein to the endoplasmic reticulum of plant cells. Plant J **10:** 935–941

Butler JH, Hu SQ, Brady SR, Dixon MW, Muday GK (1998) In vitro and in vivo evidence for actin association of the naphthylphthalamic acid-binding protein from zucchini hypocotyls. Plant J **13:** 291–301

Cande WZ, Goldsmith MHM, Ray PM (1973) Polar auxin transport and auxin-induced elongation in the absence of cytoplasmic streaming. Planta **111:** 279–296

Cox DN, Muday GK (1994) NPA binding activity is peripheral to the plasma membrane and is associated with the cytoskeleton. Plant Cell **6:** 1941–1953

Davies PJ (1995) The plant hormone concept: concentration, sensitivity and transport. *In* PJ Davies, ed, Plant Hormones: Physiology, Biochemistry and Molecular Biology, Ed 2. Kluwer Academic Publishers, Dordrecht, The Netherlands, pp 13–38

Delbarre A, Muller P, Guern J (1998) Short-lived and phosphorylated proteins contribute to carrier-mediated efflux, but not to influx, of auxin in suspension-cultured tobacco cells. Plant Physiol **116:** 833–844

Delbarre A, Muller P, Imhoff V, Guern J (1996) Comparison of mechanisms controlling uptake and accumulation of 2,4-dichlorophenoxy acetic acid, naphthalene-1-acetic acid, and indole-3-acetic acid in suspension-cultured tobacco cells. Planta **198:** 532–541

Depta H, Eisele K-H, Hertel R (1983) Specific inhibitors of auxin transport: action on tissue segments and in vitro binding to membranes from maize coleoptiles. Plant Sci Lett **31:** 181–192

Depta H, Rubery PH (1984) A comparative study of carrier participation in the transport of 2,3,5-triiodobenzoic acid, indole-3-acetic acid, and 2,4-dichlorophenoxyacetic acid by *Cucurbita pepo* L. hypocotyl segments. J Plant Physiol **115:** 371–387

Dixon MW, Jacobson JA, Cady CT, Muday GK (1996) Cytoplasmic orientation of the naphthylphthalamic acid-binding protein in zucchini plasma membrane vesicles. Plant Physiol **112:** 421–432

Friml J, Palme K (2002) Polar auxin transport—old questions and new concepts? Plant Mol Biol **49:** 273–284

Gälweiler L, Guan C, Müller A, Wisman E, Mendgen K, Yephremov A, Palme K (1998) Regulation of polar auxin transport by AtPIN1 in *Arabidopsis* vascular tissue. Science **282:** 2226–2230

Geldner N, Friml J, Stierhof YD, Jürgens G, Palme K (2001) Auxin transport inhibitors block PIN 1 cycling and vesicle trafficking. Nature **413:** 425–428

Gil P, Dewey E, Friml J, Zhao Y, Snowden KC, Putterill J, Palme K, Estelle M, Chory J (2001) BIG: a calossin-like protein required for polar auxin transport in *Arabidopsis*. Genes Dev **15:** 1985–1997

Goldsmith MHM (1977) The polar transport of auxin. Annu Rev Plant Physiol **28:** 439–478

Haseloff J, Siemering KR, Prasher DC, Hodge S (1997) Removal of a cryptic intron and subcellular localisation of green fluorescent protein are required to mark transgenic *Arabidopsis* plants brightly. Proc Natl Acad Sci USA **94:** 2122–2127

Hasenstein KH, Blancaflor EB, Lee JS (1999) The microtubule cytoskeleton does not integrate auxin transport and gravitropism in maize roots. Physiol Plant **105:** 729–738

Hawes C, Saint-Jore C, Martin B, Zheng HQ (2001) ER confirmed as the location of mystery organelles in *Arabidopsis* plants expressing GFP! Trends Plant Sci **6:** 245–246

Henderson J, Satiat-Jeunemaitre B, Napier R, Hawes C (1994) Brefeldin A-induced disassembly of the Golgi apparatus is followed by disruption of the endoplasmic reticulum in plant cells. J Exp Bot **45:** 1347–1351

Hu SQ, Brady SR, Kovar DR, Staiger CJ, Clark GB, Roux SJ, Muday GK (2000) Identification of plant actin binding proteins by F-actin affinity chromatography. Plant J **24:** 127–137

Kakimoto T, Shibaoka H (1987) Actin filaments and microtubules in the preprophase band and phragmoplast of tobacco cells. Protoplasma **140:** 151–156

Katekar GF, Geissler AE (1980) Auxin transport inhibitors: IV. Evidence of a common mode of action for a proposed class of auxin transport inhibitors: the phytotropins. Plant Physiol **66:** 1190–1195

Li HM, Altschmied L, Chory J (1994) *Arabidopsis* mutants define downstream branches in the phototransduction pathway. Genes Dev **8:** 339–349

Lomax TL, Muday GK, Rubery PH (1995) Auxin transport. *In* PJ Davies, ed, Plant Hormones: Physiology, Biochemistry and Molecular Biology, Ed 2. Kluwer Academic Publishers, Dordrecht, The Netherlands, pp 509–530

Luschnig C (2001) Auxin transport: why plants like to think BIG. Curr Biol **11:** 831–833

Mizuno K (1992) Induction of cold stability of microtubules in cultured tobacco cells. Plant Physiol **100:** 740–748

Morris DA (2000) Transmembrane auxin carrier systems—dynamic regulators of polar auxin transport. Plant Growth Regul **32:** 161–172

Morris DA, Robinson JS (1998) Targeting of auxin carriers to the plasma membrane: differential effects of brefeldin A on the traffic of auxin uptake and efflux carriers. Planta **205:** 606–612

Morris DA, Rubery PH, Jarman J, Sabater M (1991) Effects of inhibitors of protein synthesis on transmembrane auxin transport in *Cucurbita pepo* L. hypocotyl segments. J Exp Bot **42:** 773–783

Müller A, Guan CH, Gälweiler L, Tänzler P, Huijser P, Marchant A, Parry G, Bennett M, Wisman E, Palme K (1998) *AtPIN2* defines a locus of *Arabidopsis* for root gravitropism control. EMBO J **17:** 6903–6911

Muday GK (2000) Maintenance of asymmetric cellular localization of an auxin transport protein through interaction with the actin cytoskeleton. J Plant Growth Regul **19:** 385–396

Muday GK, DeLong A (2001) Polar auxin transport: controlling where and how much. Trends Plant Sci **6:** 535–542

Muday GK, Murphy AS (2002) An emerging model of auxin transport regulation. Plant Cell **14:** 293–299

Nagata T, Nemoto Y, Hasezava S (1992) Tobacco BY-2 cell line as the "Hela" cell in the cell biology of higher plants. Int Rev Cytol **132:** 1–30

Nebenführ A, Gallagher LA, Dunahay TG, Frohlick JA, Mazurkiewicz AM, Meehl JB, Staehelin LA (1999) Stop-and-go movements of plant Golgi stacks are mediated by the acto-myosin system. Plant Physiol **121:** 1127–1141

Olyslaegers G, Verbelen JP (1998) Improved staining of F-actin and co-localization of mitochondria in plant cells. J Microsc Oxford **192:** 73–77

Petrášek J, Elčkner M, Morris DA, Zažímalová E (2002) Auxin efflux carrier activity and auxin accumulation regulate cell division and polarity in tobacco cells. Planta **216:** 302–308

Raven JA (1975) Transport of indoleacetic acid in plant cells in relation to pH and electrical potential gradients, and its significance for polar IAA transport. New Phytol **74:** 163–174

Richards S, Hillman T, Stern M (1996) Mutations in the *Drosophila* push-over gene confer increased neuronal excitability and spontaneous synaptic vesicle fusion. Genetics **142:** 1215–1223

Ritzenthaler C, Nebenführ A, Movafeghi A, Stussi-Garaud C, Behnia L, Pimpl P, Staehelin LA, Robinson DG (2002) Reevaluation of the effects of brefeldin A on plant cells using tobacco bright yellow 2 cells expressing Golgi-targeted green fluorescent protein and COPI antisera. Plant Cell **14:** 237–261

Robinson JS, Albert AC, Morris DA (1999) Differential effects of brefeldin A and cycloheximide on the activity of auxin efflux carriers in *Cucurbita pepo* L. J Plant Physiol **155:** 678–684

Rubery PH (1990) Phytotropins: receptors and endogenous ligands. Symp Soc Exp Biol **44:** 119–146

Rubery PH, Sheldrake AR (1974) Carrier-mediated auxin transport. Planta **188:** 101–121

Ruegger M, Dewey E, Hobbie L, Brown D, Bernasconi P, Turner J, Muday G, Estelle M (1997) Reduced naphthylphthalamic acid binding in the *tir3* mutant of Arabidopsis is associated with a reduction in polar auxin transport and diverse morphological defects. Plant Cell **9:** 745–757

Satiat-Jeunemaitre B, Steele C, Hawes C (1996) Golgi-membrane dynamics are cytoskeleton dependent: a study on Golgi stack movement induced by brefeldin A. Protoplasma **191:** 21–33

Saint-Jore CM, Evins J, Batoko H, Brandizzi F, Moore I, Hawes C (2002) Redistribution of membrane proteins between the Golgi apparatus and endoplasmatic reticulum in plants is reversible and not dependent on cytoskeletal networks. Plant J **29:** 661–678

Sussman MR, Gardner G (1980) Solubilization of the receptor for *N*-1-naphthylphthalamic acid. Plant Physiol **66:** 1074–1078

Swarup R, Friml J, Marchant A, Ljung K, Sandberg G, Palme K, Bennett M (2001) Localization of the auxin permease AUX1 suggests two functionally distinct hormone transport pathways operate in the *Arabidopsis* root apex. Genes Dev **15:** 2648–2653

Waller F, Riemann M, Nick P (2002) A role of actin-driven secretion in auxin-induced growth. Protoplasma **219:** 72–81

Wick SM, Seagull RW, Osborn M, Weber K, Gunning BES (1981) Immunofluorescence microscopy of organized microtubule arrays in structurally stabilized meristematic plant cells. J Cell Biol **89:** 685–690

Wilkinson S, Morris DA (1994) Targeting of auxin carriers to the plasma membrane: effects of monensin on transmembrane auxin transport in *Cucurbita pepo* L. tissue. Planta **193:** 194–202

CHAPTER 4

Auxin inhibits endocytosis and promotes its own efflux from cells

Tomasz Paciorek, Eva Zažímalová, Nadia Ruthardt, **Jan Petrášek**, York-Dieter Stierhof, Jürgen Kleine-Vehn, David A. Morris, Neil Emans, Gerd Jürgens, Niko Geldner, Jiří Friml

Nature 435(7046), 1251-1256, 2005

This chapter is a result of collaboration with the laboratory of Dr. Jiří Friml (University of Tübingen). The contribution of our lab was in showing how auxins might regulate their own transport by changing the amount of auxin efflux carriers at the plasma membrane, and in the analysis of degradation of native auxin IAA. The effects of auxin on its own transport were quantitatively assessed in suspension-grown tobacco cell lines VBI-0 and BY-2 (Fig. 2o, p and supplementary fig. S10a-c) and IAA was determined in *Arabidopsis* cultivation media (fig. S5a-e).

My contribution to this article was in preparation and characterization of plant material and performing auxin-accumulation assays in tobacco cell lines BY-2 and VBI-0 together with Eva Zažímalová and David Morris. E. Zažímalová was involved in analysis of auxin degradation, and she together with D. Morris contributed substantially to writing and editing of the manuscript text and figures.

Most of the work was done on *Arabidopsis thaliana* by Tomasz Paciorek and his colleagues from Tübingen University, i.e. York-Dieter Stierhof, Jürgen Kleine-Vehn, Gerd Jürgens, Niko Geldner and Jiří Friml (corresponding author). The quantification of the effect of auxins on endocytosis using endocytotic marker FM1-43 in BY-2 cells was done by Nadia Ruthardt and Neil Emans from Aachen University. There are several other colleagues that are acknowledged for their technical assistance and discussion at the end of the paper.

Our part of this paper was supported by the Grant Agency of the Academy of Sciences of the Czech Republic, project A6038303 to Eva Zažímalová and the Royal Society of London, UK (grant to David A. Morris).

LETTERS

Auxin inhibits endocytosis and promotes its own efflux from cells

Tomasz Paciorek[1], Eva Zažímalová[2], Nadia Ruthardt[3], Jan Petrášek[2], York-Dieter Stierhof[1], Jürgen Kleine-Vehn[1], David A. Morris[2,4], Neil Emans[3], Gerd Jürgens[1], Niko Geldner[1] & Jiří Friml[1]

One of the mechanisms by which signalling molecules regulate cellular behaviour is modulating subcellular protein translocation. This mode of regulation is often based on specialized vesicle trafficking, termed constitutive cycling, which consists of repeated internalization and recycling of proteins to and from the plasma membrane[1]. No such mechanism of hormone action has been shown in plants although several proteins, including the PIN auxin efflux facilitators, exhibit constitutive cycling[2,3]. Here we show that a major regulator of plant development, auxin, inhibits endocytosis. This effect is specific to biologically active auxins and requires activity of the Calossin-like protein BIG. By inhibiting the internalization step of PIN constitutive cycling, auxin increases levels of PINs at the plasma membrane. Concomitantly, auxin promotes its own efflux from cells by a vesicle-trafficking-dependent mechanism. Furthermore, asymmetric auxin translocation during gravitropism is correlated with decreased PIN internalization. Our data imply a previously undescribed mode of plant hormone action: by modulating PIN protein trafficking, auxin regulates PIN abundance and activity at the cell surface, providing a mechanism for the feedback regulation of auxin transport.

The local, asymmetric distribution of the plant growth regulator auxin mediates a variety of developmental processes such as axis formation, organ initiation and positioning, directional growth (tropisms) and meristem activity[4–6]. Biochemical, genetic and molecular data have confirmed that auxin promotes SCF^{TIR1}-mediated ubiquitination and degradation of the auxin/indole-3-acetic acid (AUX/IAA) repressors, thus releasing auxin response factor (ARF) transcriptional regulators from inhibition[7]. In this manner the expression of different sets of genes is activated, thereby eliciting different cellular and, consequently, developmental responses. An important additional level of regulation upstream of cellular auxin signalling is a specific transport system dependent on polarly localized PIN auxin efflux regulators[8]. This dynamic auxin distribution network mediates directional (polar) auxin flow between cells, which contributes to the formation and maintenance of asymmetric auxin distribution.

PIN proteins rapidly and constitutively cycle between the plasma membrane (PM) and endosomes[2]. In *Arabidopsis* this cycling involves a brefeldin A (BFA)-sensitive regulator of vesicle budding, the guanosine exchange factor for adenosine-ribosylation-factor-type small GTPases (ARF GEF) known as GNOM[3]. BFA inhibits trafficking from endosomes to the PM and causes endosomes to aggregate into 'BFA compartments'[2], which become surrounded by Golgi stacks[3]. In contrast, trafficking from the PM to the endosomes seems to be insensitive to BFA. These differential effects of BFA on endocytosis and exocytosis lead to the internalization and accumulation of constitutively cycling proteins in the BFA compartments. Thus, in *Arabidopsis* BFA can serve as a tool for revealing subcellular protein movement between endosomes and the PM[2,3].

Several plant PM markers were rapidly and reversibly internalized in response to BFA. These included PIN auxin efflux regulators such as PIN1 (ref. 2) (Fig. 1a, b), PIN2 (ref. 3) (Supplementary Fig. S1a), PIN3 (ref. 4) and PIN4 (Supplementary Fig. S1d), the PM water channel PIP2 (Fig. 1d) and maize cell-wall pectins[9] (Supplementary Figure S1h). Plasma membrane H^+-ATPase (PM-ATPase) was preferentially internalized in rapidly elongating epidermal cells (Fig. 1c), indicating the possible existence of both dynamic and more static populations of the protein. BFA-induced reversible internalization also occurred when transcription, protein synthesis[2] or protein degradation were inhibited (Supplementary Fig. S2), confirming that proteins accumulating in BFA compartments were not synthesized *de novo* but originated from the PM. Co-localization of cycling proteins (Supplementary Fig. S1a–c), the endocytic tracer FM4-64 (Supplementary Fig. S1e–g) and endosomal markers (Fig. 2b) revealed that the proteins studied here recycle through the same endomembrane compartments. These data show that some plant PM proteins are retained at the PM, but many exhibit constitutive cycling between the PM and endosomes.

In animals, constitutive cycling is an entry point for multiple regulation, including by signalling molecules[1]. Through this mechanism, hormones such as insulin or vasopressin can control the relative rates of endocytosis and exocytosis and thereby regulate the concentrations, and thus the activity of surface-localized proteins, including ion and water channels, transporters and receptors[1]. In plants, even high concentrations of several phytohormones including abscisic acid, brassinosteroids, cytokinins, ethylene and gibberellins had no detectable effect on various trafficking processes, including BFA-induced internalization (Fig. 1h, Supplementary Fig. S3). Interestingly, however, auxins such as the naturally occurring IAA and its synthetic analogues naphthalene-1-acetic acid (NAA) and 2,4-dichlorophenoxyacetic acid (2,4-D) efficiently inhibited the internalization of PIN1, PIN2, PIN4, PM-ATPase, PIP2:GFP and maize cell wall pectins in response to BFA (Fig. 1e–g, Supplementary Fig. S1i–p). Concentrations as low as 5 μM NAA and 2,4-D were enough to elicit near-maximal effects (Fig. 1e, f, Supplementary Fig. S4) indicating that these compounds might be sufficiently active even at lower concentrations. IAA was chemically unstable under our experimental conditions (verified by high-performance liquid chromatography and mass spectroscopy; Supplementary Fig. S5), but when an antioxidant (butylated hydroxytoluene; BHT[10]) was included in the medium, IAA was also effective at concentrations as low as 5 μM (Fig. 1g, Supplementary Fig. S5). In contrast, the physiologically inactive structural isomer of

[1]Zentrum für Molekularbiologie der Pflanzen, Universität Tübingen, 72076 Tübingen, Germany. [2]Institute of Experimental Botany, ASCR, Rozvojová 135, 165 02 Praha 6, Czech Republic. [3]Cellome Research Group, RWTH Aachen University, Biology VII, Worringerweg 1, 52074 Aachen, Germany. [4]School of Biological Sciences, University of Southampton, Bassett Crescent East, Southampton SO16 7PX, UK.

NAA, naphthalene-2-acetic acid (2-NAA), had no effect even at a tenfold higher concentration (Fig. 1i). However, even at maximal effective concentrations, auxins did not completely block BFA-induced internalization. This is inferred from the observation that some accumulation of constitutively cycling PM proteins inside cells could be observed when the treatment with BFA in the presence of auxins was prolonged (Supplementary Fig. S6).

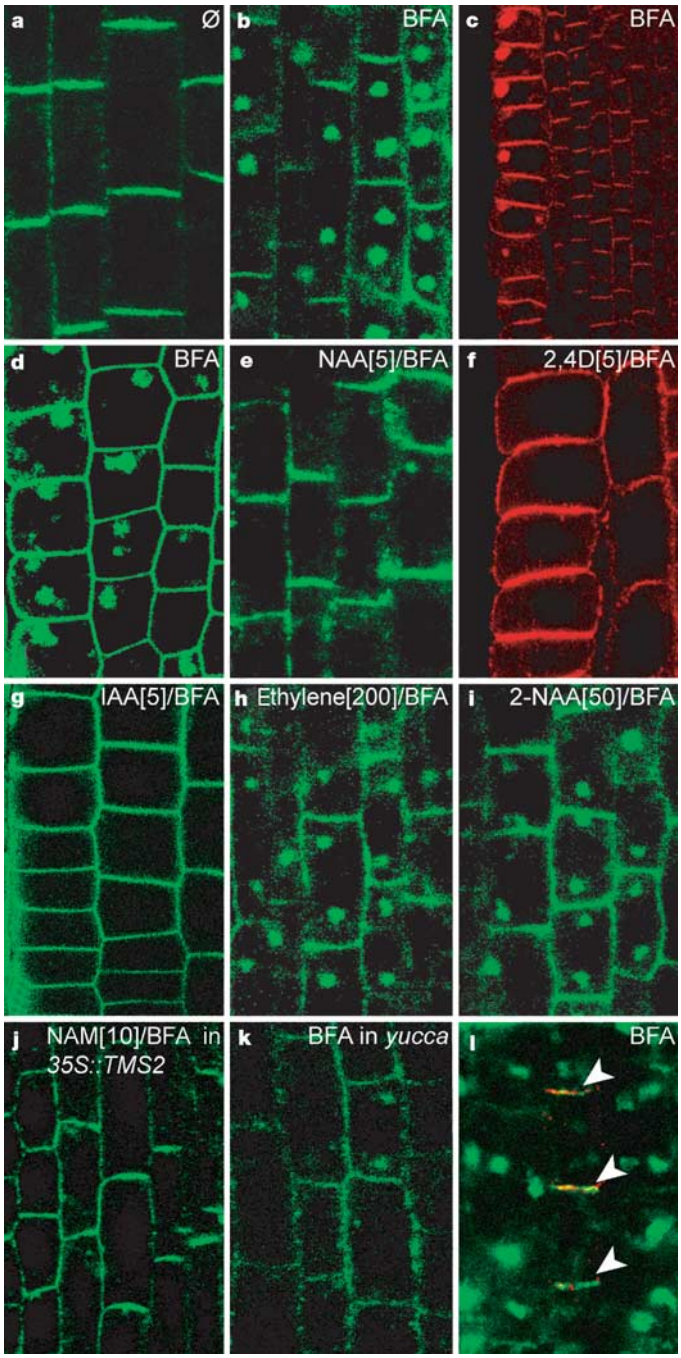

Figure 1 | Auxins inhibit internalization of constitutively cycling proteins. **a**–**d**, BFA-induced internalization of PM proteins: Polar, PM localization of PIN1 in untreated (∅) roots (**a**); PIN1 (**b**) and PIP2:GFP (**d**) internalization. BFA-sensitive (epidermis, cortex) and BFA-insensitive (stele) pools of PM-ATPase (**c**). **e**–**g**, Auxins (NAA, 2,4-D and IAA) inhibit BFA-induced internalization of PIN1 (**e**), PM-ATPase (**f**) and PIP2:GFP (**g**). **h**, **i**, Other hormones including ethylene (aminocyclopropane carboxylic acid (**h**)) or the inactive NAA analogue 2-NAA (**i**) are ineffective. **j**, NAA amide (NAM) in *35S::TMS2* plants inhibits BFA-induced internalization. **k**, *yucca* mutants show decreased PIN1 internalization. **l**, Protophloem cells marked by AUX1 (red) show less BFA-induced PIN1 (green) internalization than surrounding cells. Numbers in square brackets are concentrations in μM.

Induced increases in intracellular concentrations of endogenous auxin also had an inhibitory effect on the internalization of constitutively cycling PM proteins. *35S::TMS2* plants overexpress the amidohydrolase that converts biologically inactive auxin amides into active auxins[11]. When treated with NAA amide or IAA amide, *35S::TMS2* (Fig. 1j) but not wild-type plants (data not shown) showed inhibition of BFA-induced PIN1 internalization. Furthermore, *Arabidopsis* mutants with increased concentrations of endogenous auxin such as *superroot1* (*sur1*)[12] (data not shown) or *yucca*[13] (Fig. 1k) showed decreased PIN1 internalization after treatment with BFA in comparison with wild-type plants. Protophloem cells of root have been shown to have higher concentrations of auxin than surrounding tissues[14]. In wild-type plants grown under normal conditions, BFA-induced internalization was clearly inhibited in these cells (Fig. 1l). Together, these results show that physiological concentrations of exogenously applied and/or endogenously produced auxins downregulate the BFA-induced internalization of constitutively cycling PM proteins.

Next we examined the subcellular site(s) at which auxin acts on the BFA-induced internalization of PM proteins. An important control was the confirmation that auxins did not influence the uptake of BFA into *Arabidopsis* roots (Supplementary Fig. S7). To assess possible effects of auxin on different trafficking processes, we used established markers for various endomembrane compartments. There were no apparent effects of auxin on the distribution of ER (Sec12 (ref. 3)), presumptive trans-Golgi network (TLG2a (ref. 3)), Golgi apparatus (γ-COP (ref. 3)) or endosomal (ARF1 (ref. 15)) markers (Supplementary Fig. S8). Auxins also did not interfere with the BFA-induced formation of endosomal BFA compartments or with the aggregation of Golgi stacks at their periphery (Fig. 2a–f, Supplementary Fig. S9). Double labelling revealed that, in the same cells, auxin treatment did not affect the formation of Golgi-stack-encircled BFA compartments but prevented the internalization of PM proteins and therefore their accumulation in such compartments (Fig. 2c, f). The observation that BFA compartments (revealed as an aggregation of endocytic vesicles) still formed after treatment with auxin was confirmed by an examination of ultrastructure by electron microscopy (Fig. 2k–m). These data indicate that auxins might interfere with the endocytic step of constitutive cycling without visibly affecting other subcellular trafficking processes.

To assess directly the effect of auxin on endocytosis, we used the fluorescent dye FM4-64, an established endocytic tracer[3]. In *Arabidopsis* roots, even low concentrations of exogenously applied auxins clearly decreased the detectable uptake of FM4-64 (Fig. 2g, h), showing the inhibition of endocytosis. Furthermore, in *yucca* roots, which contain higher concentrations of endogenous IAA[13], the uptake of FM4-64 was also inhibited (Fig. 2i). To confirm and quantify the auxin effect on endocytosis, we measured the uptake of another endocytic tracer, FM1-43 (ref. 16), into suspension-grown tobacco BY-2 cells. Both 2,4-D and NAA inhibited FM1-43 uptake in a concentration-dependent manner (Fig. 2j). NAA was less effective, which is consistent with its decreased retention in tobacco cells[17]. Auxins also completely abolished the BFA-induced increase in FM1-43 internalization that results from the inhibition of membrane recycling back to the cell surface[16]. These experiments confirmed that the endocytic step of the cycling of PM proteins is the target for auxin action.

For a molecular characterization of the pathway by which auxin inhibits endocytosis, we performed a genetic screen to find mutants altered in the auxin effect on endocytosis. One group of mutants that showed resistance to the auxin effect on endocytosis was allelic to *transport inhibitor response3* (*tir3*). *tir3* was originally isolated in a screen for resistance to auxin transport inhibitors[18] and other alleles have also been identified by their involvement in light signal

transduction (*dark overexpression of CAB1* (*doc1*) and *attenuated shade avoidance* (*asa1*)) or cytokinin response (*umbrella* (*umb1*))[19,20]. The corresponding gene, since renamed *BIG*, encodes a member of the Calossin/Pushover family present in other multicellular organisms[19]. These proteins might be involved in subcellular vesicle trafficking, because they affect the subcellular localization of PIN1 after treatment with auxin efflux inhibitors[19]. We found that in both the *tir3* and *doc1* alleles of *big*, endocytosis of PM proteins was inhibited by auxins less than in the wild type. Auxin concentrations that would normally lead to the visible inhibition of BFA-induced internalization of the PIN1 protein (Fig. 3a–c) were ineffective in *big* mutants (Fig. 3e–g). Only higher auxin concentrations were able to inhibit the BFA-induced internalization (Fig. 3d, h). Other tested PM proteins such as PIN2 (data not shown) and PM-ATPase (Fig. 3i) behaved in a similar way as PIN1. Furthermore, *big* mutants also showed resistance to endogenously increased auxin concentrations in combination with *yucca* mutants, as demonstrated by a pronounced inhibition of BFA-induced internalization in *yucca* (see Fig. 1k), but not in *yucca big*, mutant roots (Fig. 3j). In addition, the inhibitory effect of auxin on the internalization of the endocytic tracer FM4-64 (see Fig. 2g–i) was less pronounced in *big* mutant roots (Fig. 3k). These data indicate that BIG is required for the auxin-mediated inhibition of endocytosis and thereby identify a molecular component of this specific pathway of auxin action.

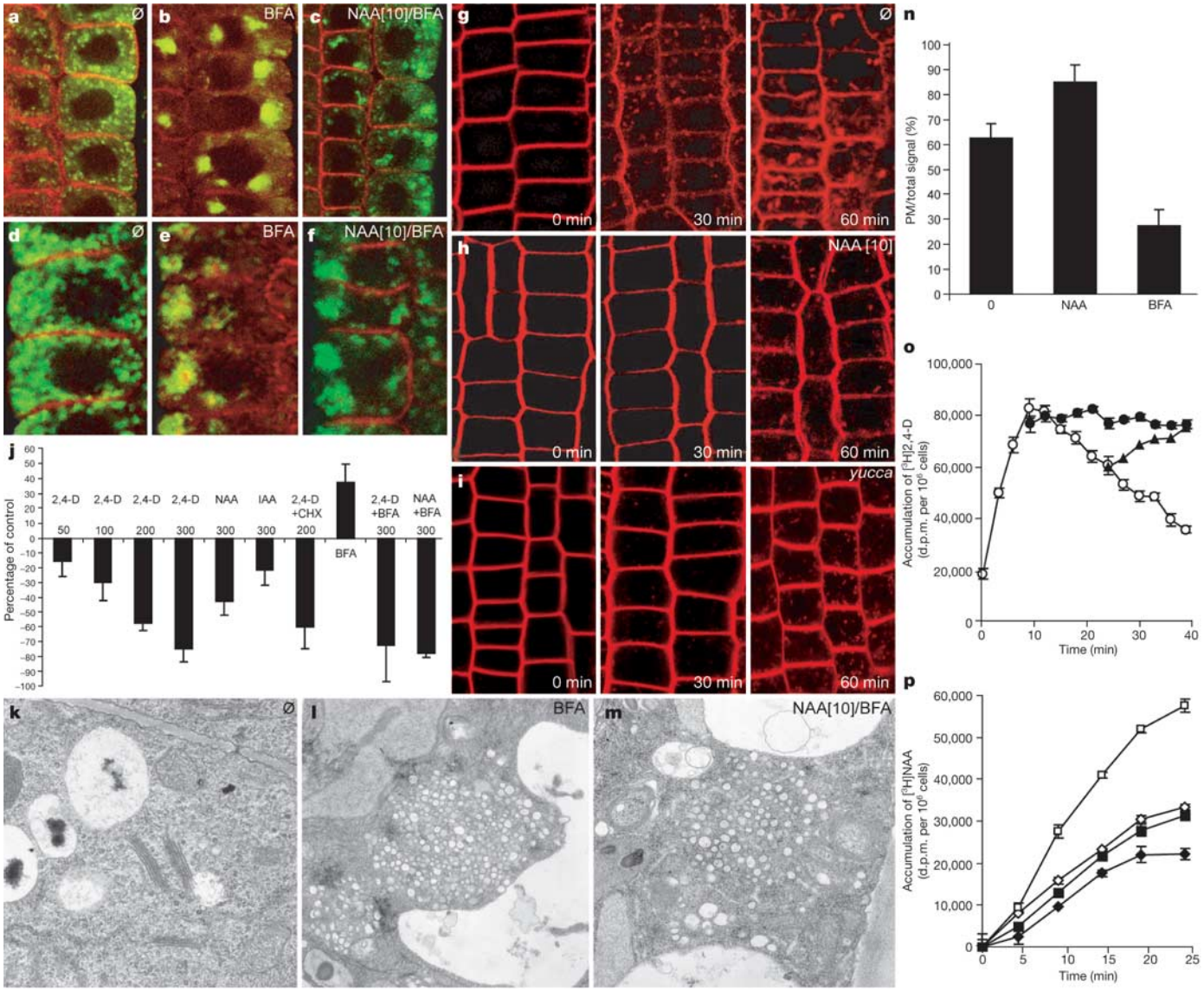

Figure 2 | **Auxin inhibits endocytosis, increases the amount of PIN2 protein at the plasma membrane and stimulates its own efflux from tobacco cells.** **a**–**c**, PM-ATPase (red) is internalized in response to BFA into ARF1-containing (green), endosomal BFA compartments (**b**). After treatment with NAA, PM-ATPase does not internalize, but ARF1-containing endosomes aggregate (**c**). **d**–**f**, γ-COP-labelled Golgi apparatus (green) aggregates around PM-ATPase-containing BFA compartments (red) (**e**). NAA prevents PM-ATPase internalization but not γ-COP aggregation (**f**). **g**–**i**, Uptake of endocytic tracer FM4-64 is slowed down in NAA-treated roots (**h**) and in *yucca* roots (**i**). **j**, 2,4-D, NAA and IAA inhibit uptake of FM1-43 into BY-2 cells in a concentration-dependent manner. Concentrations shown are in μM. CHX, cycloheximide. **k**–**m**, Ultrastructural examination of BFA compartments did not reveal any differences in ultrastructure between BFA (**l**) and NAA/BFA (**m**) treatments. **n**, The ratio of PM-located to internalized PIN2 signals (in %) increases after NAA and decreases after BFA treatments. **o**, [^{3}H]2,4-D decreases its own accumulation in VBI-0 cells over time (open circles). Concomitant BFA treatment (applied 6 min after addition of [^{3}H]2,4-D) prevents this effect (filled circles), and NAA (applied 21 min after addition of [^{3}H]2,4-D) competitively inhibits [^{3}H]2,4-D export (triangles). **p**, Pretreatment with 2,4-D for 20 min (filled diamonds) decreases [^{3}H]NAA accumulation in the BY-2 cells. BFA increases the accumulation (open squares), but this effect is prevented by pretreatment with 2,4-D (filled squares). Open diamonds, no addition. **a**, **d**, **g**, **k**, Untreated controls. Numbers in square brackets are concentrations in μM. Error bars show s.d.; ∅ relates to untreated controls.

If auxins inhibit the endocytic step of constitutive cycling, the protein pool at the PM should increase after treatment with auxin. To test this prediction we directly measured the ratio of cell surface to internalized PIN2 protein by using quantitative confocal microscopy. In the control (no auxin treatment), the PM pool composed approximately 62% of the total PIN2 protein. Treatment with auxins (NAA) increased the cell-surface signal significantly (85%, $P < 0.001$), showing higher levels of PIN2 at the PM (Fig. 2n). By contrast, treatment with BFA (inhibiting the exocytic step of the cycling) had the opposite effect and caused a massive accumulation of PIN2 inside cells, decreasing the cell-surface signal (28%, $P < 0.001$). Taken together, these data strongly indicate that auxins might inhibit the endocytic step of constitutively cycling PIN proteins, thus increasing their levels at the PM.

An auxin-dependent increase in the amount of cell-surface-localized PIN auxin efflux regulators would afford a mechanism by which auxin can control its own transport. A classical model, which attempts to explain multiple self-organizing auxin effects—the so-called canalization hypothesis—proposed feedback regulation between auxin signalling and intercellular auxin transport[21]. Earlier physiological experiments did indeed imply that auxin is required to maintain its own polar transport[22]. However, a direct effect of auxin on its own efflux has not been shown. The effects of auxin on its own transport were quantitatively assessed in suspension-grown tobacco cell lines VBI-0 and BY-2, which are well-established systems for studies of auxin transport *in vivo*[23,24]. The lines differ in their abilities to export different auxins, and the most important feature related to this study is that 2,4-D is a much better substrate for an auxin efflux machinery in VBI-0 cells than in BY-2 cells (Supplementary Fig. S10a–c). Generally, the net accumulation of radioactively labelled auxins in cells gives a measure of the relative rates of their uptake and efflux. In constant carrier-driven (and thus saturable) transport across the PM, the auxin accumulation would be expected to exhibit saturation kinetics until the uptake and efflux rates reached equilibrium. When VBI-0 cells were incubated with [^{3}H]2,4-D, after an initial increase in its internal concentration, the accumulation of [^{3}H]2,4-D decreased steadily with time instead of reaching a stable equilibrium (Fig. 2o). This effect was completely reversed by both a known inhibitor of auxin efflux (1-naphthylphthalamic acid (NPA); Supplementary Fig. S10d) and a high-affinity substrate for efflux carrier(s) in tobacco cells (NAA[17,23]; Fig. 2o). This shows that the observed decrease in 2,4-D accumulation results from an increased capacity in its carrier-driven efflux. This decrease in accumulation

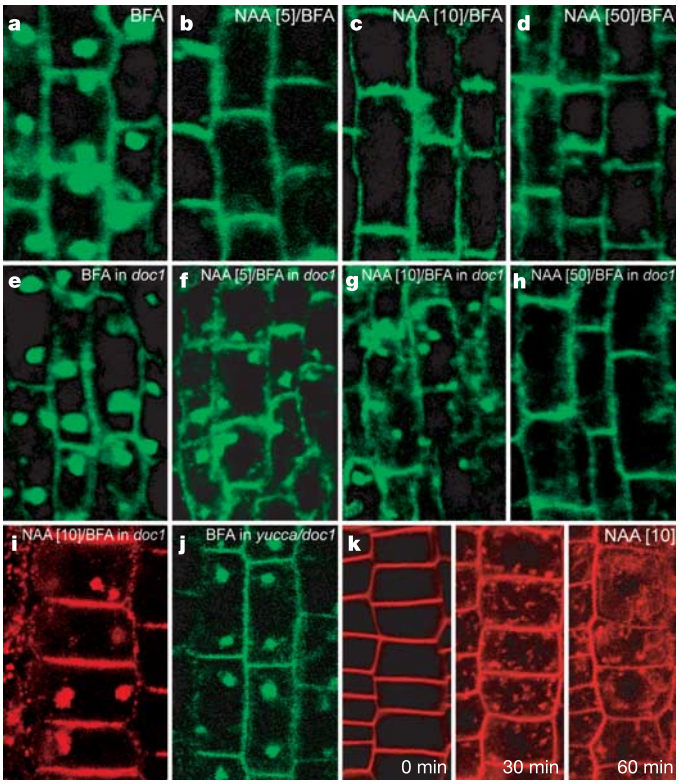

Figure 3 | BIG protein is required for the auxin-dependent inhibition of endocytosis. **a**–**h**, *doc1* mutants are partly auxin-resistant: BFA causes PIN1 internalization in control (**a**) and *doc1* roots (**e**). NAA blocks PIN1 internalization in controls (**b**, **c**) but not in *doc1* (**f**, **g**). Higher NAA concentrations are effective in both control (**d**) and *doc1* (**h**). **i**, In *doc1*, BFA-induced internalization of PM-ATPase is resistant to auxin (compare with Fig. 1f). **j**, Increase in auxin concentrations in *yucca* does not inhibit PIN1 internalization in the *yucca doc1* double mutant (compare with Fig. 1k). **k**, NAA does not inhibit the uptake of FM4-64 in the *doc1* mutant (compare with Fig. 2g, h). Numbers in square brackets are concentrations in μM.

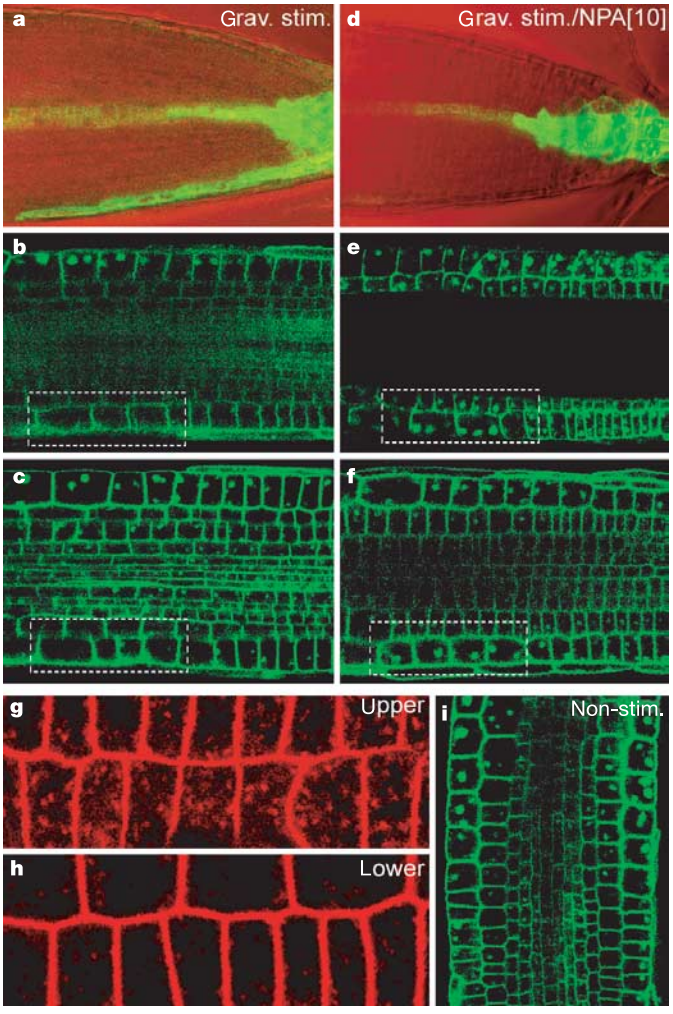

Figure 4 | Correlation between auxin translocation and the rate of PIN2 internalization in course of root gravitropism. **a**–**c**, After stimulation by gravity, auxin translocation detected by DR5rev::GFP activity (**a**) at the lower side of roots is correlated with the inhibition of BFA-induced internalization of PIN2:GFP (**b**) and PIP2:GFP (**c**). **d**–**f**, When auxin translocation is prevented by NPA, no asymmetry in DR5rev::GFP expression (**d**) or BFA-induced internalization of PIN2:GFP (**e**) and PIP2:GFP (**f**) occurs. **g**, **h**, After stimulation by gravity, FM4-64 uptake is lower in layers on the underside of the root (**h**) than in those on the upper side (**g**). **i**, Without stimulation by gravity, no asymmetry in the BFA-induced internalization of PIP2:GFP was detected. Numbers in square brackets are concentrations in μM.

(that is, an increase in efflux) was abolished by treatment with BFA (Fig. 2o), indicating that the stimulation of 2,4-D efflux was dependent on BFA-sensitive recycling of auxin efflux carriers back to PM. Next we investigated whether the pretreatment with auxin could directly affect the activity of auxin efflux. In this case, the accumulation of auxin had to be measured by using an auxin that is taken up by passive diffusion (to exclude the possible interference by the activity of auxin influx carriers) and, simultaneously, one that is a good substrate for efflux carrier(s) in tobacco cells; NAA fulfilled these criteria in both VBI-0 and BY-2 cells. In contrast, for the pretreatment, an auxin that is a weak substrate for an auxin efflux carrier had to be used to prevent competitive inhibition of NAA efflux. Because in VBI-0 cells, but not in BY-2 cells, 2,4-D is a good substrate for an efflux carrier (Supplementary Fig. S10a–c), we used BY-2 cells for this experiment. Pretreatment for 20 min with 5 μM 2,4-D significantly decreased the accumulation of [^{3}H]NAA (increased its efflux) and, moreover, abolished the inhibitory effect of BFA on auxin efflux (Fig. 2p). Together, these data show that in tobacco cells *in vivo*, auxin stimulates its own efflux by a vesicle-trafficking-dependent mechanism. All the results are consistent with the notion that auxin inhibits the internalization of constitutively cycling auxin efflux catalysts, thus increasing their incidence at the cell surface and thereby stimulating its own efflux.

We next explored *in planta* the link between the effects of auxin on endocytosis and auxin transport. Root gravitropism—the directional growth of roots along a gravity vector—is a well-characterized physiological process that involves the rapid establishment of auxin flow along the lower side of a horizontal root after gravity perception[4,8]. This process represents an ideal system in which to examine auxin translocation and endocytic recycling in parallel. After stimulation by gravity, asymmetric auxin flow resulted in auxin accumulation at the lower side of the root, as detected by the auxin response reporter DR5rev::GFP (Fig. 4a). Significantly, a similar spatial asymmetry within the root was observed for the BFA-induced internalization of PIN2:GFP and PIP2:GFP (Fig. 4b, c), indicating that their endocytic recycling might have been inhibited at the lower side of the gravistimulated root. Reduced uptake of the endocytic tracer FM4-64 was also observed at the lower side, in comparison with the upper side, of the root (Fig. 4g, h). In contrast, no asymmetry in auxin accumulation (as detected by DR5rev::GFP; Fig. 4d) and no inhibition of PM protein internalization in response to BFA occurred in non-stimulated roots (Fig. 4i) or after treatment with NPA (Fig. 4e, f), which under these conditions inhibits auxin flow but not protein cycling[2]. Thus, asymmetric auxin translocation is closely correlated spatially with the inhibition of endocytosis during the root gravitropic response. This finding strengthens the likelihood that the effects of auxin on endocytosis and on auxin transport are linked.

Our findings indicate a previously undescribed mode of action of plant hormones, namely the modulation of protein activity by regulating their intracellular trafficking. We have shown that biologically active auxins, but not their biologically inactive analogues nor other plant hormones, negatively regulate endocytosis and the internalization of constitutively cycling proteins from the PM. These auxin-induced changes in the relative rates of endocytosis and exocytosis lead to increased concentrations of PIN auxin efflux regulators at the cell surface. Concomitantly, auxins promote their own efflux by a vesicle recycling-dependent mechanism. These two previously unidentified auxin effects share similar kinetic characteristics, substrate requirements and inhibitor sensitivities. Furthermore, when assessed in parallel *in planta* during the gravitropic response, the same root cells that exhibited increased auxin translocation also displayed a decreased rate of endocytosis. Interestingly, the *sur1* mutant, which has elevated internal auxin concentrations and downregulated endocytosis, also shows increased auxin transport[25]. All these results strongly indicate that the auxin effects on endocytosis and on its own transport might be functionally linked. Thus our results show, and provide a mechanistic explanation for, a positive auxin effect on auxin transport rate.

It remains unclear which molecular pathway auxin uses to exhibit its effect on endocytosis. Mutations in the Calossin/Pushover protein BIG render endocytosis partly auxin-resistant. *BIG* is a single-copy gene present in *Arabidopsis* and other plant and animal genomes. In *Drosophila* the mutations at the corresponding locus lead to multiple defects including altered synaptic transmission and male sterility[26]; in *Arabidopsis*, *big* mutations lead to a weak physiological resistance to auxin but also affect other signalling pathways including those for ethylene, cytokinin, gibberellin or light[20]. These data do not support a direct involvement of the BIG protein in the auxin signalling pathway but rather in more general cellular processes, possibly in some aspect of endocytosis. There is no experimental support for a connection between the BIG-dependent auxin signalling pathway for inhibiting endocytosis and previously characterized SCF^{TIR1}-related auxin signalling for the regulation of gene expression. Thus it is possible that the auxin effect on endocytosis uses a previously unknown and so far molecularly uncharacterized signalling pathway that does not involve the regulation of gene expression.

METHODS

Materials and growth conditions. The following mutants and transgenic plants of *Arabidopsis thaliana* have been described previously: *AUX1:HA*[14], *GNOM-myc*[3], *PIN1:GFP*[6], *PIN2:GFP*[15], *DR5rev::GFP*[6], *doc1* (ref. 19), *sur1* (ref. 12), *tir3* (ref. 18), *yucca*[13], *yucca doc1* double mutant[19], *35S::TMS2* (ref. 11) and *EGFP-Q8* (PIP2)[27]. Experiments were performed on 4-day-old seedlings grown on vertically oriented plates containing *Arabidopsis* medium (AM; half-strength MS agar, 1% sucrose, pH 5.8). Cells of tobacco (*Nicotiana tabacum* L., lines BY-2 and VBI-0) were grown in suspension culture as described elsewhere[23,24]. Incubation of seedlings with various chemicals was performed in 24-well cell-culture plates in liquid AM medium.

Unless otherwise indicated, the following conditions were used. Pretreatments for 30 min with 5 μM NAA, 5 μM IAA plus 400 μg ml^{-1} BHT, 5 μM 2,4-D, 50 μM 2-NAA, 200 μM aminocyclopropane carboxylic acid or 10 μM NAA amide were followed by 90 min of concomitant treatment with one of the above plus 50 μM BFA. Control treatments contained an equal amount of solvent (dimethylsulphoxide or ethanol). For gravitropism experiments, plants were grown on vertically aligned plates containing a 1-mm layer of AM medium. A gravity stimulus was applied by horizontal positioning of plates; after 60 min, BFA solution was carefully added followed by incubation for 60 min. In controls, gravitational stimulation and BFA treatments were performed in the presence of 10 μM NPA. All treatments and gravity experiments were performed at least in triplicate, with a minimum of 60 roots evaluated in total in each treatment.

Genetic screen. A mutant screen to isolate plants for resistance to auxin's inhibitory effect on PM protein internalization was performed on the ethyl-methane sulphonate-mutagenized PIN1:GFP[6] population. Seedlings 5 days old were treated with 30 μM NAA for 30 min, followed by 30 μM NAA and 50 μM BFA for 90 min, and the BFA-induced internalization of PIN1:GFP was analysed with an epifluorescence microscope. From about 3,500 M1 families, we identified eight lines that under these conditions showed resistance to NAA (that is, they displayed normal internalization of PIN1:GFP into BFA compartments, as could be observed in the wild type after treatment with BFA without auxin).

Immunolocalizations. Whole-mount immunofluorescence preparations[28] and antibody staining of maize tissue sections[9] were performed as described. The rabbit anti-PIN1 polyclonal antiserum was raised against amino-acid residues 288–452 of PIN1 protein and was used previously for PIN1 localization in tissue sections[6]. For whole-mount immunolocalization in roots, immunoglobulins from the crude serum were precipitated by saturated $(NH_4)_2SO_4$ solution (2:1) and dialysed against PBS. The purified fraction was diluted 1:400. The anti-PIN2 antibody was provided by C. Luschnig and was used at a dilution of 1:400. Other antibodies were diluted as follows: anti-PIN4 (1:400)[29], anti-GFP (1:300; Molecular Probes), 9E10 anti-Myc (1:600; Santa Cruz), anti-TLG2a (1:200; Rosebiotech), anti-AtSec12 (1:50; Rosebiotech), anti-ARF1 (1:1,000)[30], anti-Atγ-COP (1:1,000)[3] and anti-PM-ATPase (1:1,000)[2]. Fluorescein isothiocyanate-conjugated and CY3-conjugated anti-rabbit secondary antibodies (Dianova) were diluted 1:200 and 1:600, respectively.

Uptake and accumulation experiments. Auxin accumulation experiments in suspension-cultured VBI-0 and BY-2 cells were performed as described previously[24]. The FM1-43 uptake experiments[16] were performed with BY-2 cells equilibrated in 2,4-D-free medium for 24 h. The measured signal was

normalized to the value of control cells at 4 °C and data were expressed relative to the 26 °C control sample. Uptake experiments with FM4-64 (Molecular Probes) in *Arabidopsis* were performed in 5-day-old seedlings, using a 5-min incubation with 1:500 dilution in AM medium.

Quantitative confocal microscopy. Quantitative confocal microscopy evaluation of the PIN2 signal was performed with Leica LCS quantification software. The scans were performed with identical microscope and laser settings for all experiments. Analysed cells on scans were selected interactively from the cortex of the same root region. Cell-border-associated and internal fluorescence were quantified separately from at least 80 cells for each treatment (10 μM NAA or 50 μM BFA for 90 min). In each experiment, inhibitors of transcription (20 μM cordycepin) and/or protein synthesis (50 μM cycloheximide) were applied to exclude any effects on PIN2 expression. Statistical significance was evaluated with Student's *t*-test.

Electron microscopy. Treatments (10 μM NAA and/or 50 μM BFA for 90 min) and ultrastructure analysis of chemically fixed root sections were performed exactly as described[2].

Received 1 February; accepted 13 April 2005.

1. Royle, S. & Murrell-Lagnado, R. Constitutive cycling: a general mechanism to regulate cell surface proteins. *BioEssays* **25,** 39–46 (2003).
2. Geldner, N., Friml, J., Stierhof, Y.-D., Jürgens, G. & Palme, K. Auxin transport inhibitors block PIN1 cycling and vesicle trafficking. *Nature* **413,** 425–428 (2001).
3. Geldner, N. *et al.* The *Arabidopsis* GNOM ARF-GEF mediates endosomal recycling, auxin transport, and auxin-dependent plant growth. *Cell* **112,** 219–230 (2003).
4. Friml, J., Wisniewska, J., Benková, E., Mendgen, K. & Palme, K. Lateral relocation of auxin efflux regulator AtPIN3 mediates tropism in *Arabidopsis*. *Nature* **415,** 806–809 (2002).
5. Friml, J. *et al.* Efflux-dependent auxin gradients establish the apical-basal axis of *Arabidopsis*. *Nature* **426,** 147–153 (2003).
6. Benková, E. *et al.* Local, efflux-dependent auxin gradients as a common module for plant organ formation. *Cell* **115,** 591–602 (2003).
7. Gray, W. R., Kepinski, S., Rouse, D., Leyser, O. & Estelle, M. Auxin regulates SCF^{TIR1}-dependent degradation of AUX/IAA proteins. *Nature* **414,** 271–276 (2001).
8. Friml, J. Auxin transport—shaping the plant. *Curr. Opin. Plant Biol.* **6,** 7–12 (2003).
9. Baluška, F. *et al.* F-actin-dependent endocytosis of cell wall pectins in meristematic root cells. Insights from brefeldin A-induced compartments. *Plant Physiol.* **130,** 422–431 (2002).
10. Von Gadow, A., Joubert, E. & Hansmann, C. F. Comparison of the antioxidant activity of aspalathin with that of other plant phenols of rooibos tea (*Aspalathus linearis*), alpha-tocopherol, BHT, and BHA. *J. Agric. Food Chem.* **45,** 632–638 (1997).
11. Karlin-Neumann, G., Brusslan, J. & Tobin, E. Phytochrome control of the *tms2* gene in transgenic *Arabidopsis*: a strategy for selecting mutants in the signal transduction pathway. *Plant Cell* **3,** 573–582 (1991).
12. Boerjan, W. *et al.* Superroot, a recessive mutation in *Arabidopsis*, confers auxin overproduction. *Plant Cell* **7,** 1405–1419 (1995).
13. Zhao, Y. *et al.* A role for flavin monooxygenase-like enzymes in auxin biosynthesis. *Science* **291,** 306–309 (2001).
14. Swarup, R. *et al.* Localisation of the auxin permease AUX1 suggests two functionally distinct hormone transport pathways operate in the *Arabidopsis* root apex. *Genes Dev.* **15,** 2648–2653 (2001).
15. Xu, J. & Scheres, B. Dissection of *Arabidopsis* ADP-RIBOSYLATION FACTOR 1 function in epidermal cell polarity. *Plant Cell* **17,** 525–536 (2005).
16. Emans, N., Zimmermann, S. & Fischer, R. Uptake of a fluorescent marker in plant cells is sensitive to brefeldin A and wortmannin. *Plant Cell* **14,** 71–86 (2002).
17. Delbarre, A., Muller, P., Imhoff, V. & Guern, J. Comparison of mechanisms controlling uptake and accumulation of 2,4-dichlorophenoxy acetic acid, naphthalene-1-acetic acid, and indole-3-acetic acid in suspension-cultured tobacco cells. *Planta* **198,** 532–541 (1996).
18. Ruegger, M. *et al.* Reduced naphthylphthalamic acid binding in the *tir3* mutant of *Arabidopsis* is associated with a reduction in polar auxin transport and diverse morphological defects. *Plant Cell* **9,** 745–757 (1997).
19. Gil, P. *et al.* BIG: a calossin-like protein required for polar auxin transport in *Arabidopsis*. *Genes Dev.* **15,** 1985–1997 (2001).
20. Kanyuka, K. *et al.* Mutations in the huge *Arabidopsis* gene BIG affect a range of hormone and light responses. *Plant J.* **35,** 57–70 (2003).
21. Berleth, T. & Sachs, T. Plant morphogenesis: long-distance coordination and local patterning. *Curr. Opin. Plant Biol.* **4,** 57–62 (2001).
22. Morris, D. A. Transmembrane auxin carrier systems—dynamic regulators of polar auxin transport. *Plant Growth Regul.* **32,** 161–172 (2000).
23. Petrášek, J., Elčkner, M., Morris, D. A. & Zažímalová, E. Auxin efflux carrier activity and auxin accumulation regulate cell division and polarity in tobacco cells. *Planta* **216,** 302–308 (2002).
24. Petrášek, J. *et al.* Do phytotropins inhibit auxin efflux by impairing vesicle traffic? *Plant Physiol.* **131,** 254–263 (2003).
25. Delarue, M., Muller, P., Bellini, C. & Delbarre, A. Increased auxin efflux in the IAA-overproducing *sur1* mutant of *Arabidopsis thaliana*: a mechanism of reducing auxin levels? *Physiol. Plant.* **107,** 120–127 (1999).
26. Richards, S., Hillman, T. & Stern, M. Mutations in the *Drosophila* pushover gene confer increased neuronal excitability and spontaneous synaptic vesicle fusion. *Genetics* **142,** 1215–1223 (1996).
27. Cutler, S., Ehrhardt, D., Griffitts, J. & Somerville, C. Random GFP::cDNA fusions enable visualisation of subcellular structures in cells of *Arabidopsis* at a high frequency. *Proc. Natl Acad. Sci. USA* **97,** 3718–3723 (2000).
28. Friml, J., Benková, E., Mayer, U., Palme, K. & Muster, G. Automated whole-mount localization techniques for plant seedlings. *Plant J.* **34,** 115–124 (2003).
29. Friml, J. *et al.* AtPIN4 mediates sink-driven auxin gradients and root patterning in *Arabidopsis*. *Cell* **108,** 661–673 (2002).
30. Pimpl, P. *et al.* In situ localization and *in vitro* induction of plant COPI -coated vesicles. *Plant Cell* **12,** 2219–2236 (2000).

Supplementary Information is linked to the online version of the paper at www.nature.com/nature.

Acknowledgements We thank C. Bellini, M. Bennett, M. Estelle, M. Grebe, W. Michalke, D. Robinson and Y. Zhao for sharing material, and E. Benková, P. Brewer, J. Eder, J. Malbeck, C. Oecking, M. Sauer, H. Stransky and D. Weijers for technical assistance and discussions. This work was supported by the Volkswagenstiftung (J.F. and T.P.), the F. Ebert Stiftung (J.K.-V.), the Deutsche Forschungsgemeinschaft (N.G., G.J. and Y.-D. S.), the Grant Agency of the Academy of Sciences of the Czech Republic (J.P. and E.Z.) and the Royal Society of London (D.A.M.).

Author Information Reprints and permissions information is available at npg.nature.com/reprintsandpermissions. The authors declare no competing financial interests. Correspondence and requests for materials should be addressed to J.F. (jiri.friml@zmbp.uni-tuebingen.de).

Auxin inhibits endocytosis and promotes its own efflux from cells

Tomasz Paciorek, Eva Zažímalová, Nadia Ruthardt, **Jan Petrášek**, Yorg-Dieter Stierhof, Jürgen Kleine-Vehn, David A. Morris, Neil Emans, Gerd Jürgens, Niko Geldner, Jiří Friml

Nature **435(7046)**: 1251-1256, **2005**.

Supplementary Data

Supplementary data 1:

Auxins inhibit BFA-induced internalisation of constitutively cycling PM markers.

a-h, BFA-induced (50 µM, 90 minutes) internalisation of PIN2 (**a**) and PM-ATPase (**b**) and their colocalisation (**c**); PIN4 (**d**); PIP2:GFP (**e**) and FM4-64 (**f**) and their colocalisation (**g**); and maize cell wall pectins (**h**). **i-p,** Exogenously applied auxin NAA inhibits internalisation of PIN2 (**i**) and PM-ATPase (**j**), their colocalisation (**k**); PIN4 (**l**); PIP2:GFP (**m**) and FM4-64 (**n**), their colocalisation (**o**); and maize cell wall pectins (**p**). Depicted concentrations are in [µM].

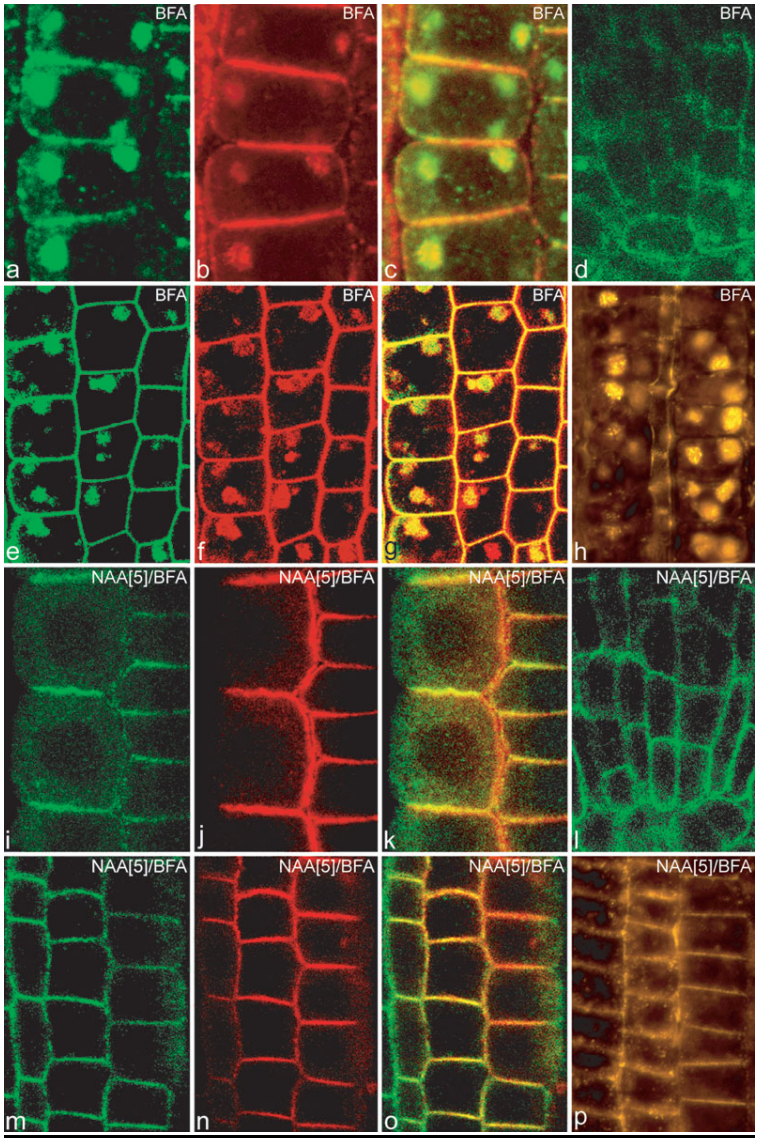

Supplementary data 2:

Inhibitors of protein expression and degradation confirm BFA-visualized constitutive cycling of PIN1.

a-d, Inhibitors of protein synthesis (CHX, 50 µM, **a**), transcription (Actinomycin D, 50 µM, **b**), (cordycepin, 50 µM, **c**), and protein degradation (MG132, 50 µM, **d**) do not interfere with BFA-induced internalisation of PIN1 in Arabidopsis root cells (BFA, 50 µM, 90 minutes).

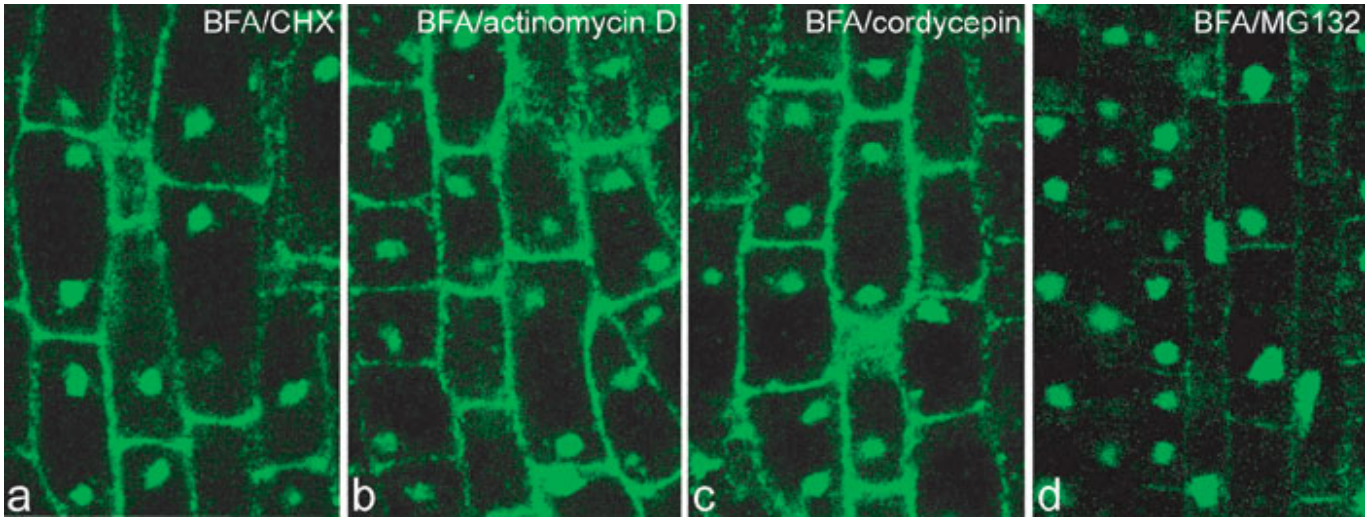

Supplementary data 3:

Other plant hormones do not inhibit internalisation of constitutively cycling proteins.

a-e, Other plant hormones including brassinosteroids (brassinolide, **a**), abscisic acid (**b**), cytokinins (zeatin, **c**), gibberellins (GA_3, **d**) and ethylene (applied as ACC, **e**) do not inhibit BFA-induced internalisation of PIN1 even at high concentrations. BFA was applied at 50 µM, for 90 minutes. Depicted concentrations are in [µM].

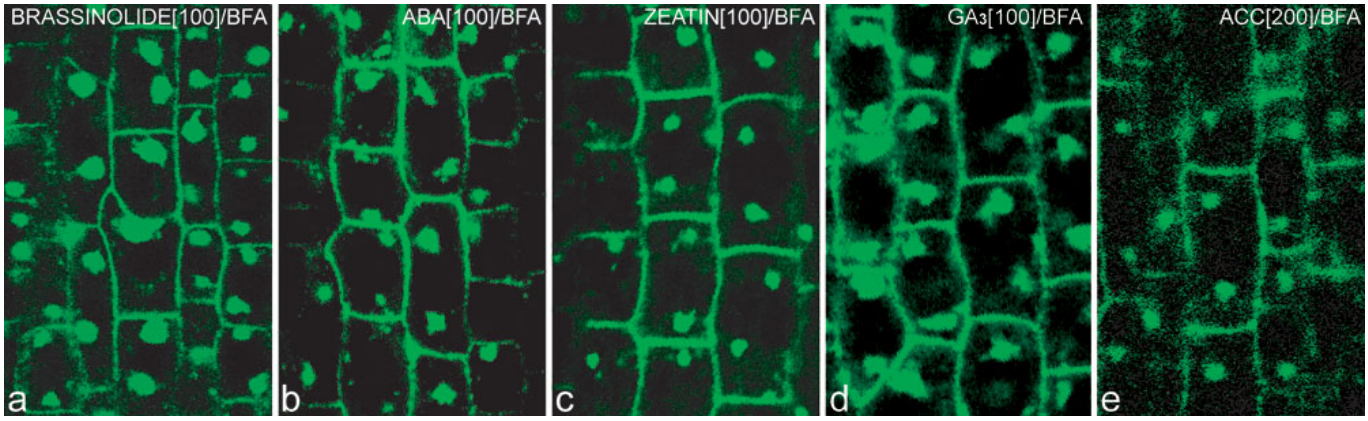

Supplementary data 4:

5 µM concentrations of NAA and 2,4-D inhibit BFA-induced internalisation of constitutively cycling proteins.

a-l, Exogenously applied auxin NAA (10 µM, 2 hours) does not visibly interfere with PM localization of PIN1 (**a**), PIP2:GFP (**e**) and PM-ATPase (**i**). Exogenously applied auxin NAA 2,5 µM does not visibly inhibit BFA-induced internalisation of PIN1 (**b**), PIP2:GFP (**f**) and PM-ATPase (**j**) but NAA 5 µM or 10 µM effectively inhibit internalisation of PIN1 (**c, d**), PIP2:GFP (**g, h**) and PM-ATPase (**k, l**). **m-p,** Exogenously applied 2,4-D (10 µM) does not interfere with localisation of PIN1 (**m**) and at 2,5 µM does not visibly inhibit internalisation of PIN1 (**n**). However, at 5 µM (**o**) and 10 µM (**p**), 2,4-D effectively blocks PIN1 internalisation. Depicted concentrations are in [µM].

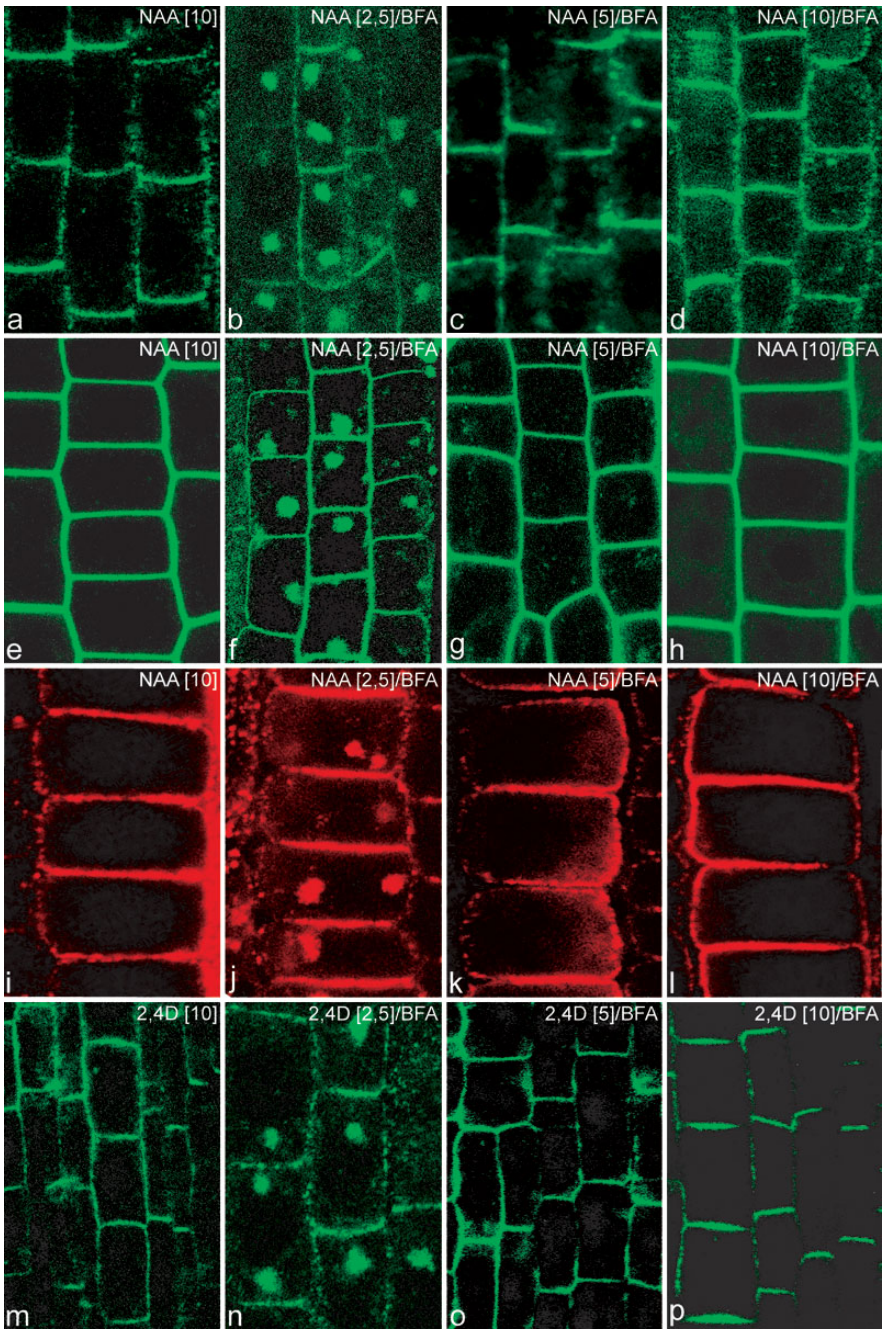

Supplementary data 5:

IAA is unstable in Arabidopsis medium but, if stabilised, it inhibits BFA-induced internalisation at 5 µM concentrations.

a-e, HPLC analysis of the chemical stability of IAA and NAA in *Arabidopsis* medium: 1 µM IAA standard solution in DMSO (**a**); 1 µM NAA standard solution in methanol (**b**). IAA (**c**) but not NAA (**d**) is very rapidly degraded in *Arabidopsis* medium. The protective effect of the antioxidant 2,6-di-t-butyl cresol (butylated hydroxytoluene, BHT, 1 mg/10 ml) on IAA (1 µM) stability (**e**). **f, g,** Exogenously applied IAA (10 µM, **f**) does not but IAA (100 µM, **g**) does effectively block BFA-induced internalisation of PIN1. **h-j,** Exogenously applied IAA (2,5 µM, **h**) does not but IAA (5 µM, **i**) does inhibit internalisation of PIN1 in presence of BHT. BHT alone (**j**) has no effect on PIN1 internalisation. Depicted concentrations are in [µM].

Method: HPLC analyses were performed using a Summit instrument (Dionex, USA) with a Spherisorb 5ODS1 column (250 x 4 mm), temperature 45^{o}C, elution with a linear gradient of acetonitrile from 88% of 5% acetonitrile + 10% of 80% acetonitrile + 2% of 5% acetic acid (time 0) to 20% of 5% acetonitrile + 78% of 80% acetonitrile + 2% of 5% acetic acid (time 35 min). Fluorescence detection was at λ_{ex} 280 nm, and λ_{em} 350 nm (detector RF2000, Dionex, USA). Each run was repeated at least three times, with the similar results. Representative runs are shown. The IAA peak was verified using MS (not shown).

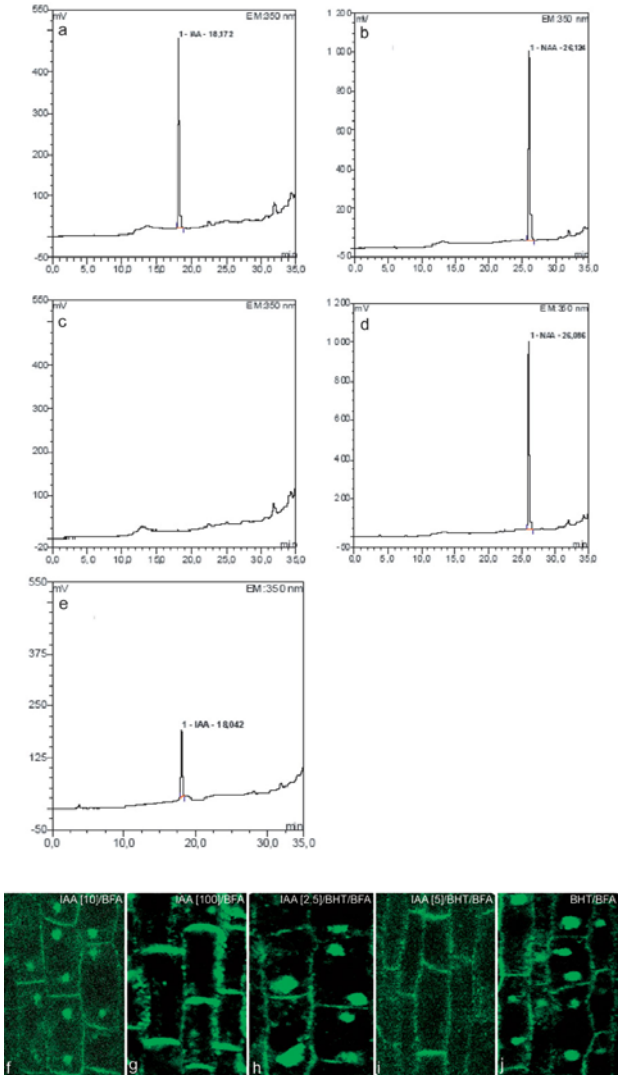

Supplementary data 6:

Auxins down-regulate but do not completely block BFA-induced internalisation of constitutively cycling proteins.

a-h, NAA does not completely block protein internalisation: after prolonged incubation with BFA (50 µM, time indicated in minutes), slow but detectable internalisation of PIP2:GFP (**c,d**) and PIN1:GFP (**g,h**) proteins were observed. Depicted concentrations are in [µM].

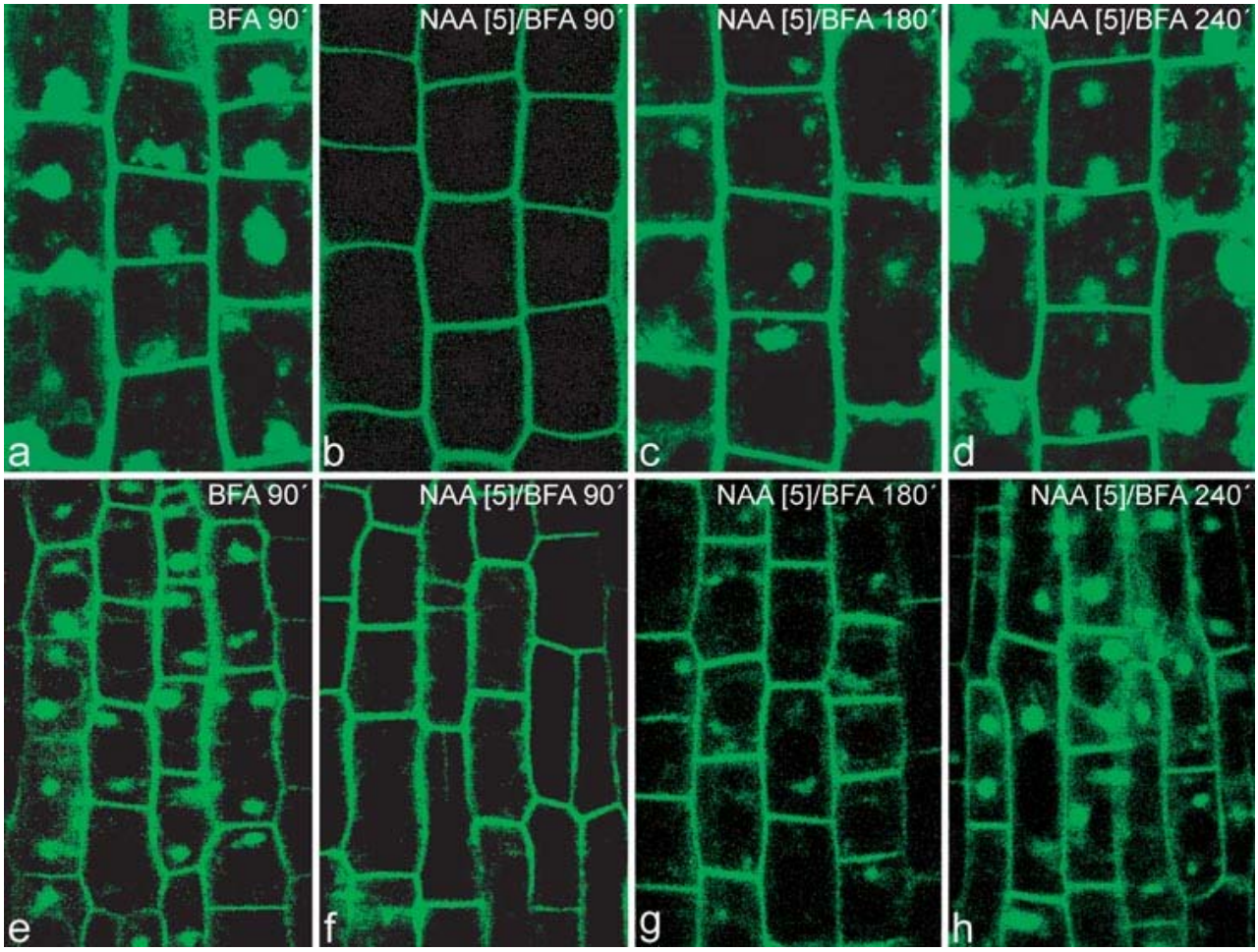

Supplementary data 7:

NAA does not influence BFA uptake in *Arabidopsis* root tissues.

a, Even high concentrations of NAA (100 µM) do not influence the uptake of BFA into *Arabidopsis* roots as demonstrated by identical uptake kinetics of [^{3}H]BFA in the presence or absence of NAA.

Method: BFA uptake studies in *Arabidopsis* roots were performed with a 100 µM solution of [^{3}H]BFA (specific radioactivity 250 MBq/mmol, ICN Biochemicals) in AM medium. An average of 100 mg fresh weight determined by triplicate measurements was used. Roots were incubated with radioactive BFA for and then put on glass fibre filters, washed three times and transferred into vials for liquid scintillation counting.

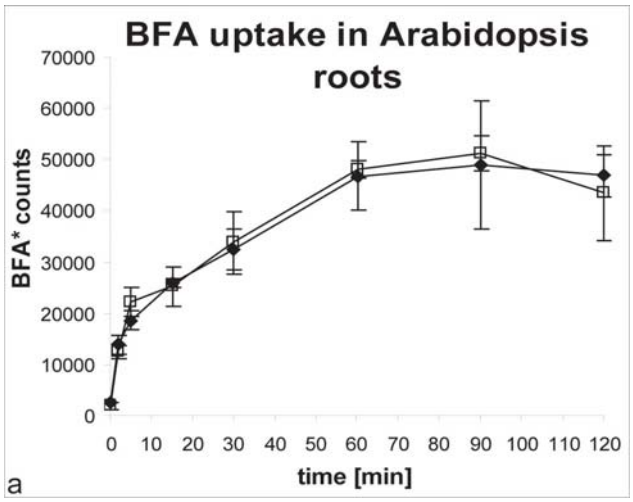

Supplementary data 8:

Auxins do not affect the morphology of selected subcellular structures.

a-h, Morphology of ER (marker Sec12, **a**), trans-Golgi network (TLG2a, **b**), Golgi apparatus (γCOP, **c**) and endosomes (ARF1, **d**) is not visibly affected by the application of NAA (2 hours) (**e-h**). Depicted concentrations are in [µM].

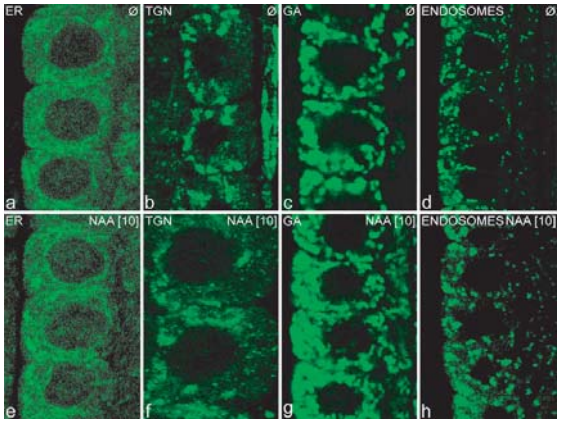

Supplementary data 9:

Auxins inhibit the BFA-induced internalisation of PM proteins but do not affect BFA-induced aggregation of endosomes.

a-g, Endosomal compartments labelled by GN-myc (red, **a-c**) and localisation of PIN2 (green, **d-f**). Control roots (**a, d**). BFA causes internalisation of PIN2 into “BFA compartments” (**e**), which also consists of aggregated GN-containing endosomes (**b**). Pre-treatment with NAA efficiently inhibits internalisation of PIN2 (**f**) but does not block aggregation of GN-containing endosomes into “BFA compartments” (**c**); Colocalisation of PIN2 and GN-myc (**g**). Depicted concentrations are in [µM].

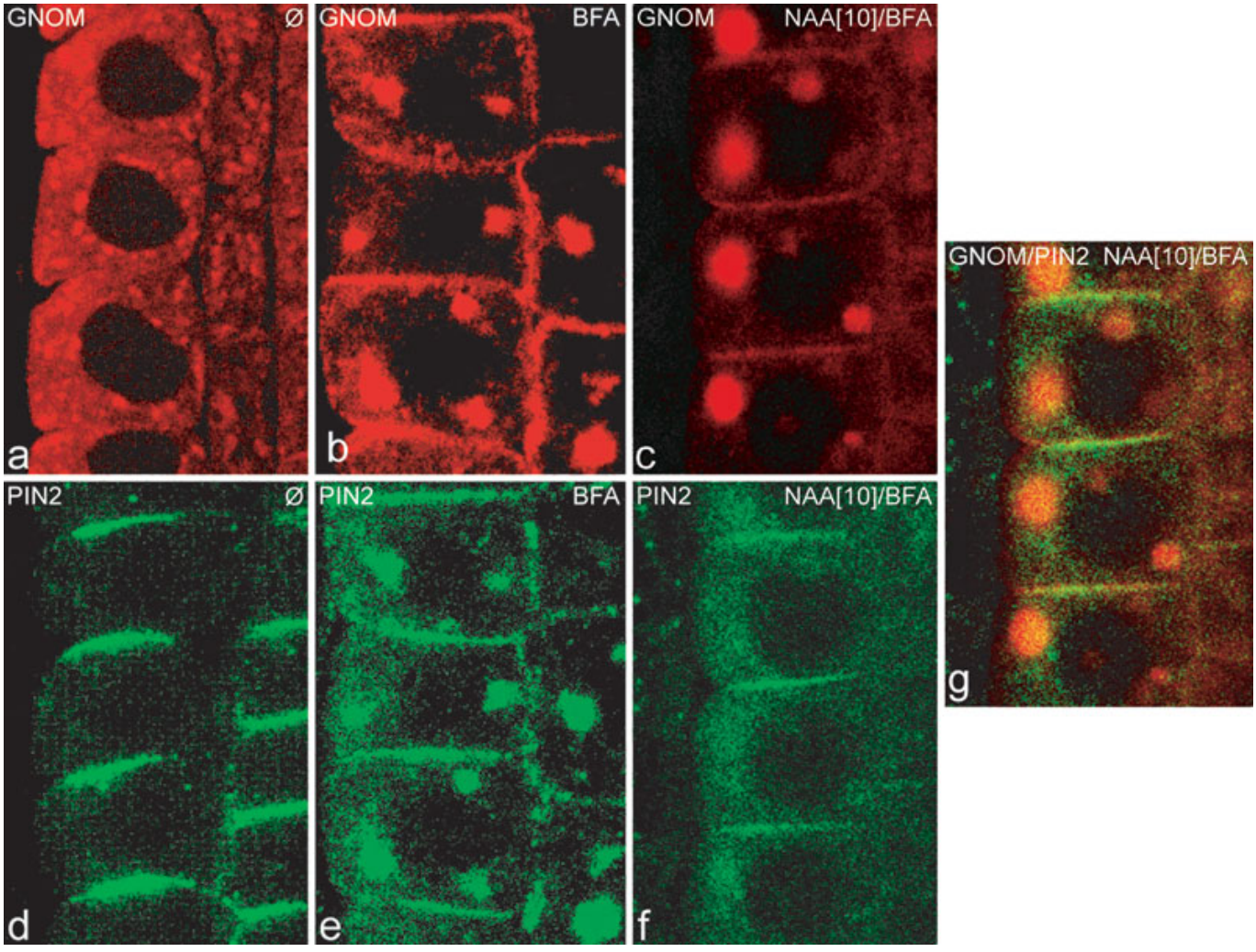

Supplementary data 10:

Auxin efflux in suspension-cultured BY-2 and VBI-0 tobacco cells.

a-c, Comparison of the rates of [^{3}H]2,4-D accumulation in cultured VBI-0 and BY-2 cells: Inhibition of auxin efflux by the competitive efflux substrate NAA (10 µM, **a**), by the efflux inhibitor 1-N-naphthylphthalamic acid (NPA, 10 µM, **b**), and by Brefeldin A (BFA, 20 µM, **c**) has a significant effect on [^{3}H]2,4-D accumulation in VBI-0 cells but not in those of BY-2. These data clearly indicate that 2,4-D is a good substrate for the efflux carrier in VBI-0 but not in BY-2. **d,** [^{3}H]2,4-D decreases its own accumulation in VBI-0 cells. Concomitant NPA treatment (applied in-flight at 6 min) significantly increases the accumulation of [^{3}H]2,4-D demonstrating that the decrease in 2,4-D accumulation occurs through the action of the auxin efflux catalysts.

Method: Comparison of the rates of accumulation of 2,4-D in VBI-0 and BY-2 tobacco cell lines determined by measuring net accumulation of [^{3}H]2,4-D (2 nM). Error bars indicate standard error of the mean (four replicates). Cells in late exponential phase of growth, cell densities were 2 x 10^5 cells and 7 x 10^5 cells per ml of suspension in VBI-0 and BY-2 respectively. Standard errors of the mean (four replicates) were in the range 5-9% and 10-15% of the means for VBI-0 and BY-2 cells respectively.

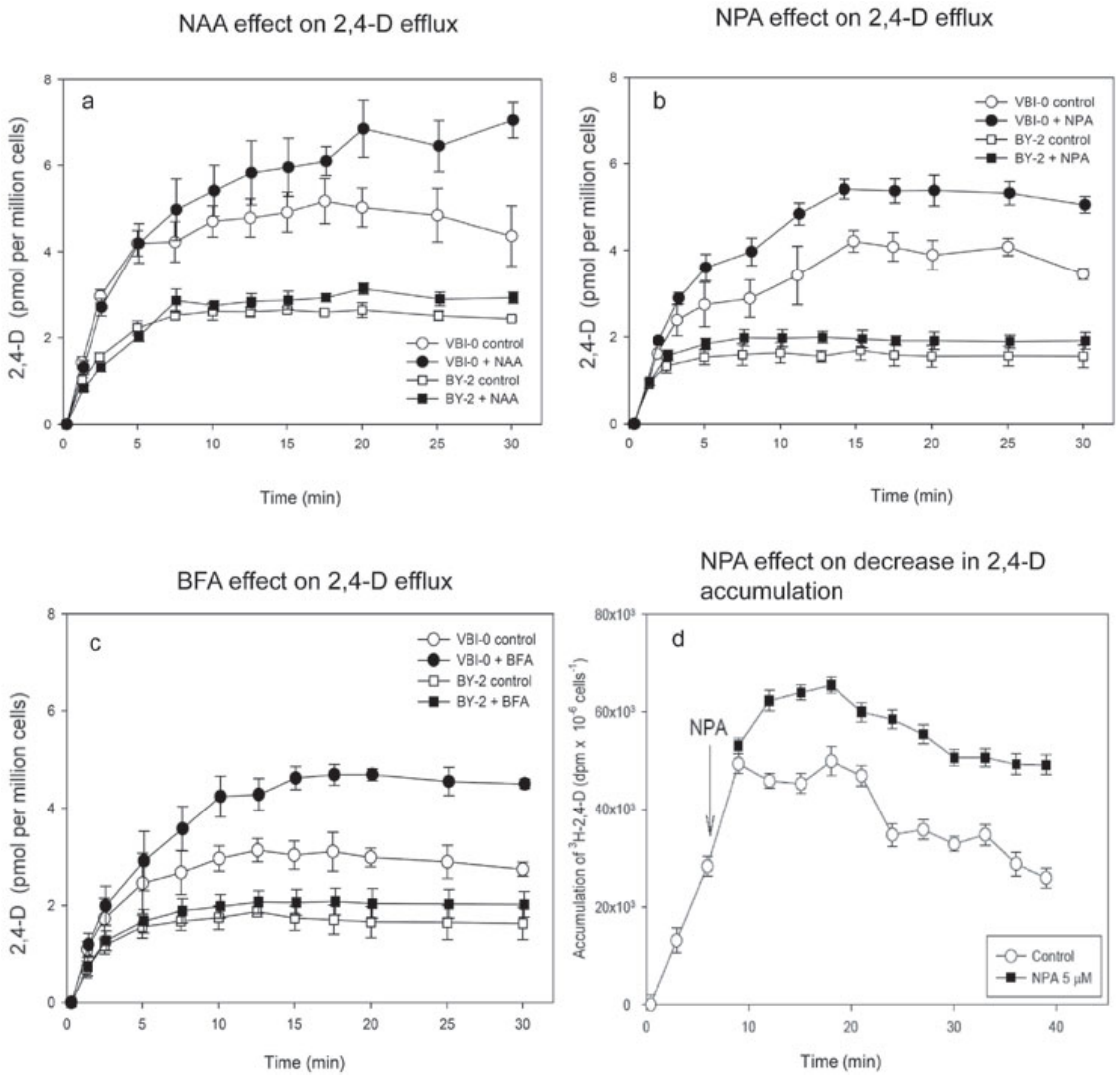

CHAPTER 5

PIN proteins perform a rate-limiting function in cellular auxin efflux

Jan Petrášek, Jozef Mravec, Rodoplhe Bouchard, Joshua J. Blakeslee, Melinda Abas, Daniela Seifertová, Justyna Wiśniewska, Zerihun Tadele, Martin Kubeš, Milada Čovanová, Pankaj Dhonukshe, Petr Skůpa, Eva Benková, Lucie Perry, Pavel Křeček, Ok Ran Lee, Gerald R. Fink, Markus Geisler, Angus S. Murphy, Christian Luschnig, Eva Zažímalová, Jiří Friml

Science 312, 914-918, 2006

This chapter is the result of collaboration of our lab with several other laboratories. Their effort has been joined by corresponding author Dr. Eva Zažímalová together with Dr. Jiří Friml to clearly show the specific and rate-limiting function of PIN proteins in cellular auxin efflux.

My contribution to this article was in the transformation of BY-2 cells with dexamethasone-inducible *PIN* genes, in testing various selection markers suitable for usage in BY-2 cells, designing the strategy for selection of transformants and in expression analyses (PCR, RT-PCR, western blotting, immunofluorescence staining), in performing auxin-accumulation assays in tobacco lines expressing inducible *PIN4*, *PIN6* and *PIN7* genes, in PIN1 and PIN7 immunofluorescence staining in *Arabidopsis* cell suspensions and tobacco BY-2 cells expressing *PIN1* and *PIN7* gene, respectively. I was also involved substantially in processing and interpretation of all measured data and in the writing and editing of the manuscript text and figures.

From Prague laboratory, Daniela Seifertová established cell suspension cultures from *Arabidopsis* lines expressing inducible PIN proteins and performed expression studies (RT-PCR) and auxin-accumulation assays in these lines as well as in BY-2 transformants (inducible PIN7). Martin Kubeš contributed with the transformation of BY-2 cells with *PGP19* and performed corresponding expression analyses (RT-PCR, immunofluorescence localization and western blot) and auxin-accumulation assays. Milada Čovanová helped with the original selection of dexamethasone-inducible PIN4,6,7 transformants. Petr Skůpa was involved in expression analyses (RT-PCR) in PIN4 and PIN6 inducible lines, Pavel Křeček performed western blots in inducible PIN7 tobacco lines, Lucie Perry co-supervised students and Eva Zažímalová (corresponding author) was involved in auxin-accumulation assays in tobacco lines and in the writing and editing of the manuscript.

At Tübingen University, various gene constructs for inducible expression of PIN and PGP proteins and *Arabidopsis* plants expressing inducible PIN proteins were prepared, expression analyses (RT-PCR) in plants overexpressing PIN and PGP proteins and gravitropism assays were performed, and namely Jiří Friml contributed substantially to coordination and covering the whole story.
In Zurich and Bern Universities, XVE-construct was prepared, and expressions of PIN7 and PIN2 proteins in yeast was done, including expression and localization analyses and auxin-accumulation assays. Mistargeted mutants of PIN2 were prepared in Whitehead Institute for Biomedical Research, Cambridge, USA, and relevant analyses were carried out at the University of Natural Resources and Applied Life Sciences-BOKU, Vienna. At Purdue University, USA, PIN7 and PIN2 were expressed in HeLa cells, and expression and localization analyses as well as auxin-accumulation assays were performed.

Our part of this paper was supported by the Grant Agency of the Academy of Sciences of the Czech Republic, project A6038303 to Eva Zažímalová and the Ministry of Education of the Czech Republic, projects MSM0021622415 and LC06034.

PIN Proteins Perform a Rate-Limiting Function in Cellular Auxin Efflux

Jan Petrášek,[1,2] Jozef Mravec,[3] Rodolphe Bouchard,[4] Joshua J. Blakeslee,[5] Melinda Abas,[6] Daniela Seifertová,[1,2,3] Justyna Wiśniewska,[3,7] Zerihun Tadele,[8] Martin Kubeš,[1,2] Milada Čovanová,[1,2] Pankaj Dhonukshe,[3] Petr Skůpa,[1,2] Eva Benková,[3] Lucie Perry,[1] Pavel Křeček,[1,2] Ok Ran Lee,[5] Gerald R. Fink,[9] Markus Geisler,[4] Angus S. Murphy,[5] Christian Luschnig,[6] Eva Zažímalová,[1]* Jiří Friml[3,10]

Intercellular flow of the phytohormone auxin underpins multiple developmental processes in plants. Plant-specific pin-formed (PIN) proteins and several phosphoglycoprotein (PGP) transporters are crucial factors in auxin transport–related development, yet the molecular function of PINs remains unknown. Here, we show that PINs mediate auxin efflux from mammalian and yeast cells without needing additional plant-specific factors. Conditional gain-of-function alleles and quantitative measurements of auxin accumulation in *Arabidopsis* and tobacco cultured cells revealed that the action of PINs in auxin efflux is distinct from PGP, rate-limiting, specific to auxins, and sensitive to auxin transport inhibitors. This suggests a direct involvement of PINs in catalyzing cellular auxin efflux.

Auxin, a regulatory compound, plays a major role in the spatial and temporal coordination of plant development (*1*–*3*). The directional active cell-to-cell transport controls asymmetric auxin distribution, which underlies multiple patterning and differential growth processes (*4*–*7*). Genetic approaches in *Arabidopsis thaliana* identified candidate genes coding for regulators of auxin transport, among them permease-like AUX1 (*8*), plant-specific PIN proteins (*9*) (fig. S1), and homologs of human multiple drug resistance transporters PGP1 and PGP19 (*10*, *11*). PGP1 has been shown to mediate the efflux of auxin from *Arabidopsis* protoplasts and heterologous systems such as yeast and HeLa cells (*12*). Similarly, PIN2 in yeast conferred decreased retention of structural auxin analogs (*13*, *14*). Plants defective in PIN function show altered auxin distribution and diverse developmental defects, all of which can be phenocopied by chemical inhibition of auxin efflux (*1*, *4*–*7*, *9*). All results demonstrate that PINs are essential components of the auxin transport machinery, but the exact mechanism of their action remains unclear.

Studies of the molecular function of PINs have been hampered mainly by the technical inability to quantitatively assess auxin flow across the plasma membrane (PM) in a multicellular system. We therefore established *Arabidopsis* cell suspension culture from the *XVE-PIN1* line, in which we placed the *PIN1* sequence under control of the estradiol-inducible promoter (*15*). Treatment with estradiol led to the activation of *PIN1* expression as shown by the coexpressed green fluorescent protein (GFP) reporter and reverse transcription polymerase chain reaction (RT-PCR) of *PIN1* in seedlings (Fig. 1A) and cultured cells (fig. S2). In estradiol-treated *XVE-PIN1* cells, the overexpressed PIN1 was localized at the PM (Fig. 1, B and C). The syn-

thetic auxin naphthalene-1-acetic acid (NAA) enters cells easily by diffusion and is a poor substrate for active uptake but an excellent substrate for active efflux (*16*). Therefore, change in accumulation of radioactively labeled NAA inside cells provides a measure of the rate of auxin efflux from cells. Untreated *XVE-PIN1* cells as well as nontransformed cells displayed [^{3}H]NAA accumulation kinetics indicative of saturable auxin efflux and sensitive to a well-established (*1*, *9*) noncompetitive inhibitor of auxin efflux: 1-naphthylphthalamic acid (NPA) (Fig. 1D). Estradiol did not influence control cells but led to substantial decrease of [^{3}H]NAA accumulation in *XVE-PIN1* cells (Fig. 1, D and E). This demonstrates that PIN1 overexpression leads to the stimulation of efflux of auxin from *Arabidopsis* cultured cells.

Arabidopsis cultured cells are not sufficiently friable to be useful in transport assays. Instead, we used tobacco BY-2 cells, a well-established model for quantitative studies of cellular auxin transport (*17*). PIN7, the most representative member of the subfamily including *PIN1*, *PIN2*, *PIN3*, *PIN4*, *PIN6*, and *PIN7* (fig. S1), was placed under the control of a dexamethasone (DEX)–inducible system (*18*) and stably transformed into BY-2 cells. The resulting line (*GVG-PIN7*) showed up-regulation of *PIN7* expression as early as 2 hours after DEX treatment and the up-regulated PIN7 protein was detected at the PM (Fig. 2A). Nontransformed cells displayed saturable, NPA-sensitive [^{3}H]NAA efflux, which was unaffected by DEX (Fig. 2B). Induction of expression of PIN7 or its close (PIN4) and the most distant (PIN6) homologs (fig. S1) resulted in a decrease in [^{3}H]NAA accumulation, to roughly half of the original level (Fig. 2C). The kinetics of NAA efflux after the initial loading of BY-2 cells (Fig. 2D), as well as displacement curves using competitive inhibition by nonlabeled NAA (fig. S3A), clearly confirm that PIN7 overexpression stimulates saturable efflux of auxin from cells. The efflux of other auxins—such as synthetic 2,4-dichlorophenoxyacetic acid (2,4-D) or naturally occurring indole-3-acetic acid (IAA), but not its precursor tryptophan—was also stimulated (Fig. 2, E and G). The PIN7-dependent efflux of all auxins was NPA sensitive (Fig. 2G), competitively inhibited by nonlabeled NAA, and unaffected by the structurally related but biologically inactive weak organic acid, benzoic acid (BeA) (fig. S3B). Furthermore, the increasing levels of induced PIN7, as achieved with the use of different concentrations of DEX for induction, and monitored by dot blot, clearly correlated with the gradual increase in [^{3}H]NAA efflux (Fig. 2F). These data imply that different PIN proteins are rate-limiting factors in NPA-sensitive, saturable efflux of auxins from BY-2 cells. This similarity in the molecular function of PINs, together with the diversity in their regulation, provides a basis for their complex functional redundancy observed in planta (*6*, *19*, *20*).

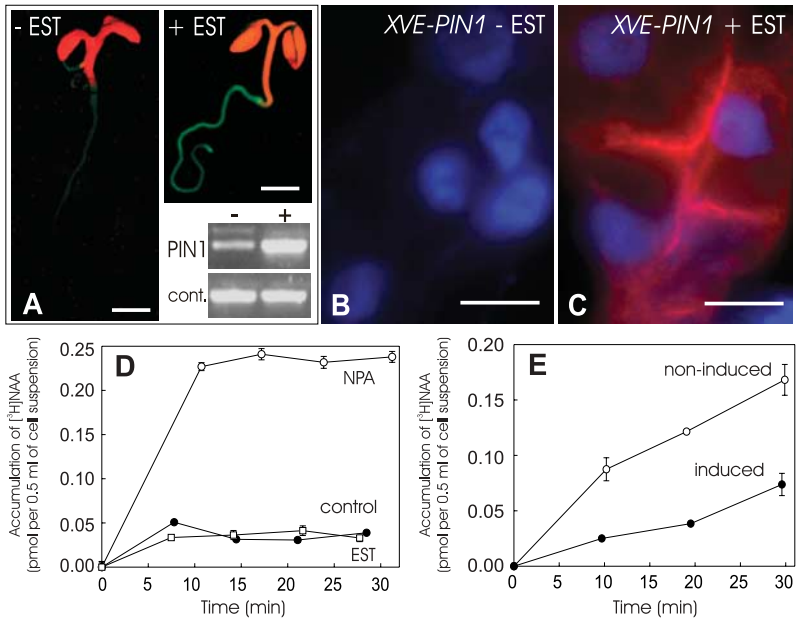

Fig. 1. PIN1-dependent auxin efflux in *Arabidopsis* cultured cells. (**A**) Up-regulation of PIN1 expression in *XVE-PIN1 Arabidopsis* seedlings after estradiol (EST) treatment (1 μM, 4 hours). The expression of coupled GFP reporter (green) and RT-PCR of *PIN1* [PGP19 expression was used as a control (cont.)] are shown. Scale bars, 3 mm. (**B** and **C**) Anti-PIN1 immunostaining (red) at the PM of *XVE-PIN1* cultured cells after EST treatment (1 μM, 24 hours) (C). There was no signal in the untreated control (B). Nuclear counterstain is shown in blue. Scale bars, 10 μm. (**D**) Auxin accumulation in *Arabidopsis* wild-type cells. NPA (10 μM) increased [^{3}H]NAA accumulation inside cells, demonstrating inhibition of auxin efflux. EST treatment (1 μM, 24 hours) had no effect on [^{3}H]NAA accumulation. (**E**) [^{3}H]NAA accumulation kinetics in *XVE-PIN1* cells, demonstrating PIN1-dependent stimulation of NAA efflux after PIN1 overexpression. Error bars show SEM (n = 4); where error bars are not shown, the error was smaller than the symbols.

The evidence from cultured cells shows that PIN proteins are key rate-limiting factors in cellular auxin efflux. This approach, however, cannot distinguish whether PINs play a catalytic role in auxin efflux or act as positive regulators of endogenous plant auxin efflux catalysts. To address this issue, we used a nonplant system: Human HeLa cells contain neither PIN-related genes nor auxin-related machinery and allow efficient heterologous expression of functional eukaryotic PM proteins (*21*). We transfected HeLa cells with *PIN7* and its more distant homolog *PIN2*. Transfected cells showed strong PIN expression (Fig. 3A), which resulted in a substantial stimulation of net efflux of natural auxin [^{3}H]IAA, compared with empty vector controls (Student's t test: $P < 0.001$) (Fig. 3B). Efflux of [^{3}H]BeA was also stimulated but to a lesser extent. These data show that PIN proteins are capable of stimulating cellular auxin efflux in the heterologous HeLa cell system, albeit with decreased substrate specificity.

To test the role of PIN proteins in another evolutionarily distant nonplant system, we used yeast (*Saccharomyces cerevisiae*). PIN2 and PIN7 were expressed in yeast and showed localization at the PM (Fig. 3A). Kinetics of relative [^{3}H]IAA retention demonstrated that expression of the PINs led to a substantial increase in IAA efflux (Fig. 3C). Efflux assays in conjunction with control experiments, including testing metabolically less active yeast in the stationary phase, or after glucose starvation (Fig. 3D), confirmed an active PIN-dependent export of IAA and, to a lesser extent, of BeA from yeast (Fig. 3C and fig. S4B). To test the requirements of the subcellular localization for PIN2 action in yeast, we performed a mutagenesis of the PIN2 sequence to isolate mistargeted mutants. One of the mutations, which changed serine-97 to glycine (pin2Gly97), led to the localization of pin2Gly97

[1]Institute of Experimental Botany, the Academy of Sciences of the Czech Republic, 165 02 Prague 6, Czech Republic. [2]Department of Plant Physiology, Faculty of Science, Charles University, 128 44 Prague 2, Czech Republic. [3]Center for Plant Molecular Biology (ZMBP), University Tübingen, D-72076 Tübingen, Germany. [4]Zurich-Basel Plant Science Center, University of Zurich, Institute of Plant Biology, CH 8007 Zurich, Switzerland. [5]Department of Horticulture, Purdue University, West Lafayette, IN 47907, USA. [6]Institute for Applied Genetics and Cell Biology, University of Natural Resources and Applied Life Sciences–Universität für Bodenkultur, A-1190 Wien, Austria. [7]Department of Biotechnology, Institute of General and Molecular Biology, 87-100 Toruń, Poland. [8]Institute of Plant Sciences, University of Bern, 3013 Bern, Switzerland. [9]Whitehead Institute for Biomedical Research, Nine Cambridge Center, Cambridge, MA 02142, USA. [10]Masaryk University, Department of Functional Genomics and Proteomics, Laboratory of Molecular Plant Physiology, Kamenice 5, 625 00 Brno, Czech Republic.

*To whom correspondence should be addressed. E-mail: eva.zazim@ueb.cas.cz

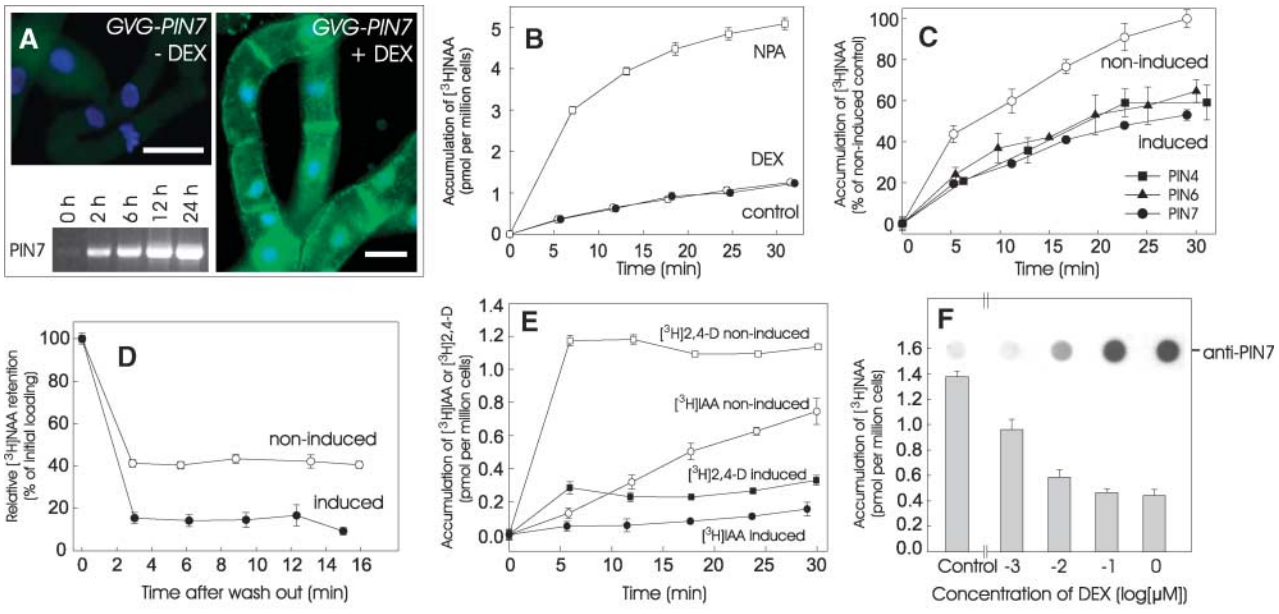

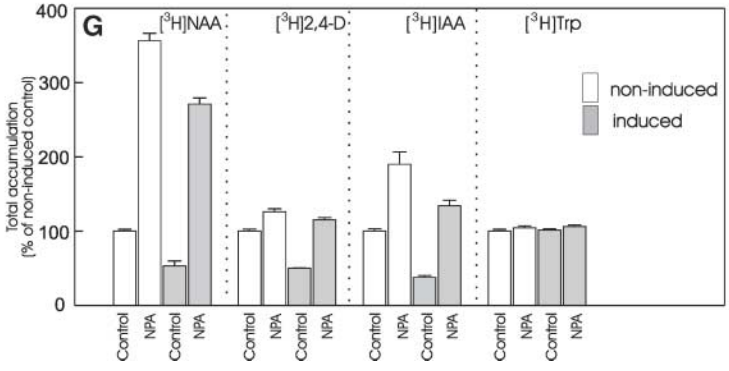

Fig. 2. PIN-dependent auxin efflux in BY-2 tobacco cultured cells. (**A**) Inducible PIN7 expression in *GVG-PIN7* tobacco cells. PIN7 immunostaining (green) is shown at the PM after DEX treatment (24 hours; 1 μM) but not in the untreated control; RT-PCR of *PIN7* was conducted within 24 hours of DEX treatment (1 μM). Nuclear counterstain is shown in blue. Scale bars, 40 μm. (**B**) Auxin accumulation in BY-2 control cells. NPA (10 μM) increased [^{3}H]NAA accumulation inside cells, demonstrating inhibition of auxin efflux. DEX treatment (1 μM, 24 hours) had no effect on [^{3}H]NAA accumulation. (**C**) [^{3}H]NAA accumulation kinetics in *GVG-PIN4*, *GVG-PIN6*, and *GVG-PIN7* cells demonstrating PIN4-, PIN6-, and PIN7-dependent stimulation of NAA efflux. Noninduced control is shown only for PIN7; those for PIN4 and PIN6 were within the range ±8% of the values for PIN7. Data are expressed as a percentage of noninduced control at 30 min after application of labeled [^{3}H]NAA. (**D**) Induced *GVG-PIN7* cells showed decreased retention of [^{3}H]NAA compared with noninduced control. (**E**) Accumulation kinetics in induced *GVG-PIN7* cells revealed PIN7-dependent stimulation of [^{3}H]IAA and [^{3}H]2,4-D efflux. (**F**) Treatments with increasing concentrations of DEX led to gradually higher levels of PIN7 in *GVG-PIN7* cells, as determined by dot blot (top) and to concomitant decrease of [^{3}H]NAA accumulation. (**G**) NPA inhibition of both endogenous and PIN7-dependent efflux of [^{3}H]NAA, [^{3}H]2,4-D, and [^{3}H]IAA. PIN7 overexpression or NPA treatment did not affect accumulation of related compound, [^{3}H]Trp. Open bars, noninduced cells; gray bars, induced cells. For all experiments, error bars show SEM (n = 4); where error bars are not shown, the error was smaller than the symbols.

in intracellular compartments (Fig. 3A). When tested in the [^{3}H]IAA efflux assay (fig. S4A), pin2Gly97 failed to mediate auxin efflux but rather increased [^{3}H]IAA accumulation inside cells (Fig. 3D). This shows that pin2Gly97 is still functional but fails to mediate auxin efflux, suggesting importance of PIN localization at PM. Overall, the results suggest that in yeast as well, PM-localized PIN proteins mediate, although with decreased specificity, a saturable efflux of auxin.

A role in auxin efflux has also been reported recently for PGP1 and, in particular, PGP19 proteins of *Arabidopsis* (*12*). PIN and PGP proteins seem to have a comparable effect on mediating auxin efflux in yeast and HeLa cells, but the genetic interference with their function in *Arabidopsis* has distinctive effects on development. All aspects of the *pin* mutant phenotypes can be mimicked by chemical interference with auxin transport (*4*–*7*, *9*). In contrast, *pgp1*/*pgp19* double mutants show strong but entirely different defects (*10*, *11*), which cannot be phenocopied by auxin transport inhibitors.

To compare the roles of PINs and PGPs in auxin efflux, we constructed the *GVG-PGP19:HA* (hemagglutinin) cell line of BY-2. DEX treatment led to the up-regulation of PGP19:HA protein, which was detected at the PM (Fig. 4A), and to a decrease in [^{3}H]NAA accumulation, similar to that observed in the *GVG-PIN4*, *GVG-PIN6*, and *GVG-PIN7* lines (Fig. 4B, compare with Fig. 2C). BeA did not interfere with [^{3}H]NAA accumulation and [^{3}H]Trp accumulation did not change after DEX treatment. However, compared with PIN-mediated auxin efflux, the PGP19-mediated NAA efflux was notably less sensitive to NPA. Whereas PIN-mediated transport was completely inhibited by NPA, about 20% of PGP19-dependent transport was NPA insensitive (Fig. 4C).

To address whether PIN action in planta requires PGP1 and PGP19 proteins, we analyzed effects of PIN1 overexpression on plant development in *pgp1*/*pgp19* double mutants. PIN1 overexpression in *XVE-PIN1* led to pronounced defects in root gravitropism, which could be detected within 4 hours after estradiol treatment. Quantitative evaluation of reorientation of root growth revealed that PIN1 overexpression in *pgp1*/*pgp19* had the same effects (Fig. 4D). These data show that PIN1 action on plant development does not strictly require function of PGP1 and PGP19 proteins, and they suggest that PINs and PGPs molecularly characterize distinct auxin transport systems. This is also supported by evidence that PIN2 mediates auxin efflux in yeast, which is known to lack homologs to *Arabidopsis* PGP proteins (*21*). It is still unclear whether these two auxin transport machineries act in planta entirely independently or in a coordinated fashion.

Rate-limiting, saturable, and specific action of PIN proteins in mediating auxin movement

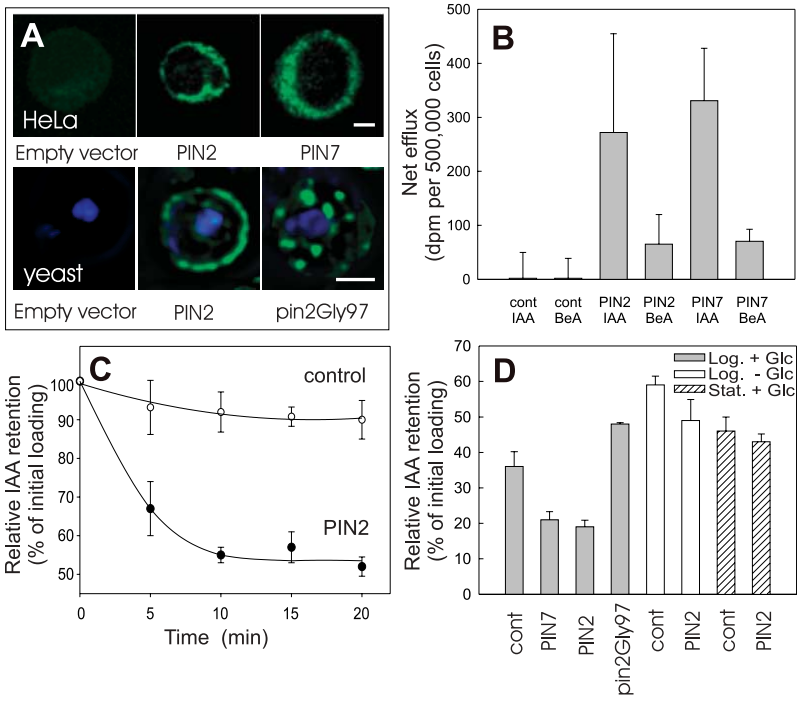

Fig. 3. PIN-dependent auxin efflux in mammalian and yeast cells. (**A**) PIN2:HA and PIN7:HA expression in HeLa and yeast. Anti-HA immunostaining detected PIN2:HA and PIN7:HA at the PM of transfected but not control (empty vector) HeLa cells (top). Anti-PIN2 immunostaining detected PIN2 at the PM and pin2Gly97 in intracellular compartments, compared with empty vector controls (bottom). Scale bars, 2 μm. (**B**) Transfected HeLa cells display PIN2- and PIN7-dependent net efflux of [^{3}H]IAA and to a smaller extent also of [^{3}H]BeA. dpm, disintegration per minute. (**C**) The kinetics of [^{3}H]IAA efflux. PIN2 stimulated saturable [^{3}H]IAA efflux in yeast JK93da strain. (**D**) [^{3}H]IAA retention measured 10 min after loading: PIN2 and PIN7 mediated [^{3}H]IAA efflux; pin2Gly97 failed to mediate efflux but increased [^{3}H]IAA retention. Yeast in stationary phase or without glucose showed much less [^{3}H]IAA efflux. Error bars show SEM (n = 4).

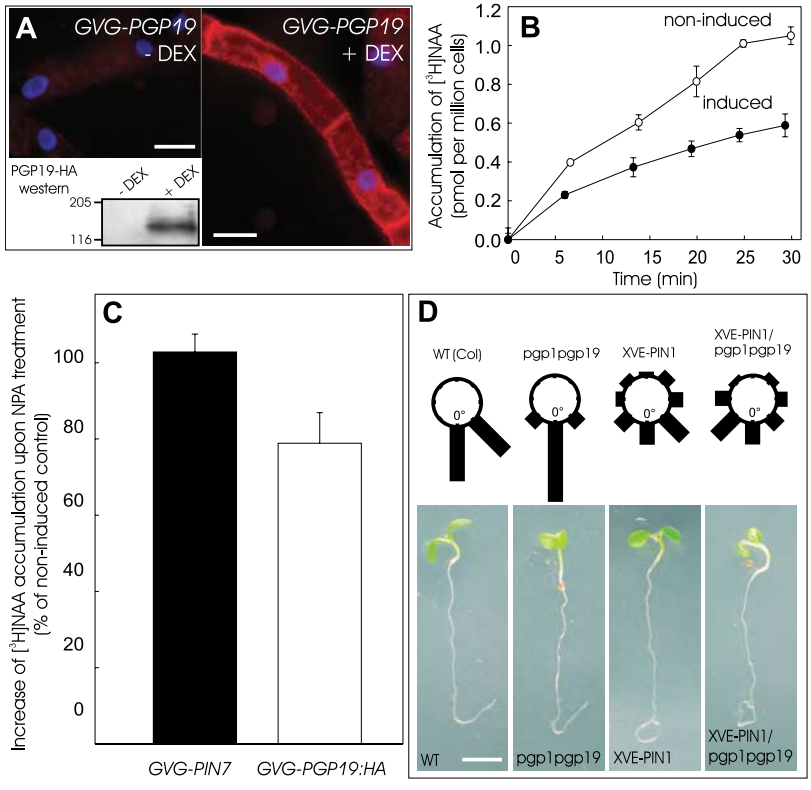

Fig. 4. Requirement of PGP function for PIN role in auxin efflux. (**A**) Inducible PGP19 expression in *GVG-PGP19:HA* tobacco cells. PGP19:HA immunostaining (red) at PM after DEX treatment (24 hours, 1 μM) is shown; no PGP19:HA immunostaining was present in the untreated control. An anti-HA immunoblot was conducted after 24 hours of DEX (1 μM) treatment. Nuclear counterstain is shown in blue. Scale bars, 40 μm. (**B**) [^{3}H]NAA accumulation decreased upon PGP19 expression, revealing function in auxin efflux in BY-2 cells. (**C**) Different sensitivities of PIN7- and PGP19-dependent [^{3}H]NAA efflux to NPA treatment (10 μM, 20 min) in *GVG-PIN7* and *GVG-PGP19:HA* cells (*23*). (**D**) Root gravitropism in *XVE-PIN1* seedlings. PIN1 overexpression (4 hours, 4 μM EST) led to gravitropic defects in *pgp1/pgp19* mutants in contrast to gravitropic growth of EST-treated nontransformed wild-type (WT) and *pgp1/pgp19* seedlings. Root gravitropism was scored 12 hours after gravity stimulation (n > 40). Scale bar, 3 mm. For (B) and (C), error bars show SEM (n = 4); where error bars are not shown, the error was smaller than the symbols.

across the PM out of plant cells largely clarifies a role of PIN proteins in intercellular auxin transport. Furthermore, the polar, subcellular PIN localization provides a vectorial component to the directional auxin flow (*22*). Therefore, transport function of PINs together with their asymmetric subcellular localization defines directional local auxin distribution underlying different developmental processes.

References and Notes

1. J. Friml, *Curr. Opin. Plant Biol.* **6**, 7 (2003).
2. A. W. Woodward, B. Bartel, *Ann. Bot. (Lond.)* **95**, 707 (2005).
3. S. Kepinski, O. Leyser, *Curr. Biol.* **15**, R208 (2005).
4. J. Friml, J. Wisniewska, E. Benková, K. Mendgen, K. Palme, *Nature* **415**, 806 (2002).
5. J. Friml *et al.*, *Cell* **108**, 661 (2002).
6. J. Friml *et al.*, *Nature* **426**, 147 (2003).
7. E. Benková *et al.*, *Cell* **115**, 591 (2003).
8. M. Bennett *et al.*, *Science* **273**, 948 (1996).
9. I. A. Paponov, W. D. Teale, M. Trebar, I. Blilou, K. Palme, *Trends Plant Sci.* **10**, 170 (2005).
10. B. Noh, A. S. Murphy, E. P. Spalding, *Plant Cell* **13**, 2441 (2001).
11. J. J. Blakeslee, W. A. Peer, A. S. Murphy, *Curr. Opin. Plant Biol.* **8**, 494 (2005).
12. M. Geisler *et al.*, *Plant J.* **44**, 179 (2005).
13. R. Chen, *Proc. Natl. Acad. Sci. U.S.A.* **95**, 15112 (1998).
14. C. Luschnig, R. A. Gaxiola, P. Grisafi, G. R. Fink, *Genes Dev.* **12**, 2175 (1998).

15. J. Zuo, Q. W. Niu, N. H. Chua, *Plant J.* **24**, 265 (2000).
16. A. Delbarre, P. Muller, V. Imhoff, J. Guern, *Planta* **198**, 532 (1996).
17. J. Petrášek *et al.*, *Plant Physiol.* **131**, 254 (2003).
18. T. Aoyama, N. H. Chua, *Plant J.* **11**, 605 (1997).
19. I. Blilou, *Nature* **433**, 39 (2005).
20. A. Vieten *et al.*, *Development* **132**, 4521 (2005).
21. M. Geisler, A. S. Murphy, *FEBS Lett.* **580**, 1094 (2006).
22. J. Wiśniewska, *Science* **312**, 883 (2006).
23. Materials and methods are available as supporting material on *Science* Online.

24. We thank N. H. Chua for providing material, V. Croy for help with HeLa studies, and P. Brewer and M. Sauer for critical reading of the manuscript. This work was supported by the European Molecular Biology Organization Young Investigator programme (J.F.), the Volkswagenstiftung (J.F., J.M., D.S., P.D.), the Grant Agency of the Academy of Sciences of the Czech Republic, project A6038303 (E.Z., M.Č., M.K., P.K., J.P., L.P., D.S., and P.S.), the Ministry of Education of the Czech Republic, projects MSM0021622415 and LC06034, the Alexander von Humboldt Foundation (Feodor Lynen fellowship to M.G.), the Foundation for Polish Science (J.W.), Margarete von Wrangell-Habilitationsprogramm (E.B.), NSF grant 0132803 (A.M., J.B., and O.L.), and Austrian Science Fund (FWF) grant 16311 (L.A. and C.L).

Supporting Online Material

www.sciencemag.org/cgi/content/full/1123542/DC1
Materials and Methods
Figs. S1 to S4
References

7 December 2005; accepted 14 March 2006
Published online 6 April 2006;
10.1126/science.1123542
Include this information when citing this paper.

www.sciencemag.org/cgi/content/full/1123542/DC1

Supporting Online Material for

PIN Proteins Perform a Rate-Limiting Function in Cellular Auxin Efflux

Jan Petrášek, Jozef Mravec, Rodolphe Bouchard, Joshua J. Blakeslee, Melinda Abas, Daniela Seifertová, Justyna Wiśniewska, Zerihun Tadele, Martin Kubeš, Milada Čovanová, Pankaj Dhonukshe, Petr Skůpa, Eva Benková, Lucie Perry, Pavel Křeček, Ok Ran Lee, Gerald R. Fink, Markus Geisler, Angus S. Murphy, Christian Luschnig, Eva Zažímalová,* Jiří Friml

*To whom correspondence should be addressed. E-mail: eva.zazim@ueb.cas.cz

Published 6 April 2006 on *Science* Express
DOI: 10.1126/science.1123542

This PDF file includes:

Supporting online material

Materials and Methods

Plant material, gene constructs, transformation and inducible expression

Arabidopsis seedlings were grown at a 16 hours light/8 hours dark cycle at 18-25 °C on 0.5 x MS with sucrose as described (*1*). The *XVE-PIN1* (Col-0) transgenic plants were obtained by introducing the $p_{G10\text{-}90}$*::XVE* activator and the *LexA::PIN1*; *LexA::GFP* reporter constructs (*2, 3*) into *pin1-7* mutant line. This line was crossed with *pgp1pgp19* double mutant (*4*) to generate *XVE-PIN1/pgp1pgp19* line. The *XVE-PIN1* construct was generated using *PIN1* cDNA (GenBank accession number AF089084). *GVG-PIN4,6,7* constructs were generated by inserting the corresponding cDNAs (*PIN4*: AF087016, *PIN6*: AF087819, *PIN7*: AF087820) into the pTA7002 vector (*5*). *GVG-PGP19:HA* construct was generated by introducing the full length genomic fragment of *PGP19* (locus name At3g28860) with C-terminal hemaglutinin tag (HA) into pTA7002 vector (*5*).
Cell suspension from *XVE-PIN1 Arabidopsis* line was established from calli induced on young leaves (*6*) and grown in liquid MS medium containing 1 μM 2,4-D. BY-2 tobacco cells (*Nicotiana tabacum* L., cv. Bright Yellow 2, (*7*)) were grown as described (*8*) and stably transformed by co-cultivation with *Agrobacterium* (*8*). Transgenic tobacco cells and calli were maintained on the media supplemented with 40 μg ml^{-1} hygromycin and 100 μg ml^{-1} cefotaxim. Expression of *PIN* and *PGP* genes in tobacco cells was induced by the addition of dexamethasone (DEX, 1 μM, 24 hours, except for stated otherwise) at the

beginning of the subcultivation period. The same approach was used for *Arabidopsis* cell culture, where 1 μM β-Estradiol (EST) was added. Both DEX and EST were added from stock solutions in DMSO (200 μM), appropriate volume of DMSO was added in controls.

Expression and localization analysis

Tobacco and *Arabidopsis* RNA was isolated using the Plant RNA Qiagen Mini-Prep and RT-PCR performed using Qiagen® OneStep RT-PCR or Invitrogen SuperSriptII kits according to the manufacturer's protocols.

Total protein fraction from *GVG-PGP19* tobacco cells was obtained after homogenization in liquid nitrogen using mortar and pestle. The frozen powder was then mixed with an equal volume of extraction buffer (50 mM Tris-HCl, pH 6.8; 2 % SDS; 36 % w/v urea; 30 % v/v glycerol; 5 % v/v mercaptoethanol; 0,5 % w/v Bromphenol Blue), vortexed for 1 min, boiled for 3 min, and centrifuged at 13,000 rpm and 4°C for 5 min. The supernatant was transferred into a new tube and re-centrifuged at 13,000 rpm and 4°C for 5 min. The resulting supernatant was defined as total protein extract and stored at –20°C until use.

Microsomal protein fraction from *GVG-PIN7* tobacco cells was used for immunoblot analysis of PIN7 protein. Briefly, cells were homogenized by sonication in extraction buffer (50mM Tris pH 6.8; 5% (v/v) glycerol; 1.5% (w/v) insoluble polyvinylpolypyrrolidone; 150mM KCl; 5mM Na EDTA; 5mM Na EGTA; 50mM NaF; 20mM beta-glycerol phosphate; 0.5% (v/v) solubilized casein, 1mM benzamidine; 1mM PMSF; 1μg/ml pepstatin; 1μg/ml leupeptin; 1μg/ml aprotinin; 1 Roche Complete Mini Protease Inhibitor tablet per 10ml). After centrifugation at 3,800 x *g* for 20 minutes, the supernatant was filtered through nylon mesh and spun again at 3,800 x *g*. The supernatant was centrifuged

at 100,000 x *g* for 90 min. The resulting pellet was homogenized and re-suspended in buffer containing 50mM Tris pH 7.5; 20% glycerol; 2mM EGTA; 2mM EDTA; 50-500µM DTE; 10µg/ml solubilized casein and protease inhibitors as in the extraction buffer. Equal amounts of protein (about 10µg) were heated at 60°C for 40 min in sample buffer (3% (w/v) SDS; 40mM DTE; 180mM Tris pH 6.8; 8M urea), and transferred on PVDF membrane using dot-blot (SCIE-PLAS, U.K.) or semi-dry electro-blot. Primary rabbit polyclonal anti-PIN7 antibody (*10*) or mouse monoclonal anti-HA antibody (Sigma) followed by secondary HRP-conjugated anti-rabbit antibody and ECL detection kit (Amersham Biosciences, U.K.) were used for dot or western blot analysis.

Indirect immunofluorescence method was used for immunolocalizations in *Arabidopsis* cell suspension (11) and BY-2 cells (*8*). Briefly, *Arabidopsis* cells were fixed for 30 min at room temperature with 4% (w/v) paraformaldehyde in 0.1 M PIPES, pH 6.8, 5 mM EGTA, 2 mM $MgCl_2$, and 0.4% (w/v) Triton X-100. Cells were then treated with the solution of 0.8% (w/v) macerozyme R-10 and 0.2% (w/v) pectolyase Y-23 in 0.4 M mannitol, 5 mM EGTA, 15 mM MES, pH 5.0, 1 mM PMSF, 10 µg/ml of leupeptin, and 10 µg/ml of pepstatin A. Then the cells were washed in PBS buffer and attached to poly-L-lysine coated coverslips and incubated for 30 min in 1% (w/v) BSA in PBS and incubated for 1 h with primary antibody. The specimens were then washed three times for 10 min in PBS and incubated for 1 h with secondary antibody. Coverslips with cells were carefully washed in PBS, rinsed with water with Hoechst 33258 (0,1µg/ml) and embedded in Mowiol (Polysciences) solution.

Tobacco BY-2 cells were pre-fixed 30 min in 100 µM MBS and 30 min in 3.7% (w/v) PFA in buffer consisting of 50 mM PIPES, 2 mM EGTA, 2 mM $MgSO_4$, pH 6.9, at 25°C and

subsequently in 3.7% (w/v) PFA and 1% Triton X-100 (w/v) in stabilizing buffer for 20 minutes. After treatment with an enzyme solution (1% (w/v) macerozyme and 0.2% (w/v) pectinase) for 7 min at 25°C and 20 minutes in ice cold methanol (at -20°C), the cells were attached to poly-L-lysine coated coverslips and treated with 1% (w/v) Triton X-100 in microtubule stabilizing buffer for 20 minutes. Then the cells were treated with 0.5% (w/v) bovine serum albumin in PBS and incubated with primary antibody for 45 minutes at 25°C. After washing with PBS, a secondary antibody in PBS was applied for 1 h at 25°C. Coverslips with cells were carefully washed in PBS, rinsed with water with Hoechst 33258 (0,1µg/ml) and embedded in Mowiol (Polysciences) solution.

The following antibodies and dilutions were used: anti- PIN1 (*13*, 1: 500), anti-PIN7 (*10*, 1:500), anti-HA (Sigma-Aldrich; 1:500), TRITC- (Sigma-Aldrich; 1:200), FITC- (Sigma-Aldrich; 1:200) anti-rabbit secondary antibodies. PIN immunostaining in yeast and HeLa cells was performed as described (*13, 14*).

All preparations were observed using an epifluorescence microscope (Nikon Eclipse E600) equipped with appropriate filter sets, DIC optics, monochrome integrating CCD camera (COHU 4910, USA) or colour digital camera (DVC 1310C, USA).

Quantitative analysis of root gravitropism

5 days old seedlings of WT-Col, *pgp1pgp19*, *XVE-PIN1* and *XVE-PIN 1/pgp1pgp19* lines grown vertically were transferred on new MS plates containing 4 µM β-estradiol for 12 hours. Seedlings were then stretched and plates turned through 135° for additional 12 hour gravity stimulation in dark. The angle of root tips from the vertical plane was measured using ImageJ software (NIH, USA). All gravistimulated roots were assigned to one of the

eight 45° sectors on gravitropism diagram. The length of bars represents the percentage of seedlings showing respective direction of root growth.

Auxin accumulation assays in plant, HeLa and yeast cells

Auxin accumulation experiments in suspension-cultured tobacco BY-2 cells were performed and the integrity of labeled auxins during the assay was checked exactly as described (*15, 8, 12*). The same protocol was used for suspension-cultured *Arabidopsis* cells. Labeled [^{3}H]IAA, [^{3}H]2,4-D and [^{3}H]Trp (specific activities 20 Ci/mmol, American Radiolabeled Chemicals, St. Louis, MO), and [^{3}H]NAA (specific radioactivity 25 Ci/mmol, Institute of Experimental Botany, Prague, Czech Republic) were used. Briefly, the accumulation was measured in 0.5-mL aliquots of cell suspension. Each cell suspension was filtered, resuspended in uptake buffer (20 mM MES, 40 mM Suc, and 0.5 mM $CaSO_4$, pH adjusted to 5.7 with KOH), and equilibrated for 45 min with continuous orbital shaking. Equilibrated cells were collected by filtration, resuspended in fresh uptake buffer, and incubated on the orbital shaker for 1.5 h in darkness at 25°C. [^{3}H]NAA was added to the cell suspension to give a final concentration of 2 nM. After a timed uptake period, 0.5-mL aliquots of suspension were withdrawn and accumulation of label was terminated by rapid filtration under reduced pressure on 22-mm-diameter cellulose filters. The cell cakes and filters were transferred to scintillation vials, extracted in ethanol for 30 min, and radioactivity was determined by liquid scintillation counting (Packard Tri-Carb 2900TR scintillation counter, Packard Instrument Co., Meriden, CT). Counts were corrected for surface radioactivity by subtracting counts obtained for aliquots of cells collected immediately after the addition of [^{3}H]NAA. Counting efficiency was determined by

automatic external standardization, and counts were corrected automatically. NPA was added as required from ethanolic stock solutions to give the appropriate final concentration. The concentration dependence of auxin accumulation in response to NPA or BFA was determined after a 20-min uptake period. For wash out experiments cells were loaded with [^{3}H]NAA (2 nM) for 30 min. After quick wash out, cells were re-suspended in fresh loading buffer but without [^{3}H]NAA; cell density before and after wash out was maintained the same. Relative NAA retention was measured as a radioactivity retained inside cells at particular time points after wash out and expressed as % of total radioactivity retained inside the cells just before wash out. The accumulation of various auxins or structurally related inactive compound (Trp) after induction of PIN or PGP expression was expressed together with SEs as the percentage of the accumulation of non-induced cells at time 30 min after application of respective labelled compound. If not indicated otherwise, 24 hours treatments with dexamethasone (1 μM) or β-estradiol (1 μM) were performed. Different sensitivities of PIN7- and PGP19-dependent [^{3}H]NAA efflux to NPA treatment (10 μM, 20 min) in *GVG-PIN7* and *GVG-PGP19:HA* cells was determined as the average value from three independent experiments. In each, the accumulation of [^{3}H]NAA was measured in NPA-treated induced and non-induced cells and scored after 20 minutes of incubation. The increase in the accumulation of [^{3}H]NAA upon NPA treatment in non-induced cells was considered as 100% and all other values expressed as the percentage of this increase.

The transient vaccinia expression system was used to transfect HeLa cells with PIN1:HA, PIN2:HA, and PIN7:HA in 6-well plates. The expression was verified by RT-PCR and western blot analysis. Auxin transport assays were performed exactly as described (*16, 14*). 16-24h after transfection cells were washed and incubated 40 min at 37°C, 5% CO_2 with

[^{3}H]IAA (26 Ci/mmol, Amersham Biosciences, Piscataway, NJ), or [^{3}H]BeA (20 Ci/mmol, American Radiolabeled Chemicals, St. Louis, MO). After incubation, cells were harvested, and retained radiolabeled substrate was quantitated. Net efflux is expressed as dpm/500,000 cells divided by the amount of auxin retained by cells transformed with empty vector minus the amount of auxin retained by cells transformed with gene of interest. Thus, the PIN-dependent decrease in retention is presented as positive efflux value expressed as means (n=3) with standard deviations. Cell viability after treatment was confirmed visually and via cell counting.

For auxin accumulation and growth assays in yeast, PIN2, PIN7 or PIN2:HA were expressed in *S. cerevisiae* strains *gef1* (*13*) and JK93da or *yap1-1* (*17*). The expression was verified by western blot analysis or immunolocalization. Export of [^{3}H]IAA (specific activity 20 Ci/mmol, American Radiolabeled Chemicals, St. Louis, MO) and [^{14}C]BeA (53 mCi/mmol, Moravek Biochemicals, Brea, CA) and growth assays were performed exactly as described (*17, 14*). The effluent species was determined by thin-layer chromatography of aliquots of exported [^{3}H]IAA (Supplementary fig. S4a) and images were taken using a phosphoimager (Cyclone, Packard Instruments) and by UV detection using [^{3}H]IAA as standard. Yeast viability before and after transport experiments was ascertained by light microscopy.

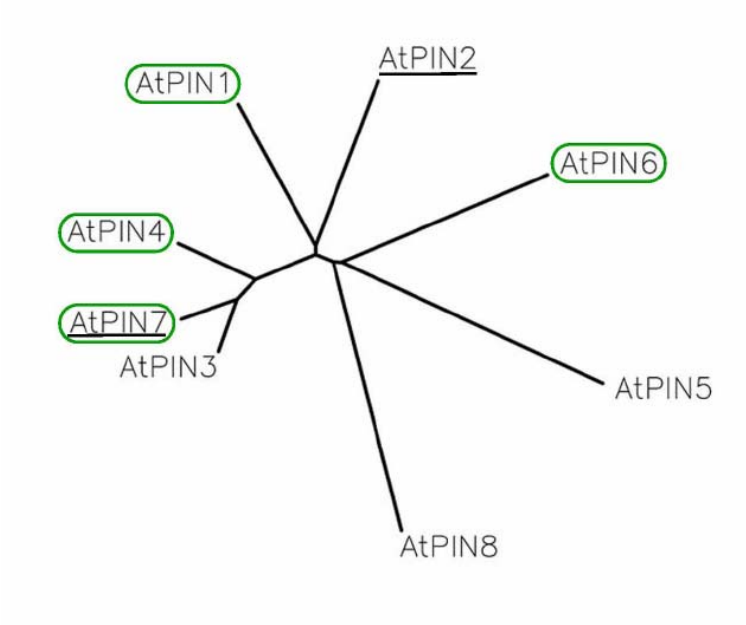

fig. S1 Arabidopsis *PIN* genes family.

Phylogenetic tree of 8 Arabidopsis *PIN* genes. Phenotypes of loss-of-function mutants in *PIN1*, *PIN2*, *PIN3*, *PIN4* and *PIN7* clearly suggest role in polar auxin transport and they all can be phenocopied by inhibitors of auxin transport (*18*). PIN6 remains functionally uncharacterized. PIN5 and PIN8 lack the middle hydrophilic domain and seem to by functionally distinct (*19*). Based on homology, *PIN7* is the most typical member of PIN family forming a distinct homologous subclade with *PIN3* and *PIN4*. *PIN6*, on the other hand, is the least homologous *PIN* from the *PIN1,2,3,4,6,7* subfamily. PIN1, PIN4, PIN6 and PIN7 (respective genes encircled in green) have been shown here to mediate auxin efflux *in planta*. PIN2 and PIN7 (genes underlined) show auxin efflux activity in heterologous systems. Notably, the confirmed expression of PIN1 in HeLa or yeast cells did not result in increased auxin efflux suggesting, in contrast to PIN2 and PIN7, that either PIN1 loses its functionality, when expressed in heterologous system, or distinctively PIN1 requires plant-specific factor(s) to mediate its function in auxin efflux.

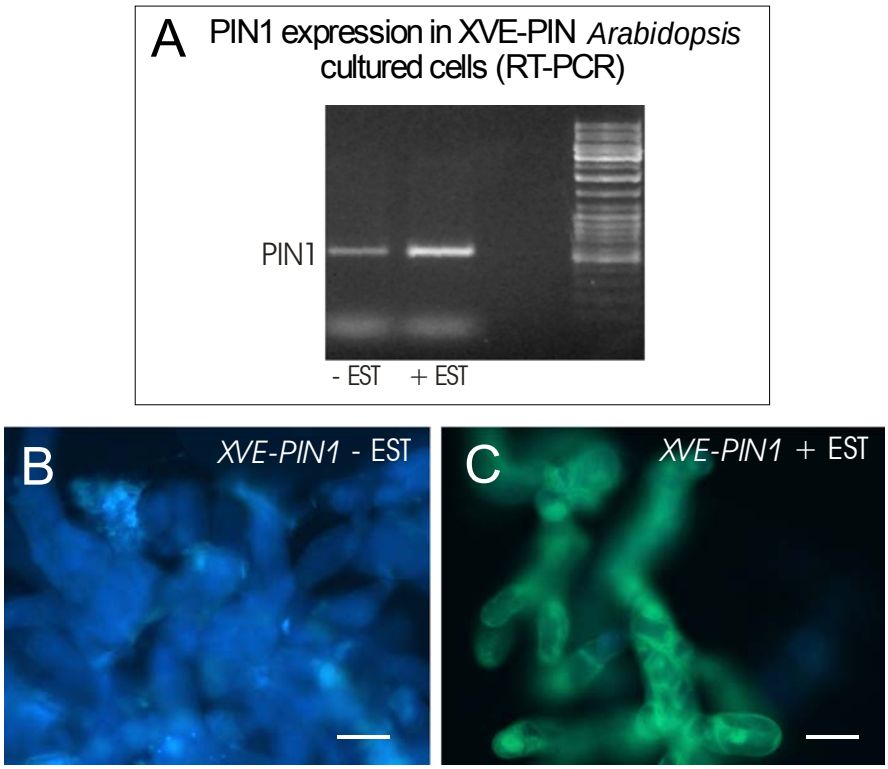

fig. S2 The expression of PIN1 in *XVE-PIN1 Arabidopsis* cultured cells

(A) RT-PCR of PIN1 in non-induced and β-estradiol-induced (1 μM, 24h) cells. (B, C) The activation of expression verified by the fluorescence of co-expressed GFP reporter. Compare the autofluorescence of cell walls in non-induced cells (B) with GFP fluorescence after 24 h incubation in 1 μM β-estradiol (C). Scale bars 30μm.

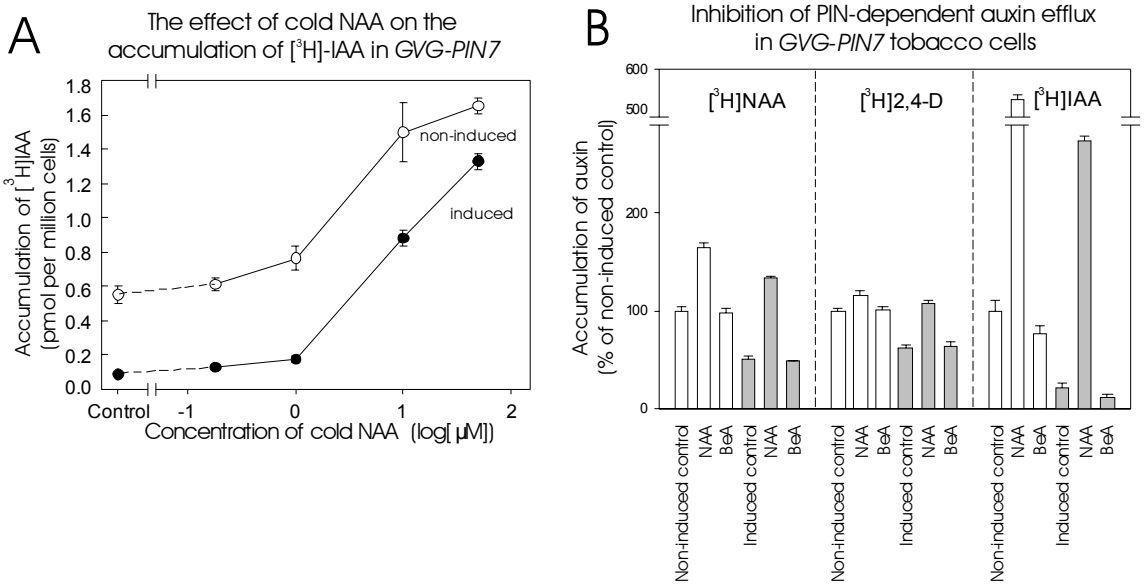

fig. S3 Auxin accumulation in *GVG-PIN7* BY-2 cells

(A) Displacement curve: The competitive inhibitory effect of cold (non-labeled) NAA on the accumulation of [^{3}H]IAA in non-induced and induced *GVG-PIN7* cells. (B) Effects of NAA and benzoic acid (BeA) on efflux of different auxins in DEX-treated (induced, full bars) and non-induced (open bars) *GVG-PIN7* cells. NAA (10 µM), a good substrate for auxin efflux machinery, interferes with both endogenous and PIN7-dependent efflux of [^{3}H]NAA, [^{3}H]2,4-D and [^{3}H]IAA in non-induced and induced *GVG-PIN7* cells, respectively. In contrast, structurally similar but inactive BeA (10 µM) does not have any detectable effect in the same experimental system.

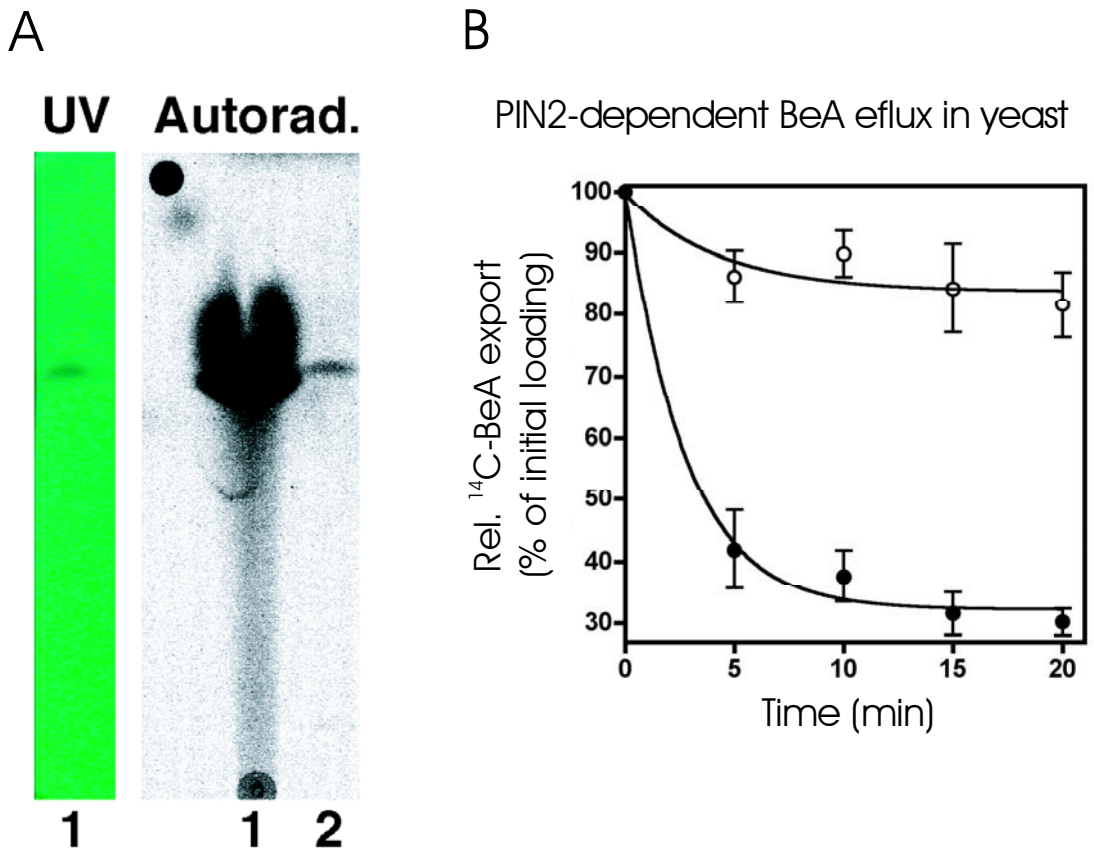

fig. S4 Control experiments for auxin efflux assays in yeast.

(A) The effluent species in yeast were determined to be [^{3}H]IAA by thin layer chromatography (lane 2). Non-exported [^{3}H]IAA was used as the standard which itself was verified by UV detection (lane 1). Images were taken using a phosphoimager (Cyclone, Packard Instruments) and by UV detection using [^{3}H]IAA as the standard. The integrity of exported [^{3}H]IAA in this assay was also proved by MS-MS, as described elsewhere (*14*).

(B) PIN2-expressing yeast show increased net efflux of [^{14}C]benzoic acid ([^{14}C]BeA)

compared to empty vector controls. [^{14}C]BeA (53 mCi/mmol, Moravek Biochemicals, Brea, CA) was used and transport experiments were performed exactly as described (*14*).

Supporting references and notes

1. E. Benková *et al.*, *Cell* **115**, 591 (2003).

2. P. J. Jensen, R. P. Hangarter, M. Estelle, *Plant. Physiol.* **116**, 455 (1998).

3. J. Zuo., Q.W. Niu, N.H. Chua, *Plant J.* **24**, 265 (2000).

4. B. Noh, A.S. Murphy, E.P. Spalding *Plant Cell* **13**, 2441 (2001).

5. T. Aoyama, N. H. Chua, *Plant J.* **11**, 605 (1997).

6. J. Mathur, C. Koncz, in *Methods in Molecular Biology: Arabidopsis Protocols*, J.M. Martinez-Zapater, J. Salinas, Eds. (Humana Press, Totowa, New Jersey, 1998), vol. 82, pp. 27-30.

7. T. Nagata, Y. Nemoto, S. Hasezawa, *Int. Rev. Cytol.* **132**, 1 (1992).

8. J. Petrášek *et al*., *Plant Physiol.* **131**, 254 (2003).

9. A. Müller, *EMBO J.* **17**, 6903 (1998).

10. J. Friml *et al.*, *Nature* **426**, 147 (2003).

11. A. P. Smertenko *et al.*, *Plant Cell* **16**, 2035 (2004).

12. T. Paciorek *et al.*, *Nature* **435**, 1251 (2005).

13. C. Luschnig, R. A. Gaxiola, P. Grisafi, G. R. Fink *Genes Dev.* **12**, 2175 (1998).

14. M. Geisler *et al*., *Plant J.* **44**, 179 (2005).

15. A. Delbarre, P. Muller, V. Imhoff, J. Guern *Planta* **198**, 532 (1996).

16. C. A. Hrycyna, *Biochemistry* **38**, 13887 (1999).

17. R. Prusty, P. Grisafi, G. R. Fink, *Proc. Natl. Acad. Sci. USA* **101**, 4153 (2004).

18. J. Friml, J. Wisniewska, in: *Annual Plant Reviews, Intercellular Communication in Plants,* A Fleming, Ed. (Blackwell Publishing, Oxford, UK, 2005), vol. 16, pp. 1-26.

19. I. A. Paponov, W. D. Teale, M. Trebar, I. Blilou, K. Palme, *Trends Plant Sci.* **10**, 170 (2005).

CHAPTER 6

The BY-2 cell line as a tool to study auxin transport

Jan Petrášek, Eva Zažímalová

Biotechnology in Agriculture and Forestry Vol. 58 "Tobacco BY-2 Cells: From Cellular Dynamics to Omics", Nagata, T., Matsuoka, K., Inzé, D. (eds), Springer-Verlag, Berlin Heidelberg, 107-115, 2006

This chapter has been published in a book devoted to tobacco BY-2 cell line. It summarizes recent progression in the field of auxin transport that has been achieved using tobacco cultured cells. Their advantages in studies of processes such as cell division, elongation and establishment of cell polarity are highlighted.

I have written this chapter completely.

All colleagues in the laboratory of Dr. Eva Zažímalová as well as in the laboratory of Dr. Jiří Friml (Tübingen University) are highly acknowledged for their excellent research mentioned here and for stimulating discussions. Special thank is due to my co-supervisor Prof. Zdeněk Opatrný, the "Guru" of cell cultures, and Dr. David Morris for his endless knowledge and enthusiasm for auxin transport studies.

This work was supported by the Grant Agency of the Academy of Sciences of the Czech Republic, project no. A6038303 to Eva Zažímalová.

II.2 The BY-2 Cell Line as a Tool to Study Auxin Transport

J. Petrášek and E. Zažímalová[1,2]

1 Introduction

Auxin transport plays a key role in the regulation of plant growth and development. Either it runs in apoplast by mass flow in the phloem together with other metabolites and/or there exists a parallel, cell-to-cell, strictly directional, carrier-mediated active transport. The major contribution to our understanding of its physiology as well as molecular background comes from studies *in planta*. However, during the last ten years, tobacco cell lines such as BY-2 have provided a major impetus for precise analysis of the machinery performing auxin flow across cell membranes at the cellular level. In this chapter recent knowledge about the molecular mechanism of auxin transport is summarized, and the data are discussed in the context of recent findings concerning the role of directional cell-to-cell transport of auxin in plant development. The results obtained using BY-2 as well as other tobacco cell lines highlight the advantages of these models in studies of auxin-regulated processes such as cell division, elongation and establishment of cell polarity.

2 Present State of the Art of Cell-to-Cell Transport of Auxins

Together with the processes of auxin biosynthesis, conjugation and degradation, unidirectional cell-to-cell transport of auxin (indole-3-acetic acid, IAA) plays a crucial role in the regulation of growth and development of plants (Blakeslee et al. 2005; Friml and Wisniewska 2005; Woodward and Bartel 2005). One of the most important features of auxin transport in the symplast is that it is unequivocally polar. The explanation of its polarity was simultaneously proposed by Rubery and Sheldrake (1974) and Raven (1975) and called the chemiosmotic polar diffusion model (Goldsmith 1977). According to this model, undissociated, a lipophilic form of native auxin molecule (IAA) can easily enter the cell cytoplasm from slightly acidic extracellular environment (pH 5.5) by passive diffusion. Since the pH of cytoplasm is more alkaline

[1] Institute of Experimental Botany ASCR, Rozvojová 135, 16502 Prague 6, Czech Republic, e-mail: petrasek@ueb.cas.cz
[2] Department of Plant Physiology, Faculty of Science, Charles University, Viničná 5, 12844 Prague 2, Czech Republic

Biotechnology in Agriculture and Forestry, Vol. 58
Tobacco BY-2 Cells: From Cellular Dynamics to Omics (ed. by T. Nagata, K. Matsuoka, and D. Inzé)

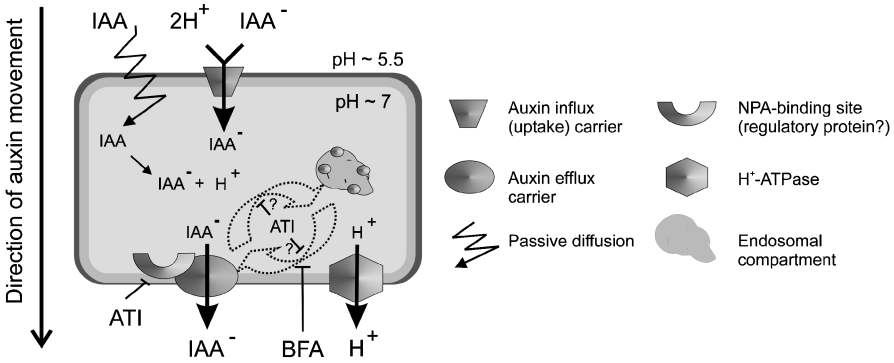

Fig. 1. Simplified scheme of auxin (IAA) transport at the cellular level. Both passive diffusion and specific auxin influx (uptake) and efflux carriers are involved in the transport of the IAA molecule and its dissociated form, auxin anion (IAA^-). In contrast to quite easy diffusion of relatively lipophilic molecules of IAA across the PM, hydrophilic IAA^- anions can be transported only actively via carriers. One of the auxin transport inhibitors (ATIs), 1-naphthylphthalamic acid (NPA), has been proposed to act via binding to the complex of auxin efflux carrier. Moreover, ATIs may have broader effect on protein trafficking processes (Muday et al. 2003). The fungal toxin brefeldin A (BFA) influences polar auxin transport by disturbing Golgi-mediated and actin-dependent vesicle transport of putative auxin efflux carriers from the intracellular space to the PM (Geldner et al. 2001, 2003)

(pH 7), IAA molecules dissociate and the resulting hydrophilic auxin anions (IAA^-) are trapped in the cytosol. The exit or uptake of IAA^- was proposed to be assisted by the auxin efflux and influx proteins, respectively, and the polarity of auxin transport was explained by their asymmetric distribution on the plasma membrane (PM) of the cell (Fig. 1).

In the last decade, genes encoding putative auxin uptake (influx) and efflux carriers have been identified in *Arabidopsis* and other species (Morris 2000; Muday and DeLong 2001; Friml and Palme 2002; Morris et al. 2004; Paponov et al. 2005). Since the intracellular concentration of auxin is, among other things, critical for the setting of various developmental programmes, it is obvious that oriented transport of auxin plays an important role in the morphoregulatory and pattern formation processes such as embryogenesis (Friml et al. 2003), root development (Friml et al. 2002a; Blilou et al. 2005; reviewed in Teale et al. 2005), organ formation (Benková et al. 2003), vascular differentiation (Mattsson et al. 2003), tropisms (Friml et al. 2002b) and phyllotaxis (Reinhardt et al. 2003).

3 Auxin Transport Studies in Planta

3.1 Auxin Transport Assays

It has always been challenging to follow the auxin distribution in plants and to understand how it is established and maintained. Besides modern instrumental techniques for the quantification of endogenous auxin content (Ljung et al. 2005) and non-invasive tracking of the expression of auxin-responding reporter genes (Ulmasov et al. 1997), the direct measurement of radiolabelled auxin distribution has been one of the most frequently used approaches in studies of auxin transport (Goldsmith 1977). Upon application of labelled auxin to one end of a tissue segment, auxin movement is usually followed by measurement of the quantity of transported radiolabel. Although this approach was recently optimized for the whole *Arabidopsis* seedling (Geisler et al. 2003) it is not applicable for the measurement of auxin transport at the cellular level.

3.2 Inhibitors of Polar Auxin Transport

One of the most fruitful approaches in studying the auxin transport machinery is the application of various inhibitors. The most widely used inhibitor of auxin efflux is 1-naphthylphthalamic acid (NPA), which belongs to a group of inhibitors known as phytotropins (Rubery 1990). The application of NPA to plant tissues results typically in an increase in auxin accumulation, presumably due to the inhibition of auxin efflux activity (Morris et al. 2004). Detailed knowledge about the mechanism, by which NPA and other phytotropins inhibit auxin efflux, is still lacking. NPA probably binds to a specific high affinity NPA-binding protein (NBP) located on the cytoplasmic face of the PM (Sussman and Gardner 1980), where it is associated with actin cytoskeleton (Cox and Muday 1994; Dixon et al. 1996; Butler et al. 1998). Recent evidence suggests that NBPs are aminopeptidases acting in cooperation with flavonoids, which are known as naturally occurring regulators of auxin efflux (Murphy et al. 2002). In addition, a more general, inhibitory effect of phytotropins on endocytotic processes was reported (Geldner et al. 2001).

Another set of results that helped the understanding of auxin transport machinery comes from studies using fungal toxin brefeldin A (BFA), the inhibitor of Golgi-mediated vesicle trafficking and endosomal recycling. BFA inhibits auxin efflux activity in zucchini hypocotyls (Morris and Robinson 1998) and blocks auxin transport through the tissue (Robinson et al. 1999). Since BFA treatment effectively changes the proportion of proteins localized at the PM and in the endosomal space (reviewed in Geldner 2004), it is an ideal tool for studying constitutive cycling of both putative auxin efflux and uptake carriers.

3.3 Genetic and Molecular Characterization of Components of the Auxin Transport Machinery

Recent research using the model plant *Arabidopsis thaliana* led to the identification of proteins involved in the auxin transport machinery. These include promising candidates for both auxin uptake (influx) carrier, AUX1/LAXs (amino-acid permease-like proteins), and regulators of auxin efflux, PINs (PIN-formed, plant-specific PM proteins) and MDR/PGPs (multidrug-resistance-like/P-glycoproteins) (see Morris et al. 2004; Blakeslee et al. 2005; Friml and Wisniewska 2005). It seems that PIN proteins establish the direction of auxin flux by their asymmetric distribution at the PM. They may form complexes with other regulatory proteins and MDR/PGPs may stabilize these complexes (Blakeslee et al. 2005).

The correct positioning of the auxin efflux complex seems to be assisted by the actin cytoskeleton. The application of actin drugs resulted in reduced polar auxin transport in maize coleoptiles (Cande et al. 1973) and in zucchini hypocotyls (Butler et al. 1998). Moreover, using BFA, it was shown that PIN proteins might undergo constitutive cycling between PM and the endosomal space, as indirectly suggested by Robinson et al. (1999), and that this process is actin-dependent (Geldner et al. 2001). It was shown that the mutation in *Arabidopsis* myosin VI led to the inhibition of basipetal auxin transport (Holweg and Nick 2004). All these observations strongly suggest that actin filaments are involved in both intracellular traffic of PINs and their correct targeting to the proper domains at the PM. The concept of trafficking and proper localization as well as function of components of the auxin efflux carrier complex has been proposed (summarized in Muday et al. 2003). In contrast to this, the mechanism(s) underlying the constitutive cycling of proteins in plants is still poorly understood (Murphy et al. 2005). Constitutive cycling of PINs is regulated by GNOM, one of the exchange factors for ADP-ribosylation factor-type GTPases (ARF-GEFs; Geldner et al. 2003, 2004) and other ARFs might also contribute to the trafficking of PINs (Xu and Scheres 2005). Interestingly, the regulation of endocytosis-dependent cycling of proteins in plant cells was shown to be regulated by auxin itself (Paciorek et al. 2005), suggesting a new mechanism of auxin action in plant cells.

4 Auxin Transport Studies in Simplified Models

4.1 Transport of Auxins in Suspension-Cultured Cells

Since it is difficult to study the biochemical aspects of auxin transport by measurements at the whole-plant and organ level (see above), plant cells cultured in liquid medium represent a valuable alternative. The accumulation of auxin can be measured in time intervals after the direct addition of radiolabelled auxin

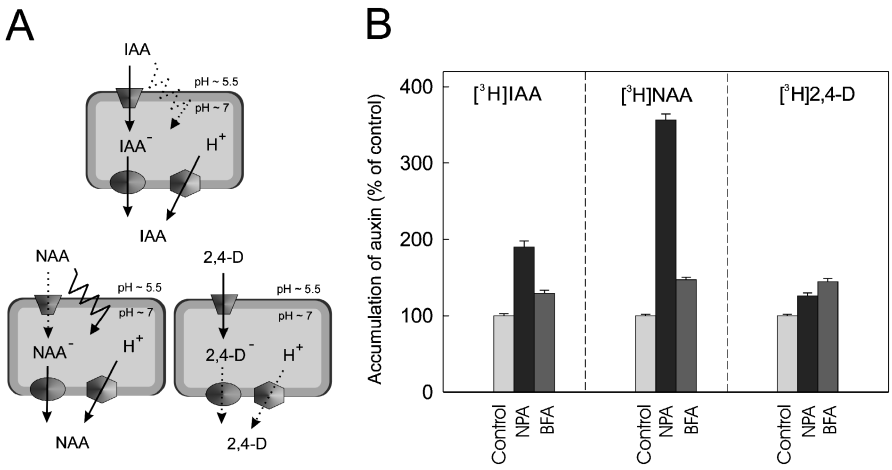

Fig. 2. Differences in the translocation of IAA and two synthetic auxins NAA and 2,4-D in tobacco cell lines. **A** Auxins are translocated across PM according to their relative lipophilicity (NAA > IAA > 2, 4-D). As shown by careful measuring of diffusion and carrier-mediated transport of NAA, IAA and 2,4-D in tobacco suspension-cultured Xanthi XHFD8 cells by Delbarre et al. (1996), the accumulation level of NAA is controlled mainly by efflux carrier activity, while the accumulation of 2,4-D is determined by the activity of an uptake carrier. Both uptake and efflux carriers, as well as passive diffusion, contribute to the accumulation of IAA. Refer to Fig. 1 for *symbol* legends. **B** The accumulation of all three types of auxins (IAA, NAA, 2,4-D) is increased upon application of inhibitors NPA or BFA, thus reflecting disturbed auxin efflux machinery in BY-2 cells (Petrášek et al. 2005)

into the cell suspension. Indeed, the most important experiments, on which the chemiosmotic hypothesis of IAA transport was based, were performed using auxin-autonomous suspensions of crown gall cells of Boston Ivy (Rubery and Sheldrake 1974), where the time of addition as well as concentrations of auxin transport inhibitors or auxin itself could be readily controlled.

The first characterization of auxin transport mechanisms at the cellular level was reported by Delbarre et al. (1994, 1996) in mesophyll protoplasts and cell suspension from tobacco cv. Xanthi XHFD8, respectively. As depicted on Fig. 2A, Delbarre et al. proposed a simple method to describe the role of passive diffusion and active carrier-mediated processes in the transport of three of the most common auxins, namely native IAA, synthetic naphthalene-1-acetic acid (NAA) and 2,4-dichlorophenoxyacetic acid (2,4-D). The same cell suspension was used for the characterization of a new class of inhibitors of auxin influx (Imhoff et al. 2000) as well as for the study of phosphorylation/dephosphorylation of proteins of the auxin efflux complex (Delbarre et al. 1998). One such regulatory protein, PINOID kinase, was recently shown to regulate polar targeting of PIN proteins in *Arabidopsis* (Friml et al. 2004).

In contrast to cell suspensions of *Arabidopsis* (which tend to form large cell clusters), the major advantage of intensively dividing cell cultures of tobacco

is that the effects on cell morphology of various inhibitors as well as of auxin itself can be observed in parallel with the measurements of auxin accumulation. Since tobacco cell lines of a good quality are completely friable, it is possible to express all measured data as an equivalent of cell number. During the period of cell division, such high-quality tobacco cell lines usually form polar cell files instead of cell clusters. Based on the studies using tobacco cell line VBI-0 (*Nicotiana tabacum* L., cv. Virginia Bright Italia; Opatrný and Opatrná 1976), the inhibition of auxin transport by NPA and the consequent rise in the internal auxin level delayed the onset of cell division and disrupted its polarity (Petrášek et al. 2002). Mathematical modelling suggested that NPA possibly disturbs the gradient in auxin concentration along the cell file (Campanoni and Nick 2003). This effect might be mediated by the actin cytoskeleton, as shown by Holweg et al. (2003), using inhibitors of myosin action. In spite of the fact that the auxin-autonomous cell line VBI-I1 containing spherical cells was derived (Campanoni et al. 2001) from 'parental' VBI-0 line, VBI-0 itself is routinely maintained on both NAA and 2,4-D. These two auxins may control cell division and cell elongation by different pathways (Campanoni and Nick 2005); therefore, the BY-2 cell line is a better model in this respect, as it is only 2,4-D-dependent.

4.2 Transport of Auxins in BY-2 Cells

The potential of simultaneous measurements of intracellular auxin accumulation and tracking of changes in various cell structures, together with directed transgenosis, makes tobacco BY-2 cells an invaluable tool for the study of auxin transport at the cellular level (Petrášek et al. 2003; Zažímalová et al. 2003) as well as for the characterization in vivo of functions of the proteins involved. BY-2 cells respond to the addition of inhibitors NPA or BFA by an immediate rise in the accumulation of IAA, NAA and 2,4-D (Fig. 2B). The transport of these auxins occurs in similar ways as suggested for tobacco Xanthi XHFD8 cells (Delbarre et al. 1996; Fig. 2A). Both the kinetics of NAA accumulation (Fig. 3A) and the arrangement of the cytoskeleton reflect differential sensitivity of BY-2 cells towards BFA and NPA (see Petrášek et al. 2003 for details).

To test the proposed role of PIN proteins in the regulation of auxin transport, BY-2 cells were transformed with *PIN1*, *PIN4*, *PIN6* and *PIN7* genes from *Arabidopsis thaliana*. For all tested PINs, their strong inducible overexpression resulted in a decrease in auxin accumulation (Fig. 3B; Skůpa et al. 2005), followed by remarkable changes in cell morphology (Fig. 3D, E, F). Similar changes have been reported previously to be typical of the response to auxin depletion (Sakai et al. 2004). Moreover, the fact that NPA, an inhibitor of auxin efflux, was capable of preventing all observed "auxin-depletion"-induced changes (Fig. 3G) strongly points to the modification in auxin transport (Petrášek et al. 2005). In vivo studies using BY-2 cells expressing *Arabidopsis* PIN1 protein fused to GFP revealed its predominant localization at transversal PMs, although

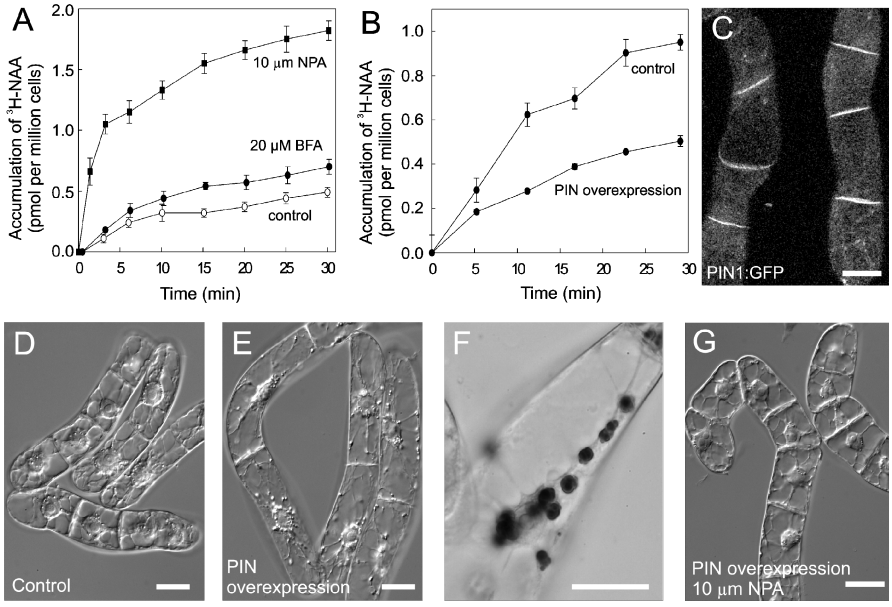

Fig. 3. Treatments with auxin efflux inhibitors or overexpression of putative auxin efflux carriers result in changed levels of endogenous auxin and distinct cell morphology in BY-2 cells. **A** Accumulation kinetics reflecting the increase in accumulation of auxin (NAA) upon application of inhibitors of auxin efflux, BFA and NPA (Petrášek et al. 2003). *Error bars* represent SEs of the mean (n = 4). **B** Decrease in accumulation of auxin upon PIN protein overexpression reflecting enhanced auxin efflux (Skůpa et al. 2005). *Error bars* represent SEs of the mean (n = 4). **C** Two-day-old BY-2 cells stably expressing *Arabidopsis* PIN1 protein in translation fusion with GFP. Merged five optical sections (each section 1 μm) through the cortical cytoplasm. The localization of PINs in BY-2 cells at transversal PMs suggests preferential direction of auxin flow. **D–G** Three-day-long overexpression of PIN proteins under strong promoter results in the cessation of cell division (**E**) and formation of starch-containing amyloplasts (Lugol staining) (**F**). All changes are rescued by simultaneous treatment with 10 μM NPA (**G**) to control-like situation (**D**), suggesting the inhibition of overexpressed PIN proteins (Petrášek et al. 2005). *Scale bars* 20 μm

a proportion of fusion protein was localized along longitudinal PMs and in the cortical cytoplasm (Fig. 3C). Thus, in the BY-2 cell line the distribution of PIN1-GFP in cell files resembles the PIN distribution pattern in the cells of the root elongation zone of *Arabidopsis thaliana*.

It was recently shown (Paciorek et al. 2005), using *Arabidopsis thaliana* plants as well as both BY-2 and VBI-0 tobacco cells, that auxins can inhibit the endocytotic step of the constitutive cycling of PM proteins including PIP2 aquaporin, PM-ATPase and PINs. According to these results, auxin increases levels of PINs at the PM and concomitantly promotes its own efflux from cells. This finding implies a novel mode of auxin action, similar to some animal hormones and consistent with pleiotropic physiological effects of auxin on plant cells.

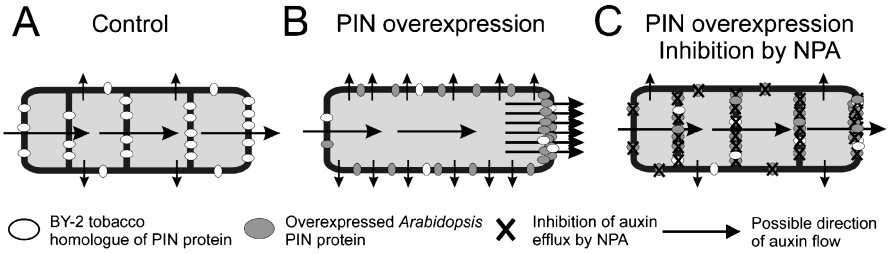

Fig. 4. Schematic diagrams summarizing the effects of overexpression of the PIN proteins in BY-2 cells. **A** Control, exponentially growing cells expressing their endogenous tobacco efflux carriers. According to BLAST search in the EST database of Matsuoka et al. (2004), EST n. 3440f1 is the most promising candidate for an Nt*PIN* gene. **B** Strong overexpression of *Arabidopsis* PIN protein stimulates auxin efflux. As a consequence, cells display typical auxin-starvation symptoms (Winicur et al. 1998; Sakai et al. 2004), such as inhibition of cell division, stimulation of amyloplast differentiation and marked cell elongation. **C** Upon inhibition of a proportion of endogenous as well as overexpressed auxin efflux carriers by NPA, cell division is restored to the control-like situation (Petrášek et al. 2005)

Altogether, our observations, summarized in Fig. 4, reveal that changes in BY-2 cell development are related to auxin transport and – from the point of view of molecular mechanisms of auxin transport – they strongly support the idea that PIN proteins are the rate-limiting components of the auxin efflux machinery, and probably the auxin efflux catalysts themselves.

5 Concluding Remarks and Future Prospects

In conclusion, the BY-2 tobacco cell line together with a few other well-defined tobacco cell lines, can serve as an invaluable alternative experimental tool for auxin transport studies complementary to *Arabidopsis* plants. In our laboratory, the collection of BY-2 cells, transformed with components of both auxin influx (Laňková et al. 2005) and efflux machinery (see above), is maintained and constantly extended. In future, these experimental materials may be useful for studies of the composition of the auxin transport machinery and quantitative aspects of its action, as well as for the characterization of the dynamics of proteins that play a role in the transport of auxin in vivo using fluorescent tags. It may also contribute to discovering the role of both auxin influx and efflux in the establishment of auxin levels inside the cell and their relation to the regulation of cell division, cell elongation and establishment and/or maintenance of cell polarity.

Acknowledgements. This work was supported by the Grant Agency of the Academy of Sciences of the Czech Republic, project no. A6038303. *PIN* gene constructs were expressed in BY-2 cells in the framework of very stimulating, informal collaboration with Dr. Jiři Friml (University of Tübingen, Germany). We also express our gratitude to Prof. Zdeněk Opatrný (Charles University,

Prague, Czech Republic) for a long-lasting fruitful collaboration on cell cultures and to Dr. David Morris (University of Southampton, UK) for collaboration and inspiring discussions on auxin transport.

References

Benková E, Michniewicz M, Sauer M, Teichmann M, Seifertová D, Jürgens G, Friml J (2003) Local, efflux-dependent auxin gradients as a common module for plant organ formation. Cell 115:591–602

Blakeslee JJ, Peer WA, Murphy AS (2005) Auxin transport. Curr Opin Plant Biol 8:494–500

Blilou I, Xu J, Wildwater M, Willemsen V, Paponov I, Friml J, Heidstra R, Aida M, Palme K, Scheres B (2005) The PIN auxin efflux facilitator network controls growth and patterning in *Arabidopsis* roots. Nature 433:39–44

Butler JH, Hu SQ, Brady SR, Dixon MW, Muday GK (1998) *In vitro* and *in vivo* evidence for actin association of the naphthylphthalamic acid-binding protein from zucchini hypocotyls. Plant J 13:291–301

Campanoni P, Nick P (2005) Auxin-dependent cell division and cell elongation. 1-naphthaleneacetic acid and 2,4-dichlorophenoxyacetic acid activate different pathways. Plant Physiol 137:939–948

Campanoni P, Petrášek J, Opatrný Z, Nick P (2001) Manipulation of cell axis, polarity and the exit from the cell cycle via the level and balance of different auxins. Proc 17th IPGSA Conference, 1–6 July, Brno, Czech Republic, p 95

Campanoni P, Blasius B, Nick P (2003) Auxin transport synchronizes the pattern of cell division in a tobacco cell line. Plant Physiol 133:1251–1260

Cande WZ, Goldsmith MHM, Ray PM (1973) Polar auxin transport and auxin-induced elongation in the absence of cytoplasmic streaming. Planta 111:279–296

Cox DN, Muday GK (1994) NPA binding activity is peripheral to the plasma membrane and is associated with the cytoskeleton. Plant Cell 6:1941–1953

Delbarre A, Muller P, Imhoff V, Morgat JL, Barbier-Brygoo H (1994) Uptake, accumulation and metabolism of auxins in tobacco leaf protoplasts. Planta 195:159–167

Delbarre A, Muller P, Imhoff V, Guern J (1996) Comparison of mechanisms controlling uptake and accumulation of 2,4-dichlorophenoxy acetic acid, naphtalene-1-acetic acid, and indole-3-acetic acid in suspension-cultured tobacco cells. Planta 198:532–541

Delbarre A, Muller P, Guern J (1998) Short-lived and phosphorylated proteins contribute to carrier-mediated efflux, but not to influx, of auxin in suspension-cultured tobacco cells. Plant Physiol 116:833–844

Dixon MW, Jacobson JA, Cady CT, Muday GK (1996) Cytoplasmic orientation of the naphthylphthalamic acid-binding protein in zucchini plasma membrane vesicles. Plant Physiol 112:421–432

Friml J, Palme K (2002) Polar auxin transport – old questions and new concepts? Plant Mol Biol 49:273–284

Friml J, Wisniewska J (2005) Auxin as an intercellular signal. In: Fleming A (ed) Annual plant reviews, vol. 16. Intercellular communication in plants. Blackwell Publishing, Oxford, pp 1–26

Friml J, Benková E, Blilou I, Wisniewska J, Hamann T, Ljung K, Woody S, Sandberg G, Scheres B, Jürgens G, Palme K (2002a) AtPIN4 mediates sink-driven auxin gradients and root patterning in *Arabidopsis*. Cell 108:661–673

Friml J, Wisniewska J, Benková E, Mendgen K, Palme K (2002b) Lateral relocation of auxin efflux regulator PIN3 mediates tropism in *Arabidopsis*. Nature 415:806–809

Friml J, Vieten A, Sauer M, Weijers D, Schwarz H, Hamann T, Offringa R, Jürgens G (2003) Efflux-dependent auxin gradients establish the apical-basal axis of *Arabidopsis*. Nature 426:147–153

Friml J, Yang X, Michniewicz M, Weijers D, Quint A, Tietz O, Benjamins R Ouwerkerk PBF, Ljung K, Sandberg G, Hooykaas PJJ, Palme K, Offringa R (2004) A PINOID-dependent binary switch in apical-basal PIN polar targeting directs auxin efflux. Science 306:862–865

Geisler M, Kolukisaoglu HU, Billion K, Berger J, Saal B, Bouchard R, Frangne N, Koncz-Kalman Z, Koncz C, Dudler R, Blakeslee J, Murphy AS, Martinoia E, Schulz B (2003) TWISTED DWARF1, a unique plasma membrane-anchored immunophilin-like protein, interacts with *Arabidopsis* multidrug resistance-like transporters AtPGP1 and AtPGP19. Mol Biol Cell 14:4238–4249

Geldner N (2004) The plant endosomal system – its structure and role in signal transduction and plant development. Planta 219:547–560

Geldner N, Friml J, Stierhof YD, Jürgens G, Palme K (2001) Auxin transport inhibitors block PIN 1 cycling and vesicle trafficking. Nature 413:425–428

Geldner N, Anders N, Wolters H, Keicher J, Kornberger W, Muller P, Delbarre A, Ueda T, Nakano A, Jürgens G (2003) The *Arabidopsis* GNOM ARF-GEF mediates endosomal recycling, auxin transport, and auxin-dependent plant growth. Cell 112:219–230

Geldner N, Richter S, Vieten A, Marquardt S, Torres-Ruiz RA, Mayer U, Jürgens G (2004) Partial loss-of-function alleles reveal a role for GNOM in auxin transport-related, post-embryonic development of *Arabidopsis*. Development 131:389–400

Goldsmith MHM (1977) The polar transport of auxin. Annu Rev Plant Physiol 28:439–478

Holweg C, Nick P (2004) Arabidopsis myosin XI mutant is defective in organelle movement and polar auxin transport. Proc Natl Acad Sci USA 101:10488–10493

Holweg C, Honsel A, Nick P (2003) A myosin inhibitor impairs auxin-induced cell division. Protoplasma 222:193–204

Imhoff V, Muller P, Guern J, Delbarre A (2000) Inhibitors of the carrier-mediated influx of auxin in suspension-cultured tobacco cells. Planta 210:580–588

Laňková M, Petrášek J, Perry L, Dobrev P, Zažímalová E (2005) Characterisation of tobacco cell lines transformed with the PaLAX1 gene. Biol Plant 49 (Suppl):S12

Ljung K, Hull AK, Celenza J, Yamada M, Estelle M, Normanly J, Sandberg G (2005) Sites and regulation of auxin biosynthesis in Arabidopsis roots. Plant Cell 17:1090–1104

Matsuoka K, Demura T, Galis I, Horiguchi T, Sasaki M, Tashiro G, Fukuda HA (2004) Comprehensive gene expression analysis toward the understanding of growth and differentiation of tobacco BY-2 cells. Plant Cell Physiol 45:1280–1289

Mattsson J, Ckurshumova W, Berleth T (2003) Auxin signaling in *Arabidopsis* leaf vascular development. Plant Physiol 131:1327–1339

Morris DA (2000) Transmembrane auxin carrier systems – dynamic regulators of polar auxin transport. Plant Growth Regul 32:161–172

Morris DA, Robinson JS (1998) Targeting of auxin carriers to the plasma membrane: differential effects of brefeldin A on the traffic of auxin uptake and efflux carriers. Planta 205:606–612

Morris DA, Friml J, Zažímalová E (2004) The transport of auxins. In: Davies PJ (ed) Plant hormones: biosynthesis, signal transduction, action! Kluwer, Dordrecht, pp 437–470

Muday GK, DeLong A (2001) Polar auxin transport: controlling where and how much. Trends Plant Sci 6:535–542

Muday GK, Peer WA, Murphy AS (2003) Vesicular cycling mechanisms that control auxin transport polarity. Trends Plant Sci 8:301–304

Murphy AS, Hoogner KR, Peer WA, Taiz L (2002) Identification, purification and molecular cloning of N-1-naphthylphthalamic acid-binding plasma membrane-associated aminopeptidases from *Arabidopsis*. Plant Physiol 128:935–950

Murphy AS, Bandyopadhyay A, Holstein SE, Peer WA (2005) Endocytotic cycling of PM proteins. Annu Rev Plant Biol 56:221–251

Opatrný Z, Opatrná J (1976) The specificity of the effect of 2,4-D and NAA on the growth, micromorphology, and the occurrence of starch in long-term *Nicotiana tabacum* cell strains. Biol Plant 18:381–400

Paciorek T, Zažímalová E, Ruthardt N, Petrášek J, Stierhof Y-D, Kleine-Vehn J, Morris DA, Emans N, Jürgens G, Geldner N, Friml J (2005) Auxin inhibits endocytosis and promotes its own efflux from cells. Nature 435:1251–1256

Paponov IA, Teale WD, Trebar M, Blilou I, Palme K (2005) The PIN auxin efflux facilitators: evolutionary and functional perspectives. Trends Plant Sci 10:170–177

Petrášek J, Elčkner M, Morris DA, Zažímalová E (2002) Auxin efflux carrier activity and auxin accumulation regulate cell division and polarity in tobacco cells. Planta 216:302–308

Petrášek J, Černá A, Schwarzerová K, Elčkner M, Morris DA, Zažímalová E (2003) Do phytotropins inhibit auxin efflux by impairing vesicle traffic? Plant Physiol 131:254–263

Petrášek J, Seifertová D, Perry L, Skůpa P, Čovanová M, Zažímalová E (2005) Expression of AtPINs in tobacco cells increases auxin efflux and induces phenotype changes typical for auxin depletion. Biol Plant 49 (Suppl):S10

Raven JA (1975) Transport of indoleacetic acid in plant cells in relation to pH and electrical potential gradients, and its significance for polar IAA transport. New Phytol 74:163–174

Reinhardt D, Pesce ER, Stieger P, Mandel T, Baltensperger K, Bennett M, Traas J, Friml J, Kuhlemeier C (2003) Regulation of phyllotaxis by polar auxin transport. Nature 426:255–260

Robinson JS, Albert AC, Morris DA (1999) Differential effects of brefeldin A and cycloheximide on the activity of auxin efflux carriers in *Cucurbita pepo* L. J Plant Physiol 155:678–684

Rubery PH (1990) Phytotropins: receptors and endogenous ligands. Symp Soc Exp Biol 44:119–146

Rubery PH, Sheldrake AR (1974) Carrier-mediated auxin transport. Planta 118:101–121

Sakai A, Miyazawa Y, Kuroiwa T (2004) Studies on dynamic changes of organelles using tobacco BY-2 as the model plant cell line. In: Nagata T, Hasezawa S, Inzé D (eds) Biotechnology in agriculture and forestry, vol. 53. Tobacco BY-2 cells. Springer, Berlin Heidelberg New York, pp 192–216

Skůpa P, Černá A, Petrášek J, Perry L, Seifertová D, Zažímalová E (2005) Characterisation of tobacco cell lines transformed with the *AtPIN1, 4, 6, 7* genes from *Arabidopsis*. Biol Plant 49 (Suppl):S12

Sussman MR, Gardner G (1980) Solubilization of the receptor for *N*-1-naphthylphthalamic acid. Plant Physiol 66:1074–1078

Teale WD, Paponov IA, Ditengou F, Palme K (2005) Auxin and the developing root of *Arabidopsis thaliana*. Physiol Plant 123:130–138

Ulmasov T, Murfett J, Hagen G, Guilfoyle TJ (1997) Aux/IAA proteins repress expression of reporter genes containing natural and highly active synthetic auxin response elements. Plant Cell 9:1963–1971

Winicur ZM, Zhang GF, Staehelin LA (1998) Auxin deprivation induces synchronous Golgi differentiation in suspension-cultured tobacco BY-2 cells. Plant Physiol 117:501–513

Woodward AW, Bartel B (2005) Auxin: regulation, action, and interaction. Ann Bot 95:707–735

Xu J, Scheres, B (2005) Dissection of *Arabidopsis* ADP-RIBOSYLATION FACTOR 1 function in epidermal cell polarity. Plant Cell 17:525–536

Zažímalová E, Petrášek J, Morris DA (2003) The dynamics of auxin transport in tobacco cells. Bulgarian J Plant Physiol Spec Issue:207–224